# DETERMINING RECENT SEDIMENTATION RATES OF THE NUECES RIVER SYSTEM, TEXAS

by

William A. White and Robert A. Morton

Assisted by Radu Boghici

Principal Investigator

Robert A. Morton

Final Report prepared for the Texas Water Development Board
under Research and Planning Fund Grant Contract No. 95-483-075

Bureau of Economic Geology
Noel Tyler, Director
The University of Texas at Austin
Austin, Texas 78713-8924

March 1996

CONTENTS

## Figures

**Tables**

# DETERMINING RECENT SEDIMENTATION RATES OF THE NUECES RIVER SYSTEM, TEXAS

## INTRODUCTION

Replacement of wetlands by water and barren flats in the lower alluvial valley and delta of the Nueces River suggests that relative sea-level rise and reductions in sediment supply have rendered the Nueces fluvial-deltaic system incapable of maintaining sufficient elevation to prevent its submergence. The Nueces River system has in the past transported a significant load of suspended sediment (Longley, 1992a), but the construction of upstream dams and reservoirs has greatly reduced the volume of sediment reaching deltaic marshes and other wetland habitats. Still, losses in deltaic environments along the Nueces River have been smaller than in other deltas of the Texas coast (White and Calnan, 1991), so there remains a potential for the Nueces River to deliver enough sediment to offset subsidence and submergence.

### Objectives

The principal objectives of this study were to determine past rates of sedimentation and relative sea-level rise for a fluvially dominated area along the Nueces River upstream from the delta. This information will be used by the Texas Water Development Board to determine the frequency, duration, and magnitude of river flooding necessary to offset submergence of wetlands (Longley, 1992b). Sedimentation rates are based on activities of $^{210}Pb$ measured in 11 cores collected in the study area (fig. 1). Rates of relative sea-level rise are based on National Ocean Service (NOS) benchmark releveling surveys, USGS reports, NOS tide gauge data, and data on relative sea-level rise presented by Paine (1993).

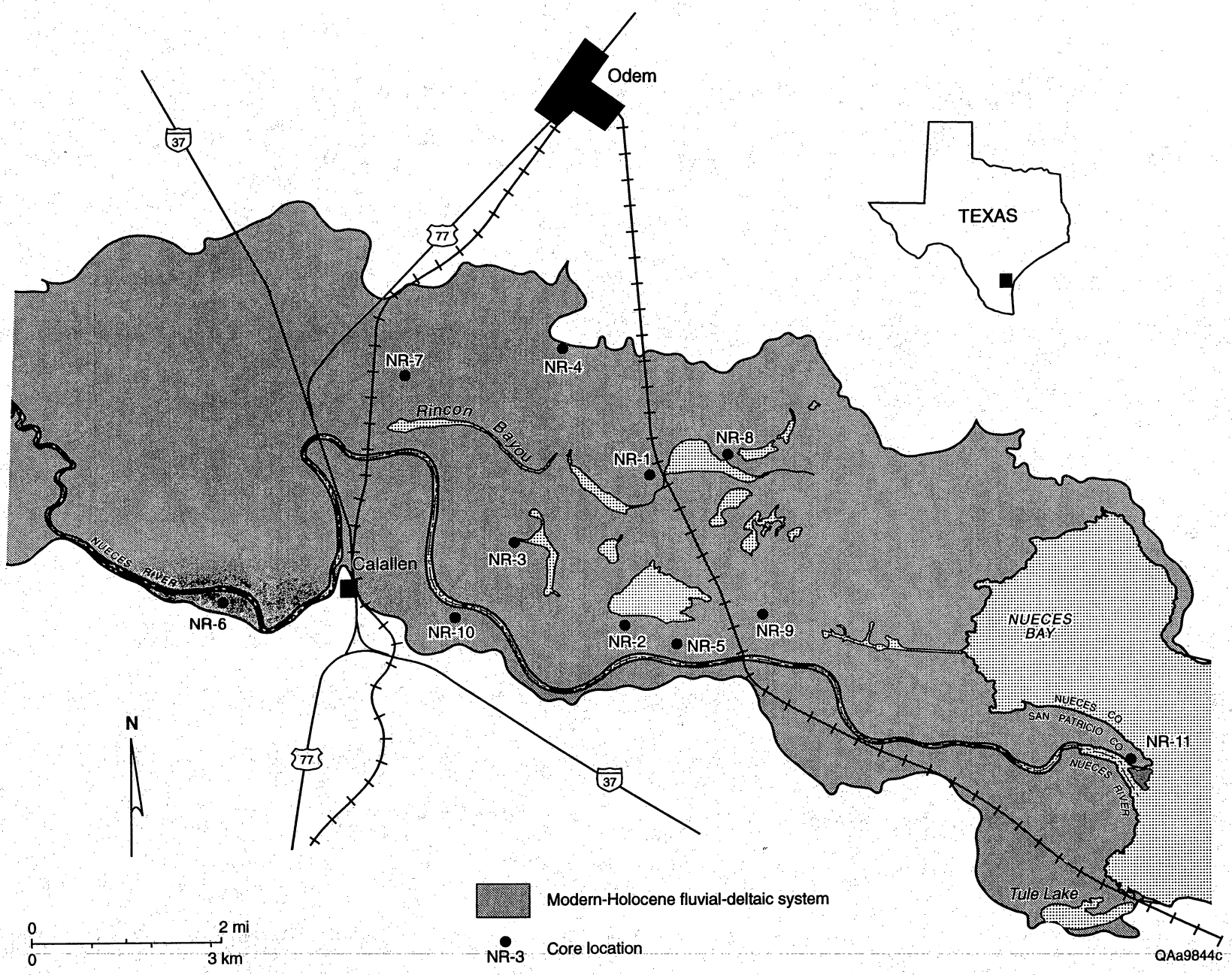


Figure 1. Index map of study area showing locations of coring sites.

## Natural Environments in the Study Area

Natural environments of the Nueces River system and alluvial valley in the study area (fig. 1) consist of salt, brackish, and fresh marshes; transitional areas; flats; open water (including lakes and abandoned river channels); fluvial woodlands, and uplands (White and others, 1983). These habitats have developed on alluvial valley fill within the entrenched valley. Inland parts of the alluvial valley are dominated by fluvial processes in contrast to deltaic areas where estuarine processes are more influential.

Average monthly median salinities in the upper part of Nueces Bay fluctuate around 21.7 ppt (Texas Department of Water Resources, 1981). However, depending on fresh-water inflows, salinities can drop to less than 1 ppt or exceed 40 ppt (Holland and others, 1975).

The Nueces River delta is generally characterized by salt marshes with salinities decreasing up the valley. In the study area, marshes are reflective primarily of salt to brackish conditions. Upstream from Interstate Highway 37, fresh marshes occur.

## Modern–Holocene Valley-Fill Deposits

Sediments in the Nueces River valley fill near Interstate Highway 37 are dominated by thick fluvial sand deposits, locally exceeding 12 m, which are overlain by thin flood basin mud deposits that vary in thickness from 1.2 to 3 m (fig. 2). The depth of the modern river channel is slightly greater than the thickness of the mud deposits; consequently, the channel is floored by sandy sediments and bars.

## Human Modifications Potentially Affecting Sedimentation

Among major human modifications in the Nueces River alluvial valley are two Missouri-Pacific (MOPAC) railroad embankments (completed before 1930), State Highway 9 (completed in 1933, preceding IH-37), Interstate Highway 37 (constructed in the late 1950s—early 1960s) (fig. 1), and Lake Corpus Christi (created originally in 1929, Mathis Dam, and enlarged in 1958, Seale Dam). Lake Corpus Christi is

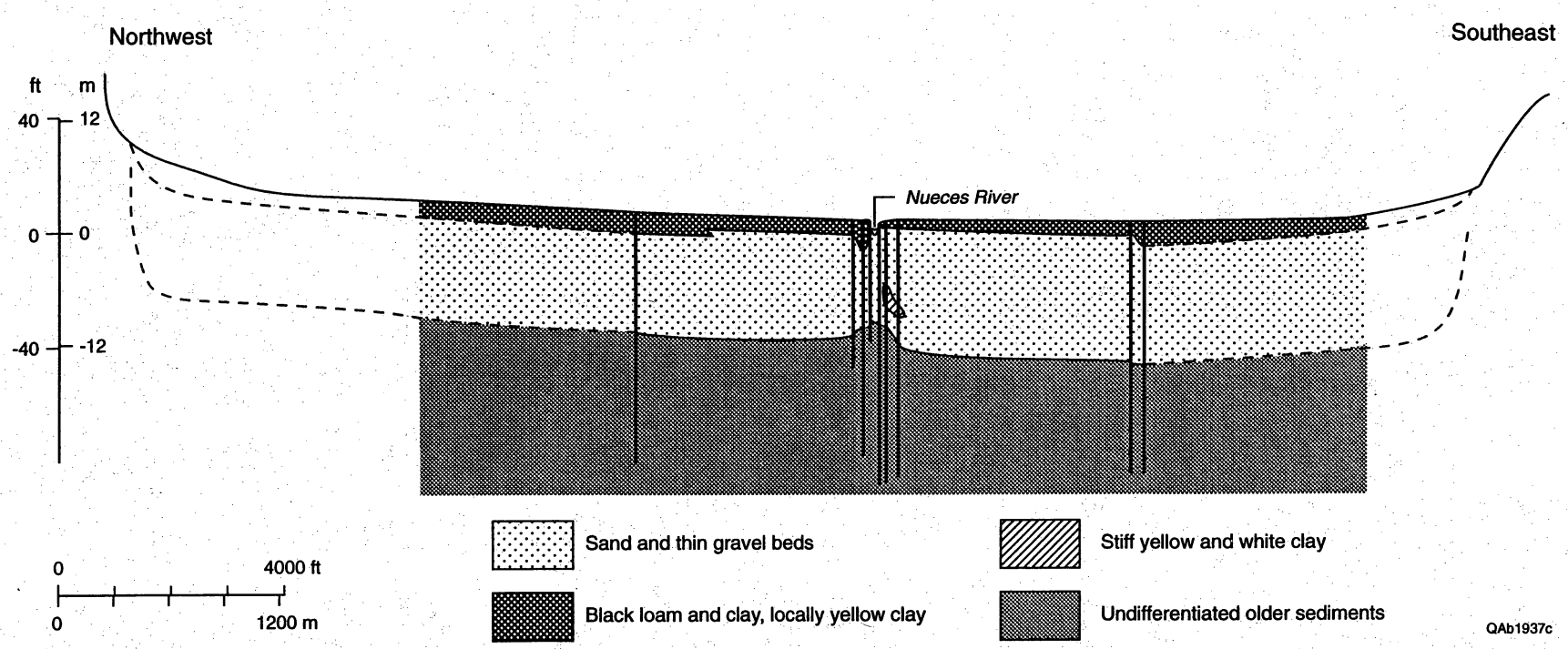


Figure 2. Cross section of Holocene sediments in the Nueces River entrenched valley at U.S. Highway 77. The lithology and thickness of sediments are based on geotechnical surveys made by the Texas Department of Transportation.

approximately 50 km upstream from the mouth of the Nueces River. Major alterations caused by MOPAC railroads include approximately 3.7 linear km of fill for the westernmost tracks near U.S. Highway 77 where the valley is about 4.3 km wide and 5.3 km of fill along the easternmost tracks where the valley is about 5.9 km wide (fig. 1). Bridge openings totaling approximately 0.6 km in length are at the Nueces River, Rincon Bayou, and narrow drainages to the north. About 90 percent of the valley is effectively dammed by the railroad fill. At IH-37, approximately 85 percent (4.35 linear km) of the valley is dammed by road fill for the highway.

The effects of human modifications in the study area on marsh sedimentation are not fully understood. It is obvious that flow patterns during flood events have been altered substantially by the MOPAC railroads and highway crossings, which extend across the valley diverting flow through bridge openings. Intuitively, one would expect sedimentation rates to be slightly higher upstream of the railroads and highway due to the partial damming effect. During floods the flow barriers may locally reduce currents and elevate water levels for longer periods of time allowing more sediments to settle upstream. However, variations in sedimentation rates, which are minimal, seem to be influenced more by the geomorphic setting and relationship of a site to the river and relict channels, rather than by location upstream or downstream of the road embankment. There is also the possibility that sediment deposition during hurricane storm surge flooding may compensate for reductions in sediment supplied to downstream sites during river flooding.

Among other artificial changes in the Nueces River valley is a 2.5-km-long navigation channel dredged for oil and gas exploration and production before the 1950s. The channel extends from the bay shoreline westward through marshes north of the river. Dredged material was deposited on mounds on the south side of the channel. No coring sites are near the channel.

Another modification to deltaic marshes is a marsh creation project that was begun in the late 1980s under the direction of the Port of Corpus Christi Authority and the U.S. Army Corps of Engineers. Approximately 80 ha was excavated in a high salt marsh (*Spartina spartinae*) to create an area of approximately 36 ha of intertidal marsh (Nicolau, 1995). Planted emergent vegetation consisted primarily

of *Spartina alterniflora*. The marsh is a mitigation project for developing a spoil disposal area near the Corpus Christi Ship Channel. The initial effort to establish *Spartina alterniflora* at the site was a failure because of incorrect elevation and slope of designated areas and higher than optimal salinity for *Spartina alterniflora* growth (Ruth, 1990; Nicolau and Adams, 1993; Nicolau, 1995). Core NR-9 is about 75 m from the edge of the site. In April of 1995, when cores were taken, the marsh restoration site was characterized primarily by open water.

## Historical Wetland Losses

In the Nueces River valley, more than 122 ha of marsh habitat was lost between the 1930s and 1979 (White and Calnan, 1990). The losses were a result of the transformation of emergent vegetation to open water and barren flats, primarily in the delta near Nueces Bay (fig. 3). Progradation ended sometime between 1930 and 1959 (Morton and Paine, 1984). Among the probable causes for the losses in wetlands are reductions in the volume of fluvial sediments reaching the delta and relative sea-level rise.

Suspended fluvial sediment reaching Nueces Bay has been reduced from 750,000 tons/yr during the first half of this century to approximately 40,000 tons/yr from 1970 to 1980 (Morton and Paine, 1984). This large reduction in sediment is caused primarily by Lake Corpus Christi.

Compounding the problem of reduced sediment supply is a rise in relative sea level. Rates of relative sea-level rise at benchmarks in the Nueces River valley along MOPAC near U.S. Highway 77 locally exceed 6 mm/yr, which is approximately three to five times higher than regional and eustatic sea-level rise (Gornitz and Lebedeff, 1987). A more detailed discussion of subsidence and sea-level rise rates is presented in the section titled "Relative Sea-Level Rise."

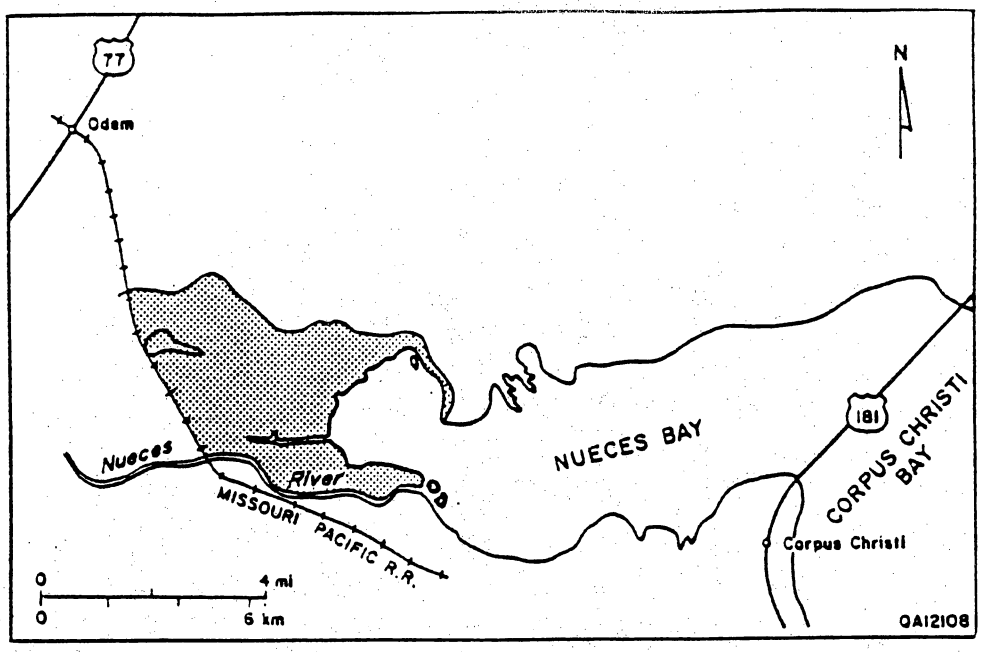


Nueces River delta index map and historical sequence of vegetated areas (in black) for the years 1930, 1959, 1975, and 1979.

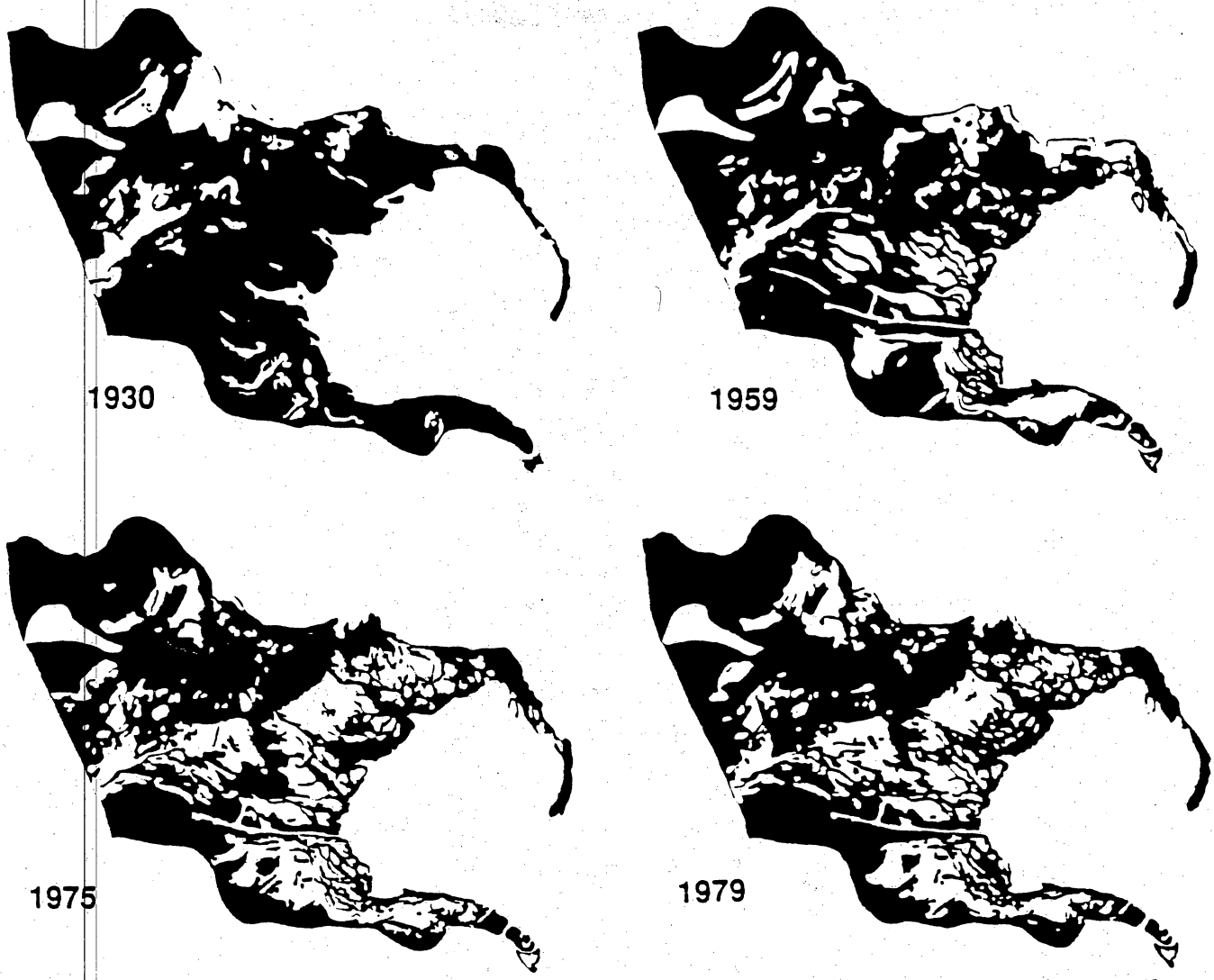


Figure 3. Historical changes in the distribution of vegetated areas (primarily marshes) in the Nueces River delta. From White and Calnan (1990).

# METHODS

## Field Methods

### Site Selection

Eleven sites were selected for coring in the Nueces River alluvial valley (fig. 1). Criteria used in selecting sites included location with respect to the modern Nueces River channel and abandoned channels such as Rincon Bayou; location with respect to the estuarine system, relative elevations, susceptibility to flooding, and types of wetland vegetation; and location with respect to existing human modifications. The approach was to sample several different wetland environments but avoid local human alterations that may have affected sedimentation rates.

Coring sites were located throughout the alluvial valley. Ten sites are located downstream from IH-37 and one is located upstream (fig. 1). Four sites are within 300 m of the river; others are at distances of about 500, 700, and 1,200 m. The remaining four core sites are north of Rincon Bayou at distances of about 200, 400, 800, and 1,900 m from the bayou. One site is near the mouth of the Nueces River at the edge of Nueces Bay, but all other sites are more than 3 km upstream from the bay shoreline, which places them in wetland areas thought to be influenced more by riverine sedimentary processes than by estuarine processes.

### Site Description

Wetland coring sites include salt-water marshes characterized by assemblages of *Spartina alterniflora* and *Salicornia-monanthochloe-Suaeda;* brackish-water marshes characterized by *Spartina spartinae, Borrichia frutescens,* and *Distichlis spicata;* and fresh to brackish assemblages of *Scirpus californicus, Typha, Scirpus maritimus,* and *Eleocharis* (table 1). Estimated elevations range from approximately 1.2 m to less than 0.3 m. Coring sites NR-1 and NR-7 had the highest estimated elevations, and site NR-11 had the lowest (table 1). Sites in high marshes and transitional areas, characterized by *Spartina spartinae* and *Borrichia frutescens,* were generally at higher elevations and were the most difficult to core because of dry soils and increasing stiffness of clay with depth. Low marshes composed

Table 1. Date of collection, core lenths, elevation, and vegetation at Nueces River coring sites.

| Core number | Date cored | Core tube length (cm) | Measured core length (cm) | Estimated elevation (m) | Predominant species | Other species nearby |
|---|---|---|---|---|---|---|
| NR-1 | 4/25/95 | 101.2 | 53.3 | 1.2 | *Spartina spartinae, local eleocharis* | |
| NR-2 | 4/24/95 | 100.9 | 64.5 | 0.6 to 0.9 | *Scirpus Californicus, Typha* sp. | *Distichlis, Borrichia, Batis, Salicornia, Monanthochloe* |
| NR-3 | 4/24/95 | 100.7 | 57 | 0.6 to 0.9 | *Eleocharis* sp. | *Borrichia, Sesbania, Spartina spartinae, Distichlis or Paspalum* |
| NR-4 | 4/25/95 | 101.5 | 48.5 | 0.9 | *Distichlis spicata*, scattered *S. maritimus* | |
| NR-5 | 4/25/95 | 101.5 | 42 | 0.9 to 1.2 | *Salicornia, Monanthochloe*, scattered *Sueada* | |
| NR-6 | 4/25/95 | 100.8 | 39 | 0.9 to 1.2 | *Typha* sp., *Scirpus maritimus* | |
| NR-7 | 4/24/95 | 100.0 | 50.0 | 1.2 | *Spartina spartinae* | |
| NR-8 | 4/26/95 | 100.8 | 76 | 0.9 | *Monanthocloe littoralis* | *Salicornia, Batis* |
| NR-9 | 4/26/95 | 100.7 | 62 | 0.9 | *Monanthochloe, Salicornia* | |
| NR-10 | 4/27/95 | 98.5 | 53.5 | 1.2 | *Borrichia frutescens* | *Saliconia, Spartina spartinae* |
| NR-11 | 4/27/95 | 101.2 | 71 | 0.15 to 0.3 | *Spartina alterniflora* | *Borrichia, Scirpus maritimus* |

predominantly of *Spartina alterniflora, Scirpus californicus, Typha, and Distichlis spicata* were less difficult to core because of softer and less compacted sediments. Sites were cored near the end of April 1995, when soils were very dry. In some cases, alternate sites, rather than those preselected on aerial photographs, were cored because of extremely dry conditions. When possible, cores were taken at sites with no evidence of surface disturbance such as burrows and cattle trails. However, effects of cattle tracks were difficult to avoid in most areas because grazing is widespread inland from the eastern MOPAC crossing.

### Coring Methods

Cores of the marsh substrate were taken by twisting and, where necessary, driving a thin-walled, sharpened metal tube, approximately 1 m long and 11.5 cm in diameter. Lengths of sediment recovered varied depending on the difficulty of penetrating the substrate and the amount of shortening. Some sediment bypassing and thinning occurred in deeper sections of cores where stiff clayey sediments were encountered, especially in transitional area levee-flank environments. Cores were dug out of the marsh soils to minimize loss of material during extraction from the substrate. The end of each core was covered with rubber caps that were tightened down with ring clamps and taped. The cores were transported to the BEG Core Research Center for processing.

### Core Shortening

The volume of unconsolidated sediments normally decreases with depth as a result of physical compaction, dewatering, and loss of organic matter. For some depth-dependent relationships, the natural compaction is taken into account and the data are normalized to equate values near the top of the core with those near the bottom of the core. Physical properties affected by natural compaction, such as water content and bulk density, are used to remove the effect of compaction so that data throughout the core can be compared on a postcompaction basis.

In the wetland literature, few references are made to artificial compaction or thinning of wetland sediments caused by the coring operation. Some reports do not address the issue of artificial compaction, and others give only vague qualitative descriptions such as minor compaction. Few studies actually attempt to quantify the

magnitude of artificial compaction and to adjust those depth-dependent parameters derived from the core.

In this report we distinguish between natural compaction and artificial compaction by referring to artificial compaction as "shortening." Shortening commonly results during coring even if steps are taken to minimize it. Adjusting the stratigraphy of the core to remove the effects of shortening is necessary because any vertical displacement of the cored sediments with respect to their natural position will result in the calculation of inaccurate sedimentation rates. Sedimentation rates calculated from shortened cores will underestimate the actual rates of sedimentation.

Penetration of the core barrel into unconsolidated sediments typically causes some minor shortening of the sediments. The amount of shortening depends on the composition and textures of the sediments, their water content, and other physical properties such as bedding. Some muds are susceptible to high shortening, whereas well-sorted, water-saturated sands are essentially incompressible. The observed shortening can occur in one of two forms. The simplest form of shortening is the physical foreshortening of the sediment column as the water and void space are reduced. For this type of shortening all the strata are represented, and the stratigraphy of the core and surrounding undisturbed sediments is the same except that the strata within the shortened intervals are closer together. The most complex type of shortening involves drag along the core barrel and expulsion of sediment so that some strata are bypassed and are not recovered in the core barrel. This type of shortening can occur where stiff sediments overlie a zone of soft sediment, and the soft sediments are driven aside as the core barrel is shoved into the ground. Drag and bypassing of sediments are observed as distorted strata in the cores. The amount of distortion observed in the core and in the x-radiographs of the core reflects the degree of sediment shortening.

Shortening of each core from the Lavaca River was anticipated because the wetland sediments are composed predominantly of mud. As the core barrel was driven into the ground, the amount of sediment shortening was estimated by periodically measuring the distance to the sediment surface on the outside and inside of the core barrel (fig. 4). By making these two measurements and by knowing the length of the core barrel, total penetration of the core barrel, and core length, the

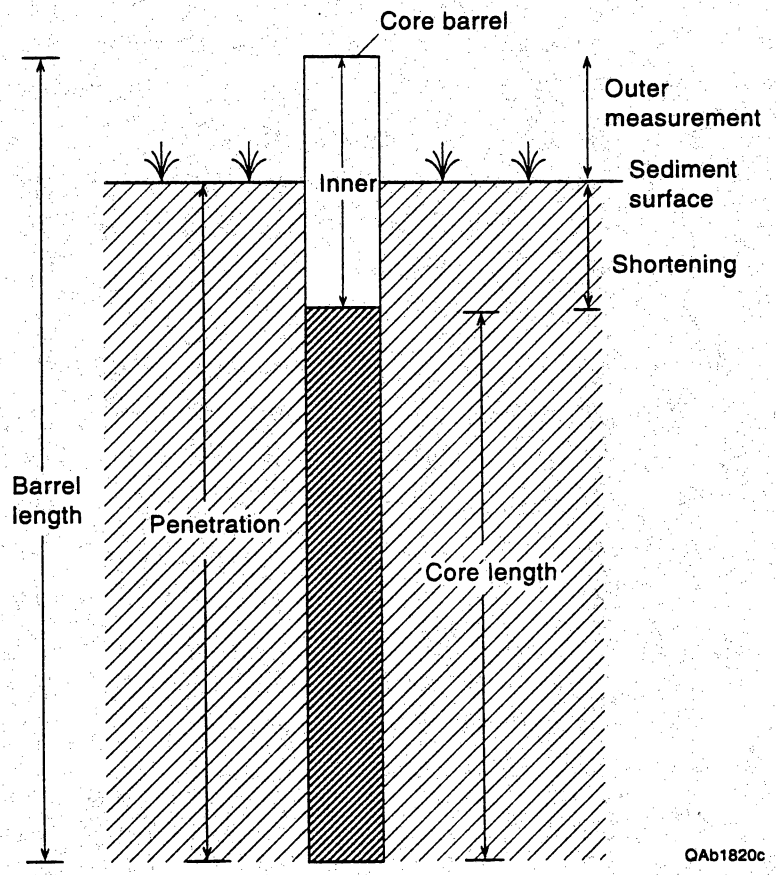


Figure 4. Illustration showing core shortening that may occur during coring.

amount of sediment shortening can be calculated (table 2 and Appendix A). The interval thickness and the amount of shortening for each interval also can be derived from these measurements (table 2) and used to illustrate the percent shortening and the depths at which it occurs. The field measurements and derived data also can be used to reconstruct the interval thickness before shortening and to calculate restored depths that are corrected for shortening (Appendix A). The depth corrections are used to adjust the core depths so that the lengths of the shortened intervals are restored to their unshortened lengths. This is done by calculating the amount of shortening ($C_i$) for each interval (i), calculating the amount of shortening for each one centimeter depth increment in the interval being corrected, and adding the fractional proportion of shortening to each depth increment. This procedure assumes that the shortening is uniformly distributed throughout the interval. The corrected depths have the numerical effect of "stretching" the core to its unshortened length.

The depth correction equation is given by:

$$D_c = P_{i-1} + (D_u - D_{u,i-1})(1+(C_i - C_{i-1})/(D_{u,i} - D_{u,i-1})$$

where

$D_c$ = corrected depth

$D_u$ = uncorrected depth

$C_i = I_i - O_i$ = shortening of interval i

$P_i = O_0 - O_i$ = penetration of interval i

and the uncorrected depth of the lower boundary of the core for which corrections are being made is $D_{u,i} = P_i - C_i$.

Before applying the above equation, the appropriate interval (i) for $D_u$ must be determined so that the proper values for shortening and penetration are used to calculate the correction factor.

Core shortening normally increases with depth, but it is not linear. In fact, the shortening curve for each core is different (Appendix A), and some cores are shortened more in the middle than at the top or the bottom. Although shortening is not linear for the entire core, it is assumed to be linear over the interval being corrected. This assumption is necessary because we do not have any information that would permit a more accurate correction.

Table 2. Total shortening and penetration of Nueces River cores and percent shortening calculated for each interval.

| Core interval i | Outer reading Oi (cm) | Inner reading Ii (cm) | Total shortening Ci | Total penetration Pi | Depth of shortened interval (Du,i) | Interval shortening % |
|---|---|---|---|---|---|---|
| | | | **NR-1** | | | |
| 0 | 101.0 | 101.0 | 0.0 | 0.0 | 0.0 | 0.0 |
| 1 | 80.5 | 80.5 | 0.0 | 20.5 | 20.5 | 0.0 |
| 2 | 69.4 | 69.6 | 0.2 | 31.6 | 31.4 | 1.8 |
| 3 | 59.8 | 60.0 | 0.2 | 41.2 | 41.0 | 0.0 |
| 4 | 57.2 | 57.4 | 0.2 | 43.8 | 43.6 | 0.0 |
| 5 | 52.6 | 53.0 | 0.4 | 48.4 | 48.0 | 4.3 |
| 6 | 49.6 | 50.0 | 0.4 | 51.4 | 51.0 | 0.0 |
| 7 | 47.0 | 47.6 | 0.6 | 54.0 | 53.4 | 7.7 |
| | | | **NR-2** | | | |
| 0 | 100.9 | 100.9 | 0.0 | 0.0 | 0.0 | 0.0 |
| 1 | 83.8 | 83.8 | 0.0 | 17.1 | 17.1 | 0.0 |
| 2 | 78.2 | 78.2 | 0.0 | 22.7 | 22.7 | 0.0 |
| 3 | 73.8 | 74.0 | 0.2 | 27.1 | 26.9 | 4.5 |
| 4 | 71.8 | 72.0 | 0.2 | 29.1 | 28.9 | 0.0 |
| 5 | 62.8 | 63.0 | 0.2 | 38.1 | 37.9 | 0.0 |
| 6 | 58.0 | 60.0 | 2.0 | 42.9 | 40.9 | 37.5 |
| 7 | 56.2 | 58.4 | 2.2 | 44.7 | 42.5 | 11.1 |
| 8 | 52.4 | 54.8 | 2.4 | 48.5 | 46.1 | 5.3 |
| 9 | 44.8 | 47.4 | 2.6 | 56.1 | 53.5 | 2.6 |
| 10 | 43.8 | 46.4 | 2.6 | 57.1 | 54.5 | 0.0 |
| 11 | 40.0 | 42.6 | 2.6 | 60.9 | 58.3 | 0.0 |
| 12 | 36.4 | 39.0 | 2.6 | 64.5 | 61.9 | 0.0 |
| 13 | 32.8 | 35.8 | 3.0 | 68.1 | 65.1 | 11.1 |
| | | | **NR-3** | | | |
| 0 | 100.7 | 100.7 | 0.0 | 0.0 | 0.0 | 0.0 |
| 1 | 89.6 | 90.0 | 0.4 | 11.1 | 10.7 | 3.6 |
| 2 | 76.0 | 76.4 | 0.4 | 24.7 | 24.3 | 0.0 |
| 3 | 64.2 | 64.6 | 0.4 | 36.5 | 36.1 | 0.0 |
| 4 | 59.6 | 60.0 | 0.4 | 41.1 | 40.7 | 0.0 |
| 5 | 51.8 | 52.2 | 0.4 | 48.9 | 48.5 | 0.0 |
| 6 | 49.4 | 49.8 | 0.4 | 51.3 | 50.9 | 0.0 |
| 7 | 45.0 | 46.0 | 1.0 | 55.7 | 54.7 | 13.6 |
| 8 | 41.0 | 42.6 | 1.6 | 59.7 | 58.1 | 15.0 |

Table 2 (cont.)

| Core interval i | Outer reading Oi (cm) | Inner reading Ii (cm) | Total shortening Ci | Total penetration Pi | Depth of shortened interval (Du,i) | Interval shortening % |
|---|---|---|---|---|---|---|
| | | | **NR-4** | | | |
| 0 | 101.0 | 101.0 | 0.0 | 0.0 | 0.0 | 0.0 |
| 1 | 87.0 | 87.0 | 0.0 | 14.0 | 14.0 | 0.0 |
| 2 | 80.0 | 80.0 | 0.0 | 21.0 | 21.0 | 0.0 |
| 3 | 74.8 | 75.0* | 0.2 | 26.2 | 26.0 | 3.8 |
| 4 | 70.2 | 70.4* | 0.2 | 30.8 | 30.6 | 0.0 |
| 5 | 54.0 | 54.2 | 0.2 | 47.0 | 46.8 | 0.0 |
| 6 | 51.6 | 51.8 | 0.2 | 49.4 | 49.2 | 0.0 |
| 7 | 46.0 | 46.2 | 0.2 | 55.0 | 54.8 | 0.0 |
| 8 | 42.4 | 42.6 | 0.2 | 58.6 | 58.4 | 0.0 |
| 9 | 39.4 | 40.2 | 0.8 | 61.6 | 60.8 | 20.0 |

*Field data modified to avoid negative numbers.

| | | | | | | |
|---|---|---|---|---|---|---|
| | | | **NR-5** | | | |
| 0 | 101.2 | 101.2 | 0.0 | 0.0 | 0.0 | 0.0 |
| 1 | 87.8 | 88.2 | 0.4 | 13.4 | 13.0 | 3.0 |
| 2 | 82.0 | 82.4* | 0.4 | 19.2 | 18.8 | 0.0 |
| 3 | 72.4 | 72.8* | 0.4 | 28.8 | 28.4 | 0.0 |
| 4 | 66.6 | 67.0 | 0.4 | 34.6 | 34.2 | 0.0 |
| 5 | 63.2 | 63.8 | 0.6 | 38.0 | 37.4 | 5.9 |
| 6 | 61.0 | 62.6 | 1.6 | 40.2 | 38.6 | 45.5 |
| 7 | 58.6 | 60.2 | 1.6 | 42.6 | 41.0 | 0.0 |
| 8 | 56.6 | 58.2 | 1.6 | 44.6 | 43.0 | 0.0 |

*Field data modified to avoid negative numbers.

| | | | | | | |
|---|---|---|---|---|---|---|
| | | | **NR-6** | | | |
| 0 | 100.4 | 100.4 | 0.0 | 0.0 | 0.0 | 0.0 |
| 1 | 81.0 | 81.0 | 0.0 | 19.4 | 19.4 | 0.0 |
| 2 | 76.0 | 76.0 | 0.0 | 24.4 | 24.4 | 0.0 |
| 3 | 72.8 | 73.0 | 0.2 | 27.6 | 27.4 | 6.3 |
| 4 | 70.6 | 70.8 | 0.2 | 29.8 | 29.6 | 0.0 |
| 5 | 65.0 | 68.0 | 3.0 | 35.4 | 32.4 | 50.0 |
| 6 | 57.0 | 63.0 | 6.0 | 43.4 | 37.4 | 37.5 |
| 7 | 52.0 | 61.6 | 9.6 | 48.4 | 38.8 | 72.0 |
| | | | **NR-7** | | | |
| 0 | 100.0 | 100.0 | 0.0 | 0.0 | 0.0 | 0.0 |
| 1 | 86.0 | 86.0 | 0.0 | 14.0 | 14.0 | 0.0 |
| 2 | 81.0 | 81.0 | 0.0 | 19.0 | 19.0 | 0.0 |
| 3 | 79.8 | 79.8 | 0.0 | 20.2 | 20.2 | 0.0 |
| 4 | 71.8 | 71.8 | 0.0 | 28.2 | 28.2 | 0.0 |
| 5 | 66.6 | 66.6 | 0.0 | 33.4 | 33.4 | 0.0 |
| 6 | 60.4 | 60.4 | 0.0 | 39.6 | 39.6 | 0.0 |

Table 2 (cont.)

| Core interval i | Outer reading Oi (cm) | Inner reading Ii (cm) | Total shortening Ci | Total penetration Pi | Depth of shortened interval (Du,i) | Interval shortening % |
|---|---|---|---|---|---|---|
| 7 | 55.6 | 55.6 | 0.0 | 44.4 | 44.4 | 0.0 |
| 8 | 51.2 | 51.4 | 0.2 | 48.8 | 48.6 | 4.5 |
| 9 | 48.2 | 49.4 | 1.2 | 51.8 | 50.6 | 33.3 |
| | | | **NR-8** | | | |
| 0 | 100.6 | 100.6 | 0.0 | 0.0 | 0.0 | 0.0 |
| 1 | 89.0 | 89.0* | 0.0 | 11.6 | 11.6 | 0.0 |
| 2 | 82.8 | 82.8 | 0.0 | 17.8 | 17.8 | 0.0 |
| 3 | 77.8 | 78.0 | 0.2 | 22.8 | 22.6 | 4.0 |
| 4 | 58.6 | 59.0 | 0.4 | 42.0 | 41.6 | 1.0 |
| 5 | 44.8 | 45.6 | 0.8 | 55.8 | 55.0 | 2.9 |
| 6 | 31.4 | 32.8 | 1.4 | 69.2 | 67.8 | 4.5 |
| 7 | 20.0 | 22.0 | 2.0 | 80.6 | 78.6 | 5.3 |
| | | | **NR-9** | | | |
| 0 | 100.3 | 100.3 | 0.0 | 0.0 | 0.0 | 0.0 |
| 1 | 87.5 | 87.5 | 0.0 | 12.8 | 12.8 | 0.0 |
| 2 | 83.6 | 83.6 | 0.0 | 16.7 | 16.7 | 0.0 |
| 3 | 72.0 | 72.0 | 0.0 | 28.3 | 28.3 | 0.0 |
| 4 | 62.0 | 62.0 | 0.0 | 38.3 | 38.3 | 0.0 |
| 5 | 53.5 | 53.5 | 0.0 | 46.8 | 46.8 | 0.0 |
| 6 | 44.5 | 44.5 | 0.0 | 55.8 | 55.8 | 0.0 |
| 7 | 37.0 | 38.0 | 1.0 | 63.3 | 62.3 | 13.3 |
| | | | **NR-10** | | | |
| 0 | 98.5 | 98.5 | 0.0 | 0.0 | 0.0 | 0.0 |
| 1 | 79.0 | 79.0 | 0.0 | 19.5 | 19.5 | 0.0 |
| 2 | 74.0 | 74.0 | 0.0 | 24.5 | 24.5 | 0.0 |
| 3 | 61.0 | 61.0 | 0.0 | 37.5 | 37.5 | 0.0 |
| 4 | 55.0 | 55.0 | 0.0 | 43.5 | 43.5 | 0.0 |
| 5 | 49.5 | 50.5 | 1.0 | 49.0 | 48.0 | 18.2 |
| 6 | 45.0 | 47.0 | 2.0 | 53.5 | 51.5 | 22.2 |
| 7 | 42.0 | 45.0 | 3.0 | 56.5 | 53.5 | 33.3 |
| | | | **NR-11** | | | |
| 0 | 101.2 | 101.2 | 0.0 | 0.0 | 0.0 | 0.0 |
| 1 | 79.5 | 79.5 | 0.0 | 21.7 | 21.7 | 0.0 |
| 2 | 67.0 | 67.5 | 0.5 | 34.2 | 33.7 | 4.0 |
| 3 | 58.0 | 60.0 | 2.0 | 43.2 | 41.2 | 16.7 |
| 4 | 51.0 | 53.0 | 2.0 | 50.2 | 48.2 | 0.0 |
| 5 | 42.5 | 44.5 | 2.0 | 58.7 | 56.7 | 0.0 |
| 6 | 36.5 | 38.5 | 2.0 | 64.7 | 62.7 | 0.0 |
| 7 | 32.5 | 34.5 | 2.0 | 68.7 | 66.7 | 0.0 |
| 8 | 28.0 | 30.0 | 2.0 | 73.2 | 71.2 | 0.0 |

*Field data modified to avoid negative numbers.

Most cores from the Nueces River system underwent some shortening, and most of the cores are shortened from 1 to 2 cm (table 2 and Appendix A). Core 1 is the least shortened (0.6 cm), whereas core 6 is the most shortened (9.6 cm). Most of the shortening in core 6 occurred below 30 cm. Core lengths estimated from the shortening and penetration measurements generally agree within 1 cm of the actual core length. Larger discrepancies between the depth of penetration and the length of core recovered suggest that some of the sediment dropped out of the end of the core barrel as it was being retrieved.

## Laboratory Methods

### Core Preparation and Handling

Cores were split in half by first cutting horizontally down each side of the metal tube and then by cutting the core in half with a thin wire or band saw. The top section of each core, and in several cases the entire core, was cut with a fine-toothed band saw to limit disturbance of the root-matted zone. The two half cores were then separated, each half retained in the half tube. One half of the core was wrapped in plastic, sealed in an airtight clear plastic liner, and transported to the USGS laboratory in Denver for x-radiography and analysis of $^{210}Pb$ and $^{226}Ra$ activity, moisture content, loss on ignition, bulk density, and texture.

The other halves of the cores were archived and retained in the BEG Core Research Center where they were subsampled for other physical and chemical analysis. Immediately after the cores were split, a measured volume of material was collected from near the top, middle, and bottom of each core for analysis of moisture content, chlorinity, and bulk density.

Each half core was trimmed with an osmotic knife and physically described. Information recorded on core description sheets included core depth, sediment color, sediment type (visual description), nature of contacts, textural trends, sedimentary structures, state of oxidation, and presence of accessories (organic material and caliche nodules). The cores were then photographed to produce large-format color prints and 35-mm slides.

When not in use, the archived core halves were covered with plastic wrap, placed in labeled boxes, and stored in a climate-controlled room. The archived core half serves as a permanent record of the sediment types encountered and the types of material sampled for textural and geochemical analyses.

## Analytical Methods

**$^{210}$Pb Analysis.** Isotopic analysis of cores (Appendix B) was completed under the supervision of Dr. Charles Holmes of the U.S. Geological Survey using procedures developed by the USGS (Holmes and Martin, 1976; Martin and Rice, 1981), which is a modified version of that described by Flynn (1968) (Appendix C). The specific activity of $^{210}$Pb was measured indirectly by determining the activity of the granddaughter isotope $^{210}$Po. Samples were analyzed at 1-cm intervals down to a depth of 20 to 21 cm, below which analyses were at 2-cm intervals. Samples were separated by textural composition before isotopic analysis. Only the mud fractions (silt and clay, or particles <62 μm in size) were used in the $^{210}$Pb analyses.

**$^{226}$Ra Analysis.** Isotopic analysis of $^{226}$Ra, which is the source of supported $^{210}$Pb, was completed under the supervision of Dr. Charles Holmes at the USGS. A representative sample was ground and placed in a counting cup. The cup was placed in a high-resolution planar gamma-ray detector (germanium, lithium-drifted) from which a spectrum was accumulated for 24 h. The resulting value was compared to a standard of known value and reported as disintegrations per minute per gram (dpm/g). The activity of $^{226}$Ra was determined by analysis of $^{214}$Bi, which has a strong gamma emission and is easy to measure. $^{214}$Bi is one of several short-lived intermediate daughters of $^{226}$Ra and is assumed to be in equilibrium with it (fig. 5) (Dr. Charles Holmes, personal communication, 1995). This relationship between $^{226}$Ra and $^{214}$Bi is also reported by Appleby and others (1988) and Brenner and others (1994).

The isotope $^{214}$Bi is one of several short-lived intermediate daughters of $^{226}$Ra; these daughters decay in a matter of minutes into $^{210}$Pb (fig. 5). $^{226}$Ra occurs in minerals in the sediments and is the source of the supported $^{210}$Pb through the decay chain, including $^{222}$Rn, shown in figure 5. The source of the "excess," or unsupported, $^{210}$Pb is from $^{222}$Rn that has outgassed into the atmosphere from multiple source areas (Robbins, 1978). Although there may be some "leakage" of

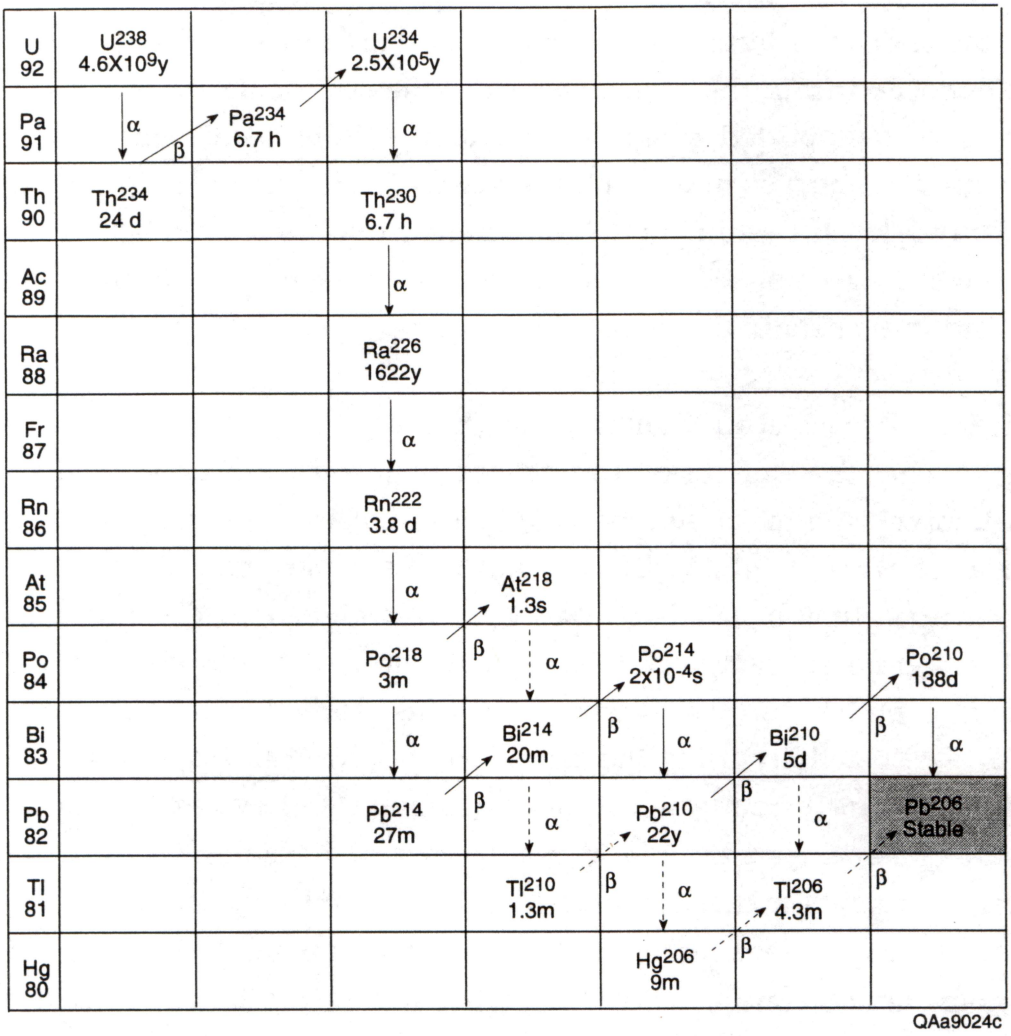


Figure 5. Relationship between various isotopic elements including $^{226}Ra$, $^{214}Bi$, and $^{210}Pb$. Solid arrows indicate major decay modes. From Robbins (1978).

$^{222}Rn$ into the atmosphere from the sediments measured in cores, it is apparently insignificant relative to the entire system. Atmospheric $^{222}Rn$ decays (as it does in the sediments) through the intermediate daughters including $^{214}Bi$ (fig. 5), but because of the short half-lives of these isotopes relative to $^{210}Pb$, only the $^{210}Pb$ is effectively deposited from the atmosphere into the sediments, where it constitutes the "excess" or unsupported component of total $^{210}Pb$. $^{214}Bi$ from atmospheric $^{222}Rn$ does not become a significant part of the sediment and, thus, is not part of the $^{214}Bi$ measured in the sediment to determine supported $^{210}Pb$. A total of 44 samples were analyzed for $^{226}Ra$; results are presented in the "Results" section of this report and in Appendix B.

**Bulk Density, Moisture Content, and Organic Matter (USGS).** Samples were collected by slicing the half core (of measured diameter) into 1- or 2-cm wafers to produce a known volume of sediment for bulk density measurements. The wet sediment wafers were weighed, divided into two samples, one of which was then dried at a temperature of 60°C for 24 h, and reweighed to determine moisture content. The second subsample was separated into its textural components (sand, silt, and clay) as outlined in the "Textural Analysis" section. The mud fraction was analyzed for $^{210}Pb$ activity using the procedure described in Appendix C. Organic content was determined from weight loss-on-ignition (LOI) by heating the sample to a temperature of 450°C for 6 to 12 h. Wet and dry bulk densities, water content, LOI, and mineral (inorganic) matter are presented in Appendix B. It was assumed that sediments in the cores were carbonate free, but four cores (NR-4, NR-5, NR-7, and NR-10) contain minor concentrations of carbonates in the form of small nodules and tiny fragments of $CaCO_3$, which are most abundant in the lower half of the cores.

**Bulk Density (BEG).** A measured volume of sediment was obtained by subsampling each half core with a cork borer of known diameter (1.17 cm), and measuring the thickness of the half core, usually about 5 cm. Lengths were based on the thickness of the half core rather than the removed sample plug because of shortening of the plug when it was collected. Three subsamples were taken from each core near the top, middle, and bottom. The subsamples were placed in pre-weighed containers, weighed, then dried at 105°C to constant weight. A total of 33 subsamples were analyzed. From these data, dry bulk density and moisture content were determined (Appendix D).

**Textural Analysis.** All samples were analyzed for textural composition by the USGS following procedures detailed by Starkey and others (1984). Disaggregated samples were wet sieved through a 230-mesh sieve to separate particles larger than sand size, >62 μm (which included sand, caliche nodules, and gross organics), from silt and clay. The silt and clay fractions were separated by centrifugation, which is essentially a settling technique that operates according to Stoke's law.

**Salinity (Chlorinity) (BEG).** For sediments with a high salt content, excess $^{210}Pb$ activities should be determined on a salt-free basis (Church and others, 1981). Total chloride was measured by ion chromatography following BEG procedures (Specific Work Instruction 1.15: Determination of anions by ion chromatography). Three samples from each core (top, middle, and bottom) were analyzed. Chlorinity was converted to salinity using a factor of 1.80655 (Duxbury, 1971).

## RESULTS

Results of the $^{210}Pb$ analysis are presented in Appendix B along with measurements of $^{226}Ra$ activity, water content, loss on ignition, mineral matter, wet bulk density, and dry bulk density. Bulk density was determined for each sample by the USGS. A few samples from each core were also analyzed for bulk density by BEG. In general, bulk densities measured by the USGS were higher by an average of about 1.5 times than those determined by BEG. The reason for this difference is not clear, but may be related to the variation in methods used to take subsamples of the cores (see "Methods" section). Because USGS measurements were made on every sample that was analyzed for $^{210}Pb$, the USGS bulk densities provide the most complete data for analyzing cumulative inorganic mass and for determining dates and sedimentation rates.

### $^{210}Pb$ Activity Profiles

The objective of this investigation was to determine sedimentation rates based on $^{210}Pb$ activity. Accordingly, results of other physical and chemical analyses are discussed primarily in terms of their influence on or relationship with the distribution of $^{210}Pb$ activity within a core. $^{210}Pb$ activity profiles were completed

for each core and examined carefully to determine trends and probable causes for variations in trends.

### Variations in $^{210}Pb$ and Probable Causes

Plots of $^{210}Pb$ activity against depth indicate some scatter and local variations from linear trends for some cores. However, the amount of scatter in Nueces River cores is much less than that found in Lavaca-Navidad River cores (White and Morton, 1995). This reduction in the amount of scatter is attributed to a change in procedures in which only the fine fraction (mud) was analyzed for $^{210}Pb$ activity. Fluctuations in $^{210}Pb$ activity in the Lavaca-Navidad River cores were caused partly by variations in sand content in the analyzed samples. Pronounced variations in slope of the plots should define variations in sedimentation rates, which can be correlated with sediment deposition by the Nueces River. But local variations in excess $^{210}Pb$ activity involving individual samples or a few samples are not fully understood. Some are apparently related to bioturbation and organic properties, presence of carbonates, and other changes in sediment chemistry, and some are possibly due to radioactivity counting errors.

**Bioturbation.** According to some researchers, for example Nittrouer and others (1979), the relatively uniform $^{210}Pb$ activity in near surface layers of some cores indicates a zone of bioturbation and mixing of sediments (fig. 6). In most Nueces River cores, distinct evidence of bioturbation was not apparent in either X-rays or dressed and described cores. Below the root zones, cores are homogeneous in appearance and profiles of total $^{210}Pb$ against depth show that activities generally decline in a relatively linear fashion to depths of about 5 to 20 cm, below which there is a flattening of the profile for most cores. We believe that the flattening occurs as background or supported $^{210}Pb$ levels are approached and reached at depth. Varying from this general trend is core NR-10, which is nonlinear in the upper 15 cm. The nonlinearity may be a result of bioturbation, physical mixing, variations in organic matter or erosion and deposition during flood events. The specific reason for the "saw-tooth" nature of the $^{210}Pb$ profile is not totally clear, but may be related to variations in deposition. This site appears to be one of the first sites inundated during floods along the Nueces River.

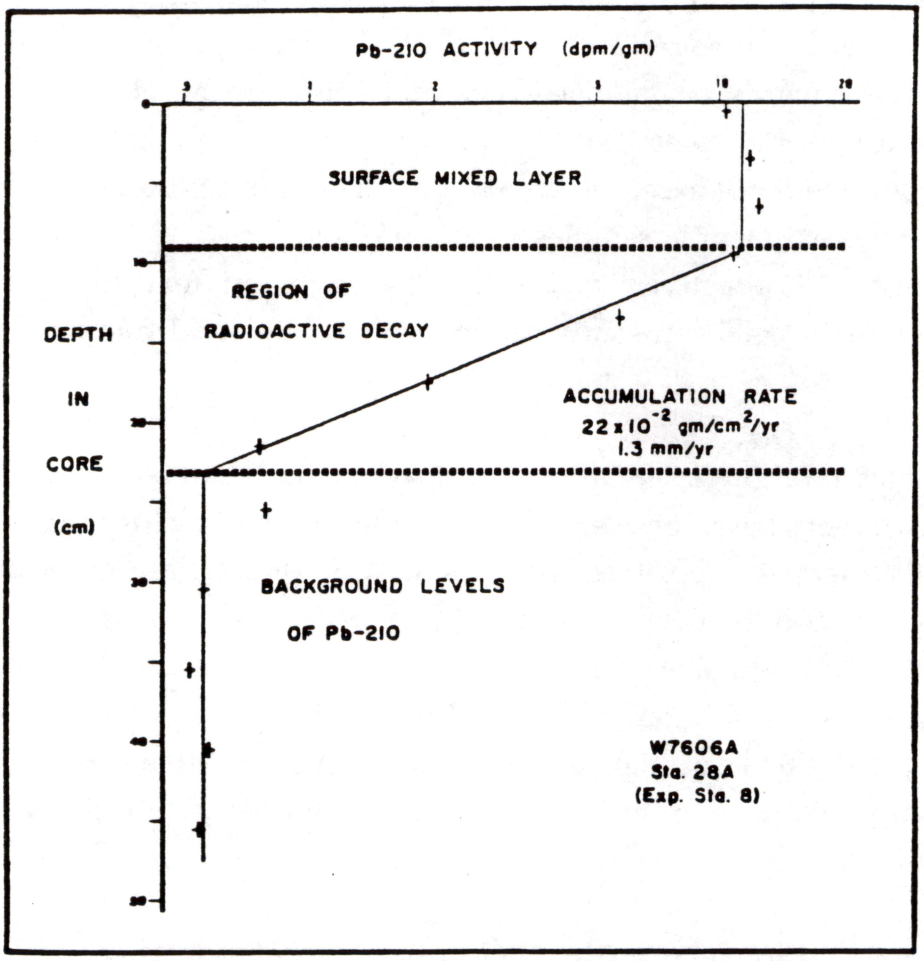


Figure 6. Profile of $^{210}Pb$ activity of a sediment core from the Washington continental shelf showing the mixed surface layer. Bioturbation in marsh surface layers can produce similar "flat" activities. From Nittrouer and others (1979).

**Texture.** Textural variations can influence excess $^{210}Pb$ activity (fig. 7). Activity levels are higher in finer sediments, apparently because Pb, like many other metals, is sequestered by fine-grained particles such as clay minerals, organic matter, and Fe-Mn oxides (Nittrouer and others, 1979). Sediment in cores taken in this study consists primarily of homogeneous mud (silt and clay), but sand was higher than expected in some cores. Still, sand is a minor constituent overall (less than 20 percent) (Appendix B) except in core NR-9 where it composes, on average, almost 40 percent of the sediment in samples analyzed (fig. 8).

Because $^{210}Pb$ activity is affected by sediment texture, exemplified by depressed $^{210}Pb$ activities in sandy sediments, only the mud fraction was analyzed for $^{210}Pb$.

**Organics (Weight Loss-On-Ignition).** The association between $^{210}Pb$ activity and organic content, based on weight loss-on-ignition (LOI), varies from core to core, but generally there is a positive correlation. Correlations are especially high for some cores when only the top sections are considered and when one or two anomalous values are excluded. Under these conditions the square of the correlation coefficient ($R^2$) ranged from 0.746 to 0.945 in eight of the cores, and six of the cores had $R^2$ of 0.818 or higher. Two of the highest positive correlations between LOI and total $^{210}Pb$ were in cores NR-1 (fig. 9) and NR-6 (fig. 10). The cores with the lowest correlations were NR-2 and NR-9.

**Calcium Carbonate (Caliche Nodules).** Caliche nodules can influence $^{210}Pb$ activity. Fortunately, large nodules (1–2 cm in diameter) were not found in Nueces River cores. Analysis of nodules from Trinity River cores (White and Morton, 1993) indicated that they can be "hot spots" where $^{210}Pb$ activity is substantially higher than in surrounding sediments (Dr. Charles Holmes, personal communication, 1993). In Nueces River cores, calcium carbonate specks were observed in the lower portions of a few cores, but there is no obvious evidence that $^{210}Pb$ activity was affected. Carbonates of sand size or larger would have been separated from the mud fraction before analysis of $^{210}Pb$.

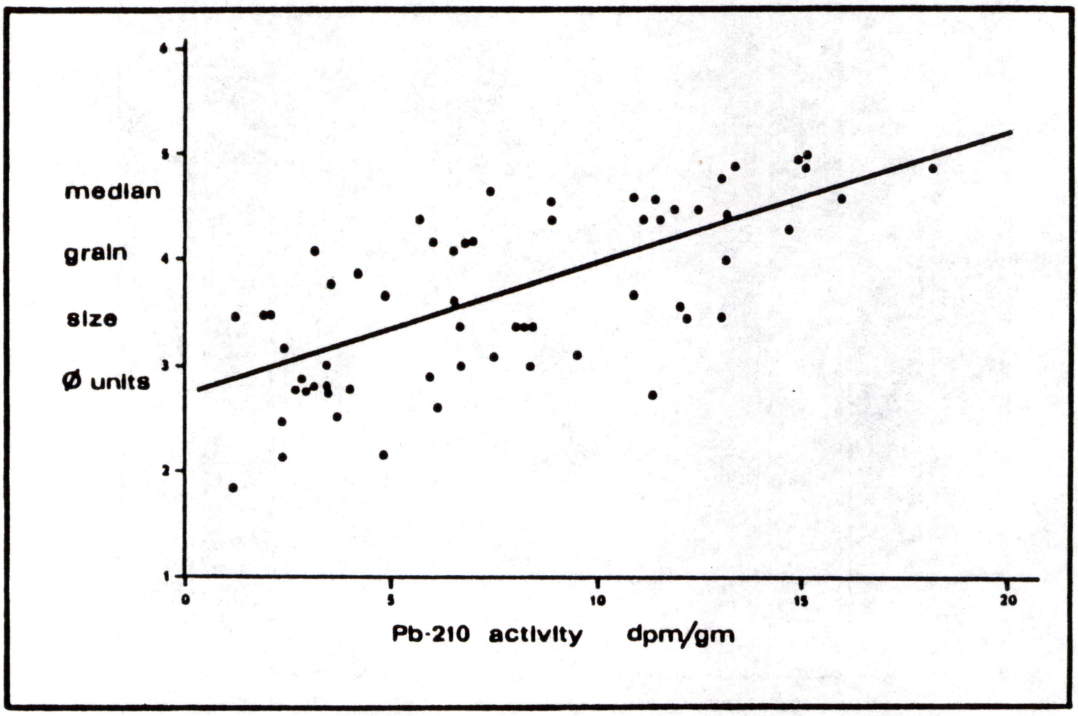


Figure 7. Relationship between grain size and initial $^{210}Pb$ activity. From Nittrouer and others (1979).

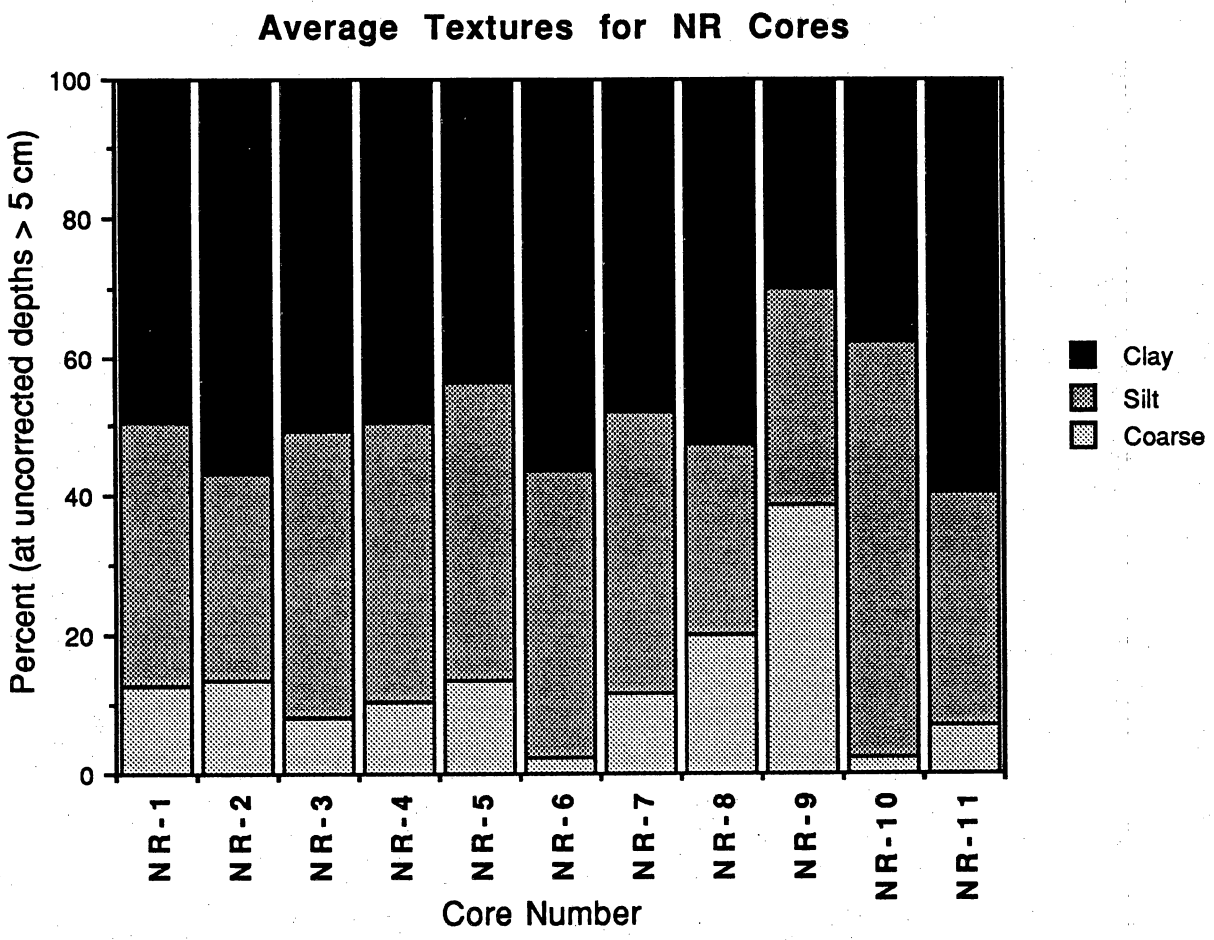


Figure 8. Average percentages of clay, silt, and coarse textures in Nueces River cores.

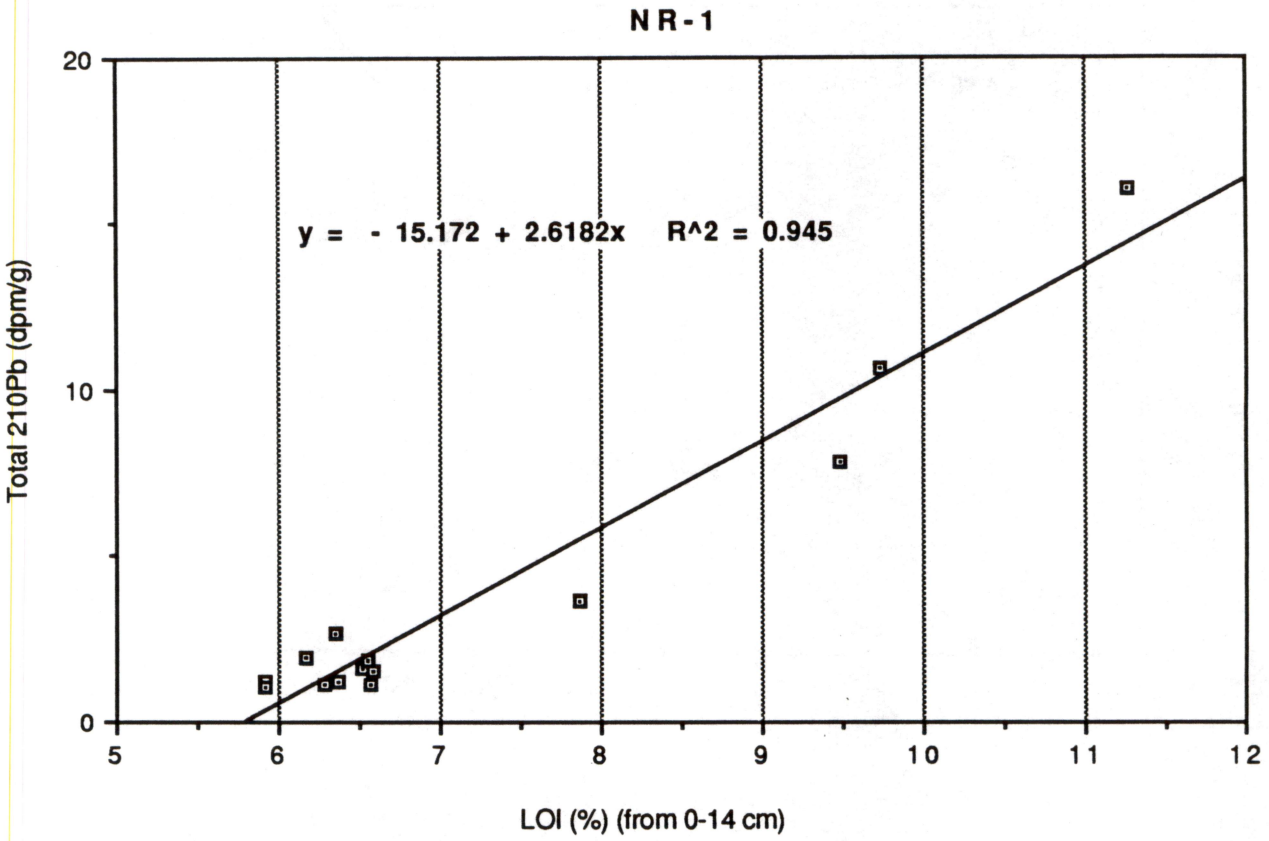


Figure 9. Correlation between percent LOI and total $^{210}Pb$ activity in core NR-1.

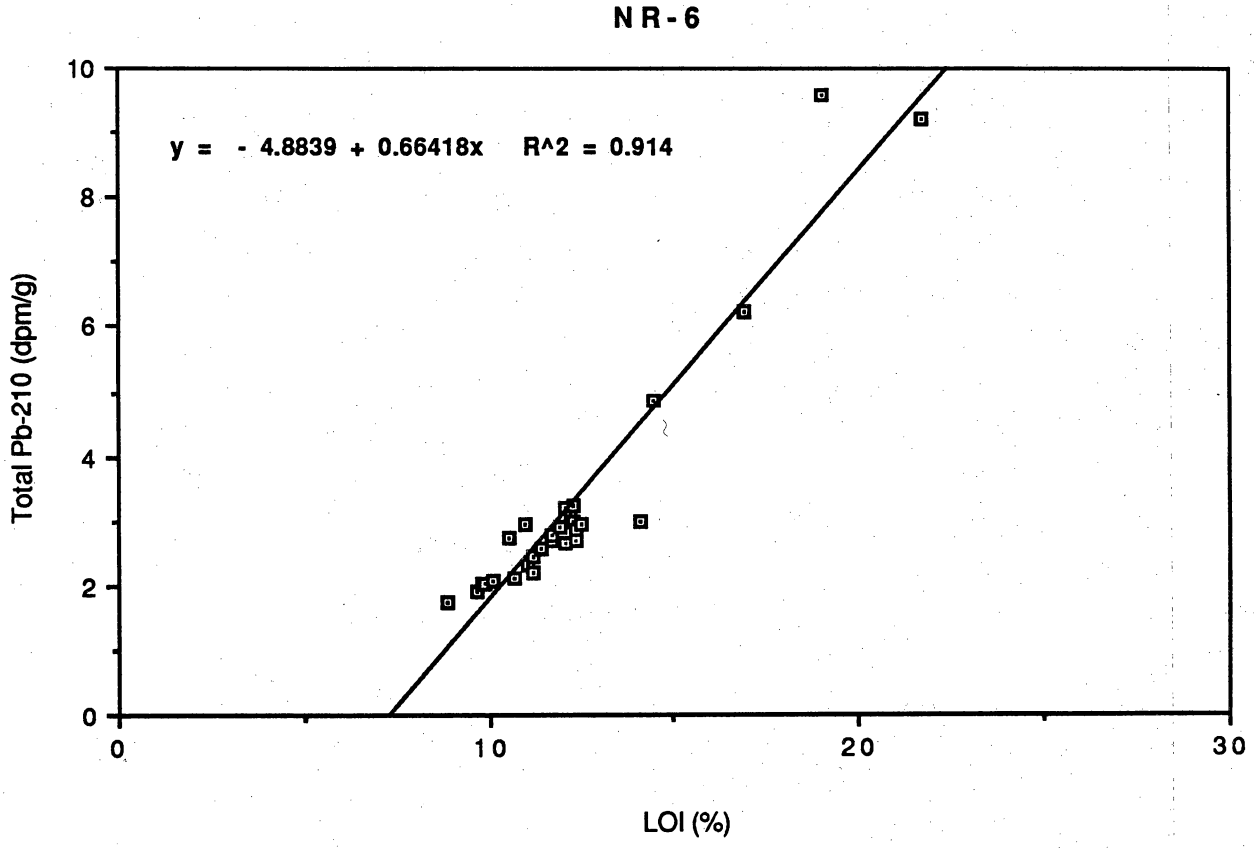


Figure 10. Correlation between percent LOI and total $^{210}Pb$ activity in core NR-6.

**Salinity**. Results show that sediments at three core sites, NR-5, NR-8, and NR-9, are the most saline, each exceeding 20,000 ppm (fig. 11). The high salinities in these three cores was expected because they were taken in vegetated "salt" flats where plant species with a high salt tolerance are the dominant vegetation (table 1). The deepest subsample from NR-10 also exceeded 20,000 ppm, which was not expected because the dominant vegetation at the surface was *Borrichia frutescens*. The two sites with the lowest salinities are NR-1 and NR-6. Vegetation at each of these sites indicated low salinities, especially at NR-6, where *Typha* sp. was dominant (table 1). The high salinities at several of the cores suggest that $^{210}Pb$ should be determined on a salt-free basis for those cores to evaluate whether sedimentation rates are significantly altered.

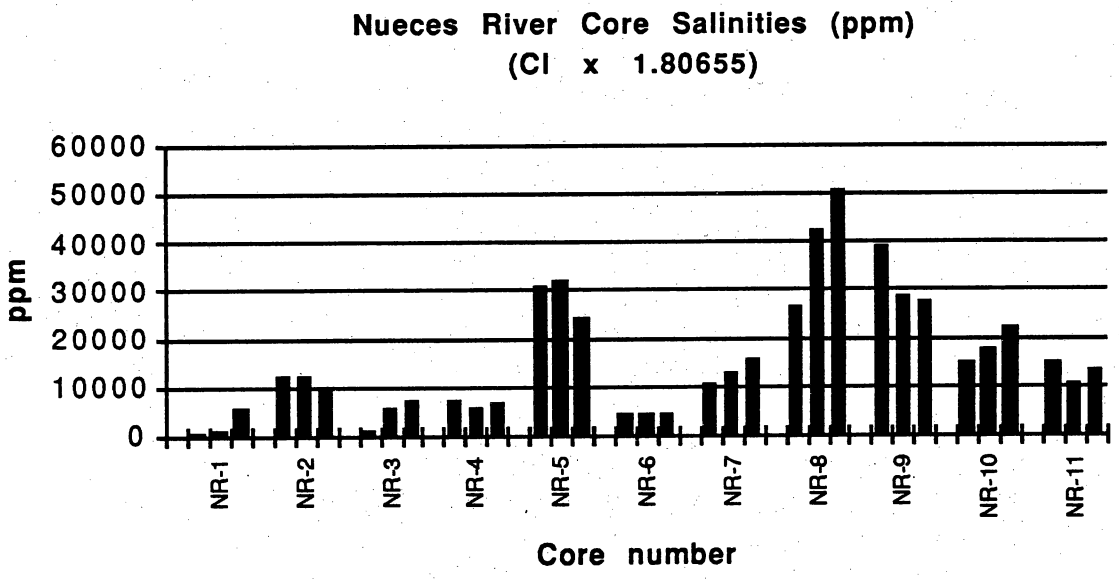


Figure 11. Salinities of sediments subsampled from cores taken in the Nueces River delta and alluvial valley.

Table 3. Salinity of samples analyzed in cores.

| Location/ depth (cm) | Cl (mg/kg @105°C) | Salinity (ppm) (Cl × 1.80655) |
|---|---|---|
| NRD1/ 5 | 297 | 536 |
| NRD1/23 | 519 | 938 |
| NRD1/50 | 2,967 | 5,359 |
| NRD2/ 5 | 6,803 | 12,290 |
| NRD2/35 | 6,639 | 11,994 |
| NRD2/62 | 5,347 | 9,660 |
| NRD3/ 5 | 606 | 1,095 |
| NRD3/33 | 2,885 | 5,211 |
| NRD3/54 | 4,077 | 7,366 |
| NRD4 / 5 | 4,044 | 7,306 |
| NRD4 /25 | 3,087 | 5,577 |
| NRD4 /45 | 3,479 | 6,284 |
| NRD5/ 5 | 17,001 | 30,714 |
| NRD5/24 | 17,708 | 31,990 |
| NRD5/39 | 13,249 | 23,935 |
| NRD6/11 | 2,450 | 4,426 |
| NRD6/22 | 2,315 | 4,181 |
| NRD6/36 | 2,306 | 4,166 |
| NRD7/11 | 5,645 | 10,198 |
| NRD7/25 | 6,855 | 12,384 |
| NRD7/44 | 8,526 | 15,403 |
| NRD8/12 | 14,647 | 26,460 |
| NRD8/42 | 23,311 | 42,112 |
| NRD8/72 | 28,067 | 50,704 |
| NRD9/ 5 | 21,663 | 39,135 |
| NRD9/32 | 15,870 | 28,670 |
| NRD9/59 | 15,216 | 27,489 |
| NRD10/10 | 8,298 | 14,991 |
| NRD10/27 | 9,753 | 17,620 |
| NRD10/48 | 12,209 | 22,055 |
| NRD11/28 | 8,335 | 15,058 |
| NRD11/62 | 5,691 | 10,281 |
| NRD11/67 | 7,256 | 13,109 |

**Visible Physical and Chemical Variations.** Most cores in the Nueces River system were homogeneous in appearance. Variations in appearance occurred in the upper 5–10 cm of most cores where plant roots were abundant. Changes in color generally occurred in deeper portions of the cores, but the color changes did not correspond to changes in $^{210}Pb$ activities, which were relative "flat" indicating background, or supported, $^{210}Pb$ levels had been reached. There was little evidence of oxidation in any of the cores. In contrast, almost all cores from the Trinity River system showed evidence of oxidation in the upper halves of the cores.

**Accuracy of Analysis at Low $^{210}Pb$ Concentrations.** Some fluctuations in $^{210}Pb$ activity in the lower part of a core may be a result of low concentrations of $^{210}Pb$ as background levels are approached. According to Dr. Charles Holmes (USGS), the analytical variance (error bar) for samples with activities below approximately 0.5 dpm/g is larger than for samples with higher concentrations. Therefore some of the sample to sample variations are simply related to counting errors.

## Determination of Excess (Unsupported) $^{210}Pb$

**$^{226}Ra$.** One method used by researchers to determine supported $^{210}Pb$ activities is to analyze $^{226}Ra$ from which supported $^{210}Pb$ is derived and with which it is assumed to be in equilibrium (see "Analytical Methods" section). In some settings, however, $^{226}Ra$ may be unusable because of possible disequilibrium between $^{226}Ra$ and $^{210}Pb$ (Brenner and others, 1994). Still, in many coastal settings $^{226}Ra$ has been used to estimate supported $^{210}Pb$. The USGS analyzed $^{226}Ra$ in a selected number of samples in all cores (Appendix B). Averages in cores varied from 0.87 to 1.57 dpm/g (table 4).

Table 4. Average activities of $^{226}Ra$ in selected sediment samples from Nueces River cores.

| Core no. | Average $^{226}Ra$ (dpm/g) | Number of samples |
|---|---|---|
| NR-1 | 0.89 | 2 |
| NR-2 | 1.04 | 3 |
| NR-3 | 1.29 | 11 |
| NR-4 | 1.09 | 3 |
| NR-5 | 1.11 | 3 |
| NR-6 | 0.87 | 3 |
| NR-7 | 0.98 | 3 |
| NR-8 | 0.91 | 3 |
| NR-9 | 0.99 | 3 |
| NR-10 | 1.57 | 8 |
| NR-11 | 0.94 | 2 |

**Supported $^{210}Pb$ Based on Activity Profiles.** The concentration of $^{210}Pb$ in most Nueces River cores approaches a constant level at depths generally less than 20 cm. Estimates of supported $^{210}Pb$ concentrations can be made from total $^{210}Pb$ activity in the lower part of each profile where it becomes "flat" as excess $^{210}Pb$ approaches zero. Estimates of supported $^{210}Pb$ levels based on total $^{210}Pb$ activity profiles are typically higher than those based on $^{226}Ra$ (table 5). For example, averages are 1.36 and 1.06 dpm/g, respectively, for the activities listed in table 5. In deeper parts of the cores, $^{226}Ra$ and $^{210}Pb$ should be in secular equilibrium and activities should be equal. Lower activities of $^{226}Ra$ compared to $^{210}Pb$ (table 5) have also been reported by other researchers, for example Robbins and others (1978), who found $^{226}Ra$ activities to be 10 to 30 percent lower than $^{210}Pb$ and attributed this difference to small intercalibration errors, to actual departures in secular equilibrium, or to differences in leachability of $^{226}Ra$ and $^{210}Pb$ in the analytical process. Generally, activities of $^{226}Ra$ appear to provide the best estimate of supported $^{210}Pb$ activities except in a few cases, discussed in the following section.

Table 5. Estimated supported $^{210}Pb$ levels based on average $^{226}Ra$ activities, and average, or lowest, activities of total $^{210}Pb$ near base of cores.

| Core Number | Supported $^{210}Pb$ based on average $^{226}Ra$ Activity (dpm/g) | Supported $^{210}Pb$ based on $^{210}Pb$ activities near base of core (dpm/g) | Cumulative excess $^{210}Pb$ using average $^{226}Ra$ for supported $^{210}Pb$ (dpm/cm$^2$) |
|---|---|---|---|
| NR-1 | 0.89 | 1.09 | 31.33 |
| NR-2 | 1.04 | 1.05 | 38.13 |
| NR-3 | 1.29 | 1.31 | 33.19 |
| NR-4 | 1.09 | 1.60 | 27.51 |
| NR-5 | 1.15 | 1.00 | 28.46 |
| NR-6 | 0.87 | 1.60* | 58.88 |
| NR-7 | 0.98 | 1.06 | 40.94 |
| NR-8 | 0.91 | 1.70 | 37.37 |
| NR-9 | 0.99 | 0.95 | 9.31 |
| NR-10 | 1.57 | 1.88 | 25.63 |
| NR-11 | 0.94 | 1.60 | 53.41 |

* Based in part on $^{226}Ra$ activity and averages of $^{210}Pb$ near base of core.

## Cumulative Inventories of Excess $^{210}Pb$ Activity

Estimates of total unsupported residual, or cumulative excess, $^{210}Pb$ activity for the Nueces River system cores were made using average $^{226}Ra$ activities as a measure of supported $^{210}Pb$ (table 5). Based on these data, cumulative inventories of excess $^{210}Pb$ for all cores range from 9.31 dpm/cm$^2$ to 58.88 dpm/cm$^2$. Eight of the cores have cumulative excess Pb inventories ranging from approximately 26 dpm/cm$^2$ to 41 dpm/cm$^2$. Core NR-9 has an atypically low cumulative inventory (9.31 dpm/cm$^2$), apparently because too few samples were analyzed in the upper part of the core to provide sufficient data for calculating the total cumulative inventory (Appendix B). Cores NR-6 and NR-11 have the highest cumulative inventories of 58.88 and 53.41 dpm/cm$^2$, respectively (table 5). If the higher supported $^{210}Pb$ activities derived from total $^{210}Pb$ data are used (table 5), cumulative inventories are reduced to 35.11 dpm/cm$^2$ in core NR-6 and 29.97 dpm/cm$^2$ in NR-11. These inventories are more in line with those in other cores.

## Sedimentation Rates Based on $^{210}Pb$ Activities

Sedimentation rates derived from three models CFS (constant flux–constant sedimentation), CRS (constant flux, or constant rate of supply), and CIC (constant initial concentration) (Robbins, 1978; Oldfield and Appleby, 1984) were compared to determine the consistency and utility of the $^{210}Pb$ data in calculating rates. Using the CFS method, rates at coring sites range from less than 1 mm/yr to more than 5 mm/yr (table 6 and fig. 12). The lowest rate of 0.6 mm/yr at core NR-1 is in agreement with rates determined using the CRS and CIC models (fig. 13) and is supported by a rate based on archeological evidence found at the edge of Rincon Bayou near the coring site. (Best agreement between models for NR-1 was achieved by using a supported $^{210}Pb$ activity of 1.09 dpm/g from table 5). The archeological evidence, which consists of a thin stratum of shells and faunal bones, was discovered at a depth of 25 cm by Mike Blum (University of Nebraska) and was dated by Bob Ricklis (Archeologist, Corpus Christi) at 500 to 1,000 years B.P. (Before Present). Using the more recent date of 500 years yields an average sedimentation rate of 0.05 cm/yr for the 25 cm of sediment above the archeological horizon. This rate is within 0.01 cm/yr of the rates determined from $^{210}Pb$ data. The geomorphic setting of coring site NR-1 is consistent with the low sedimentation rate. The site is approximately 3 km north of the Nueces River (fig. 1) and is partially "protected" from flooding by an upland terrace that curves around the western (upstream) side of the site.

Table 6. Average sedimentation rates for given core intervals. Rates are based on a least-squares fit of Ln plots of excess $^{210}Pb$ against corrected depths (CFS model, Oldfield and Appleby, 1984).

| Core no. | Sedimentation rate (CFS model) (cm/yr) | Corrected depth interval used (cm) | $R^2$ | Supported $^{210}Pb$ (dpm/g) |
|---|---|---|---|---|
| NR-1 | 0.06 | 1-13 | 0.962 | 1.09 |
| NR-2 | 0.55 | 1-29 | 0.834 | 1.04 |
| NR-3 | 0.20 | 1-10 | 0.872 | 1.29 |
| NR-4 | 0.20 | 1-15 | 0.917 | 1.09 |
| NR-5 | 0.13 | 1-6 | 0.912 | 1.15 |
| NR-6 | 0.10 | 1-6 | 0.916 | 0.87 |
| NR-7 | 0.16 | 1-12 | 0.926 | 0.98 |
| NR-8 | 0.13 | 1-13 | 0.832 | 0.91 |
| NR-9 | 0.10 | 1-9 | 0.918 | 0.99 |
| NR-10 | 0.32 | 1-20 | 0.852 | 1.57 |
| NR-11 | 0.45 | 1-25 | 0.899 | 0.94 |

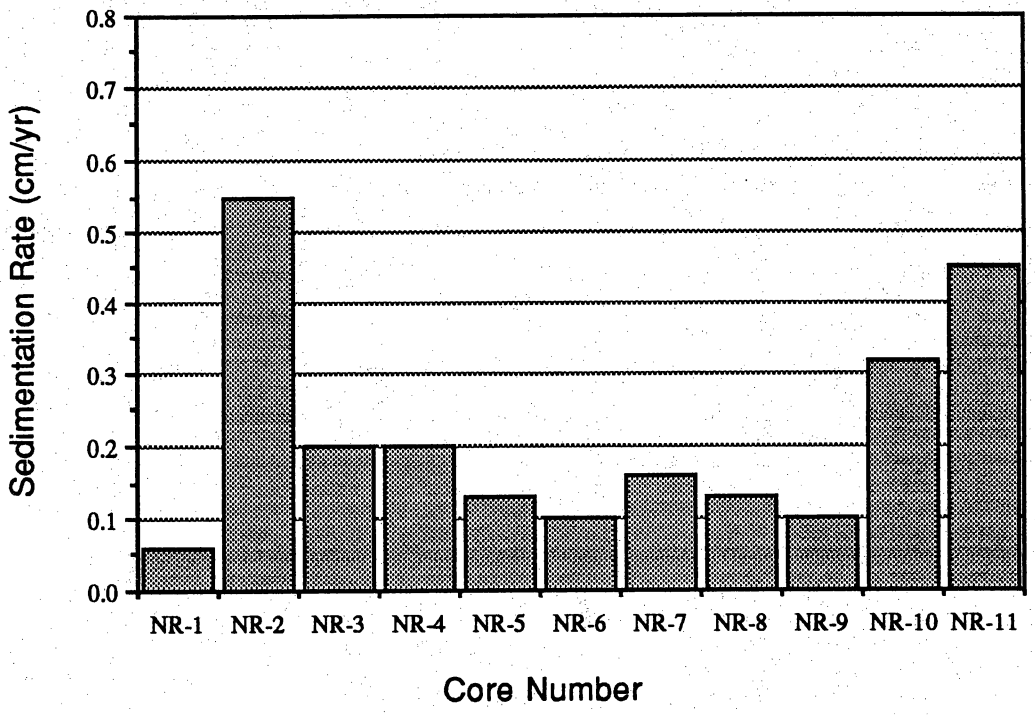


Figure 12. Sedimentation rates of Nueces River cores using CFS model (table 6). Depths are generally less than 15 cm. Supported $^{210}Pb$ for each core is based on average $^{226}Ra$.

The highest sedimentation rates are at coring sites NR-2 and NR-11. Core NR-11 was collected from an intertidal *Spartina alterniflora* marsh that receives sediment from the Nueces River and Nueces Bay (fig. 1). Core NR-2 was collected in a brackish-water marsh that had developed in a depression near the margin of a tidally influenced lake. The average sedimentation rate at the two sites is 0.45 cm/yr for NR-11 (fig. 14) and 0.55 cm/yr for NR-2. The rate at NR-11 is equal to the average rate of relative sea-level rise of 0.45 cm/yr at the Rockport tide gauge for the period from the late 1940s to mid-1980s (fig. 15). Other researchers have also reported a close relationship between rates of relative sea-level rise and rates of estuarine

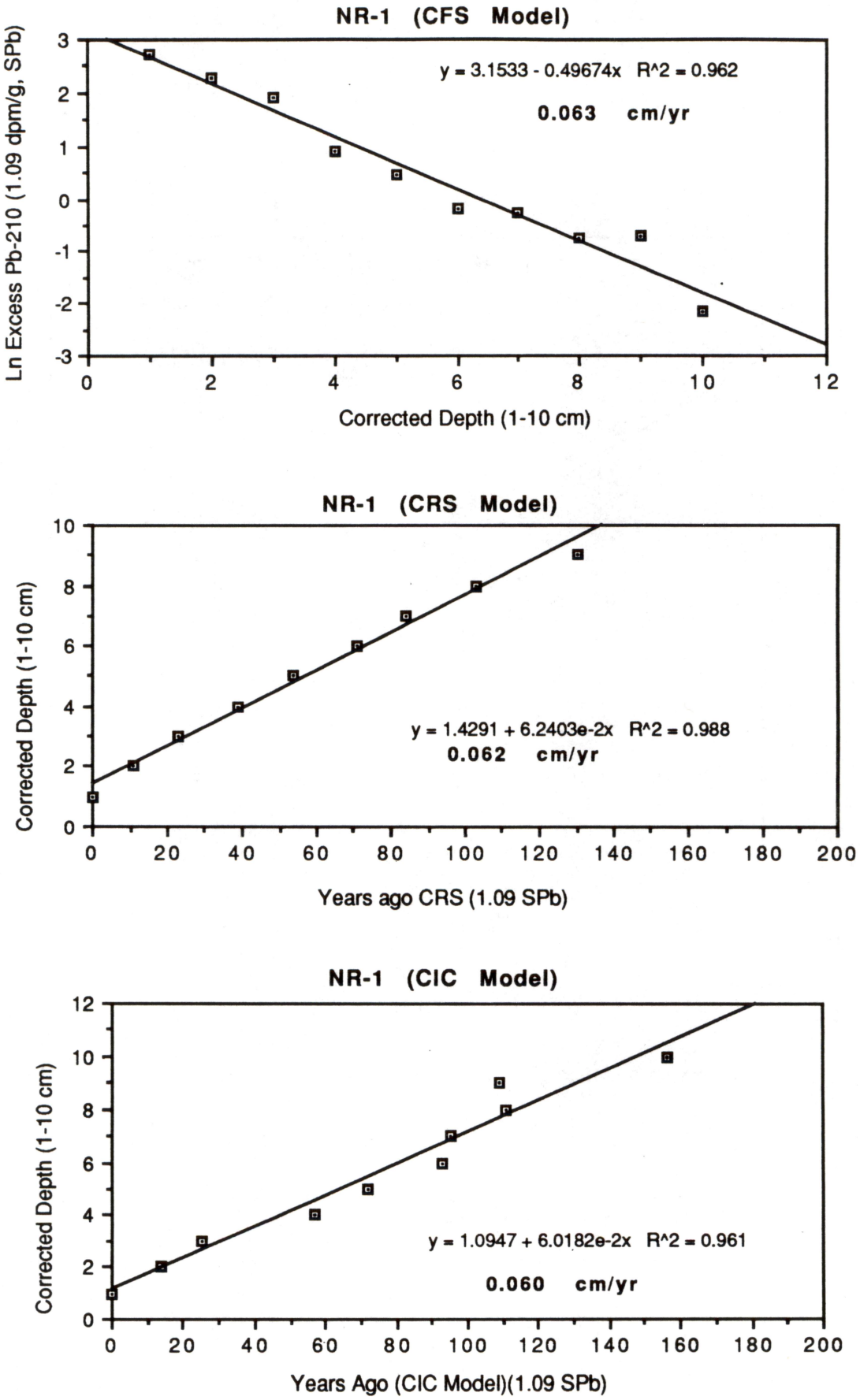


Figure 13. Average sedimentation rates at core site NR-1 based on CFS, CRS, and CIC models.

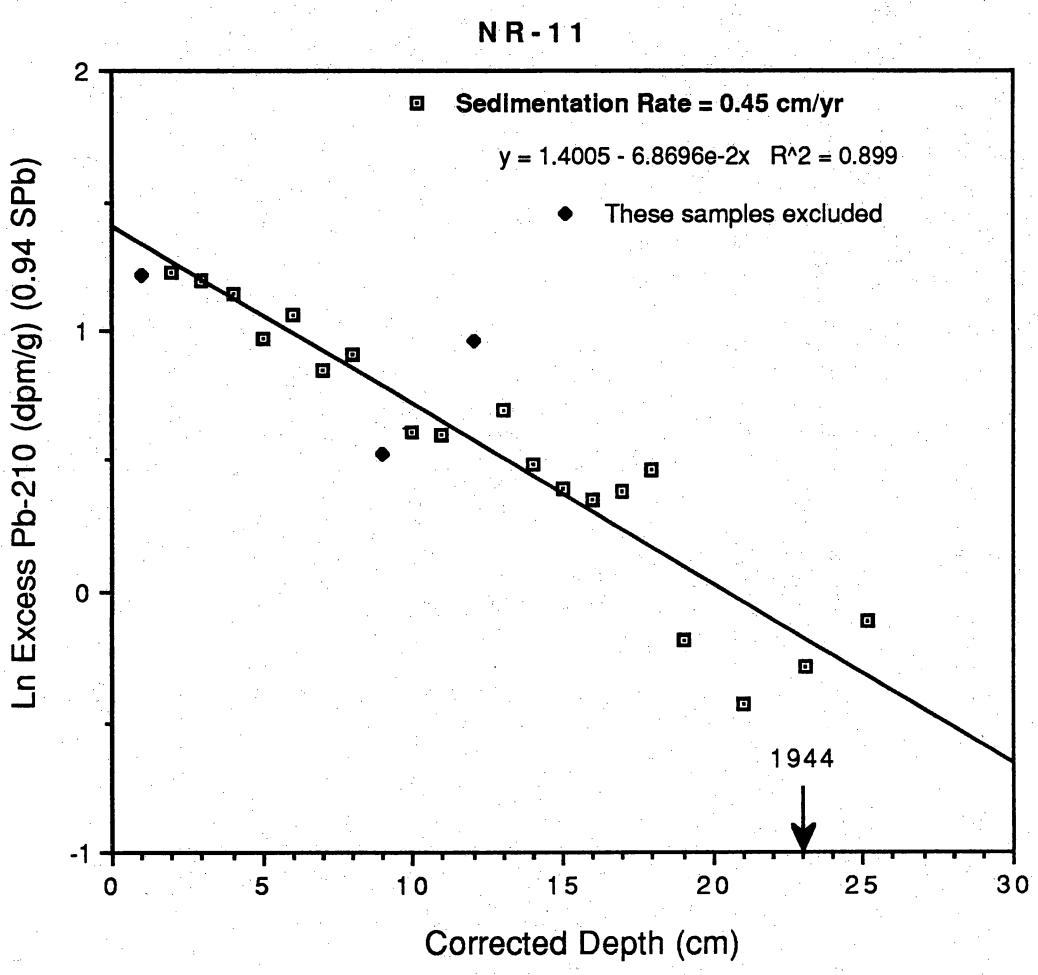


Figure 14. Average sedimentation rate at core site NR-11 based on the CFS model.

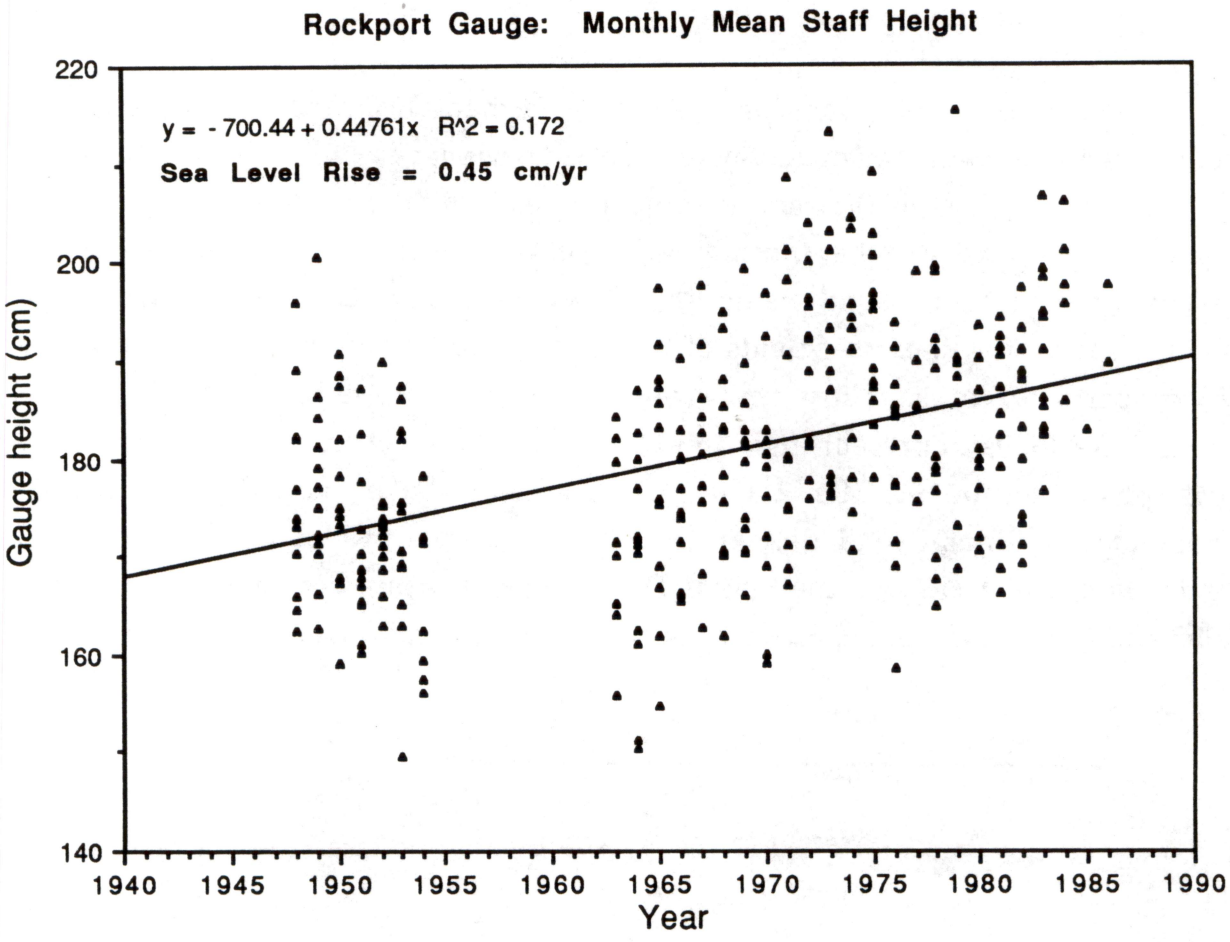


Figure 15. Average rate of sea-level rise at the Rockport tide gauge for the period from the 1940s to mid-1980s. Average monthly tide levels from National Oceanic and Atmospheric Administration (NOAA).

salt marsh sediment accumulation (for example, McCaffrey, 1977). Rates indicated by cores from other locations in the Nueces River area are much lower and range from 0.32 cm/yr at NR-10 to ≤0.20 cm/yr at the remaining sites (table 6).

Preliminary relationships between sedimentation rates, river suspended sediment loads, dam construction, and relative sea-level rise were investigated for several cores. The results show some interesting and, in some cases, puzzling trends depending on the sedimentation model used. There appears to be a relatively consistent trend using the CFS model and calculating two rates of sedimentation for linear segments of the $^{210}Pb$ profiles representing the upper and lower parts of cores. Most cores show reductions in sedimentation rates from around the 1930s to present (figs. 16 to 20). The Mathis Dam at Lake Corpus Christi was constructed in 1929 (fig. 21) and is estimated to have trapped 75 percent of the suspended sediment load delivered along the Nueces River (Brune, 1953). The Seale Dam, which flooded the Mathis Dam at Lake Corpus Christi, was completed in 1958 and traps more than 95 percent of the suspended sediment (Liebbrand, 1987).

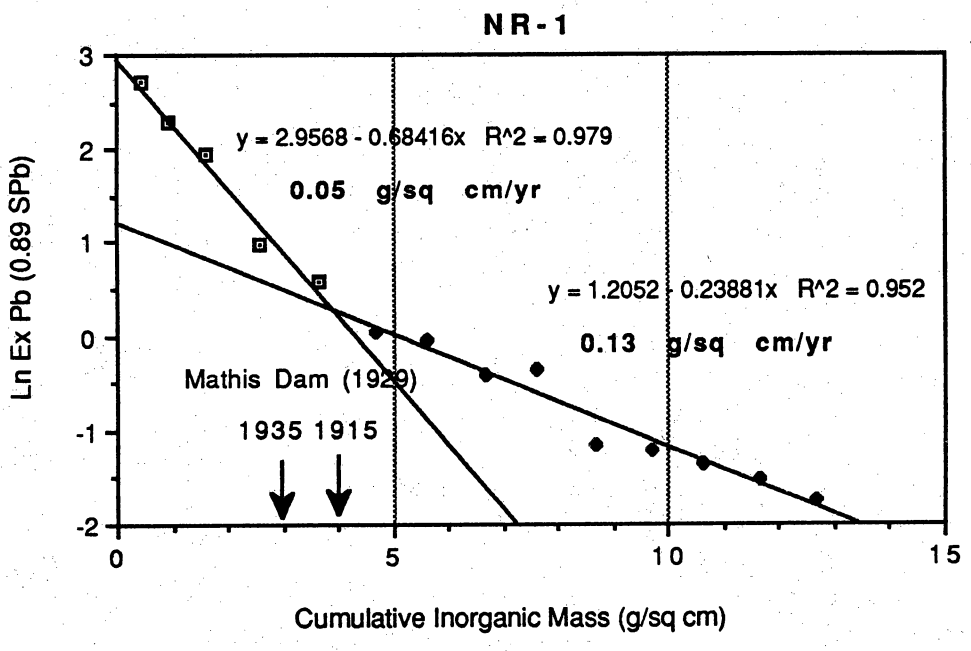


Figure 16. $^{210}Pb$ profile of core NR-1 showing decreasing rates of sedimentation after approximately 1929 when the Mathis Dam was constructed on Nueces River to form Lake Corpus Christi. Based on the CFS model and cumulative mass.

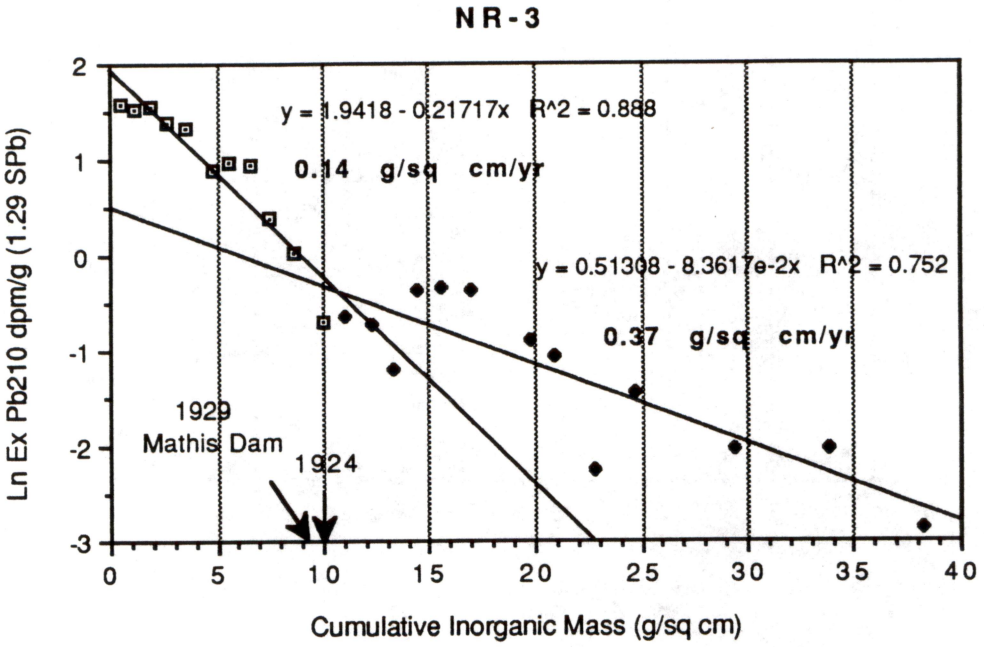


Figure 17. $^{210}Pb$ profile of core NR-3 showing decreasing rates of sedimentation after the Mathis Dam was constructed on the Nueces River in 1929. Based on CFS model and cumulative mass.

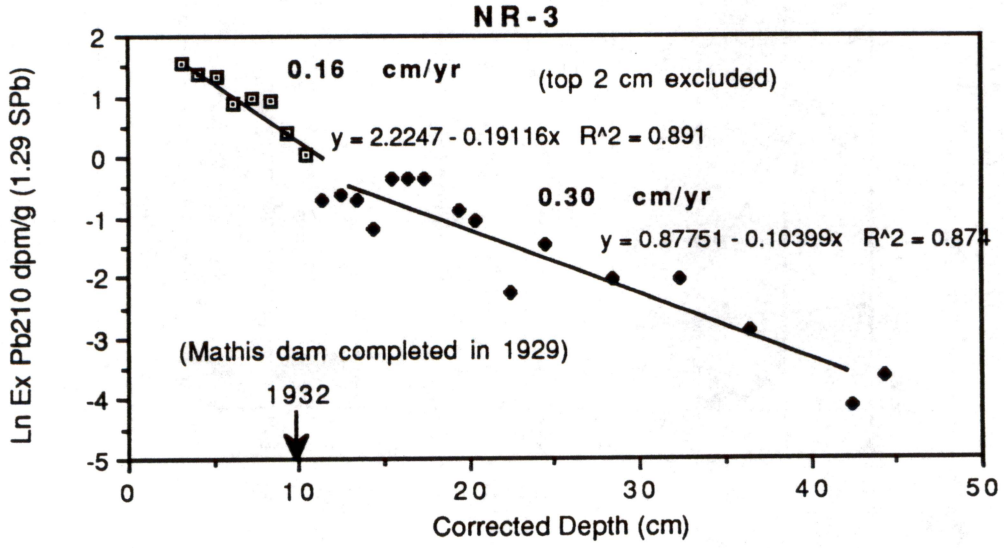


Figure 18. $^{210}Pb$ profile of core NR-3 showing decreasing rates of sedimentation after the Mathis Dam was constructed on the Nueces River in 1929. Based on CFS model and corrected depth.

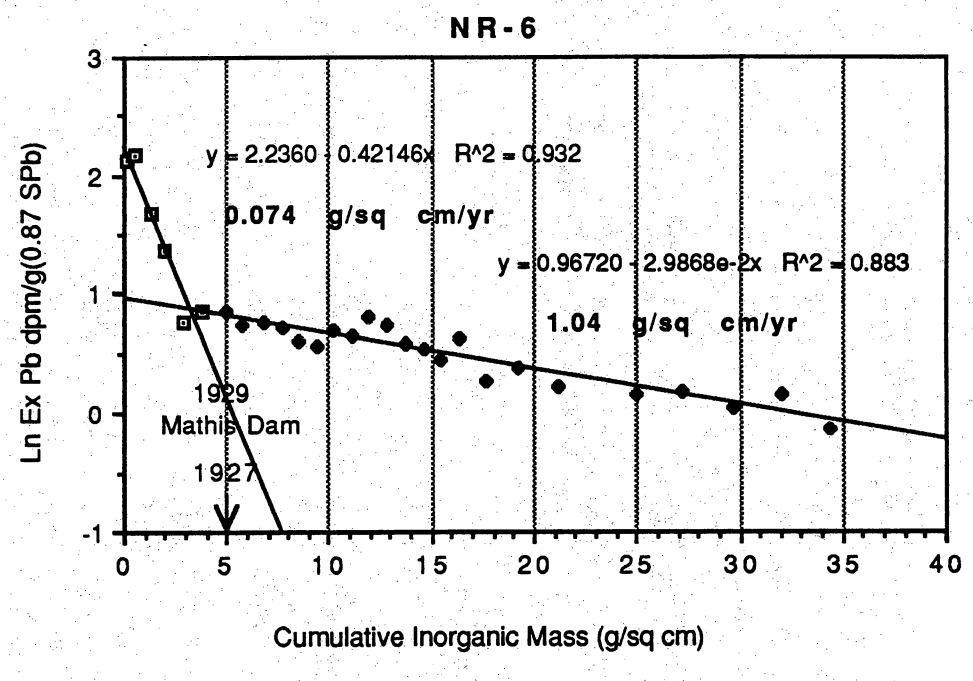


Figure 19. $^{210}Pb$ profile of core NR-6 showing decreasing rates of sedimentation after the Mathis Dam was constructed on the Nueces River in 1929. Based on CFS model and cumulative mass.

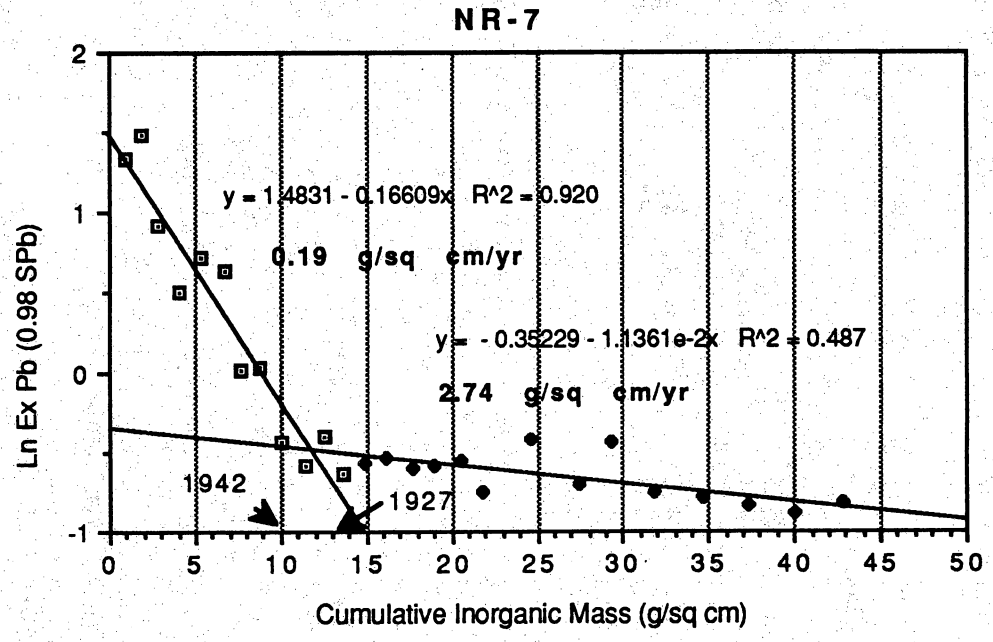


Figure 20. $^{210}Pb$ profile of core NR-7 showing decreasing rates of sedimentation after the Mathis Dam was constructed on the Nueces River in 1929. Based on CFS model and cumulative mass.

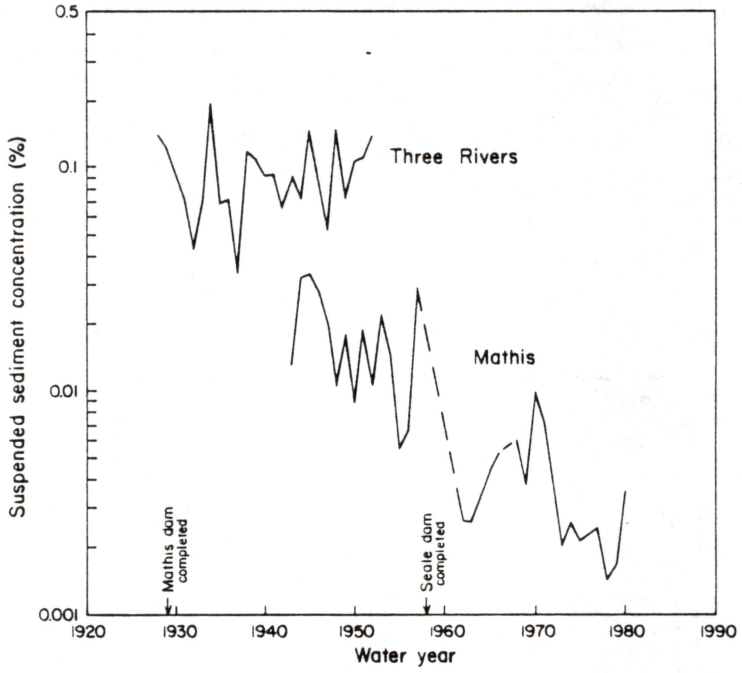


Figure 21. Suspended sediment load (percent by weight) for the Nueces River. The Three Rivers station is upstream from Lake Corpus Christi, and Mathis station is downstream. No data for dashed segments. Note the time of completion of the Mathis and Seale Dams that formed Lake Corpus Christi. From Morton and Paine (1984).

Rates of sedimentation derived from the three models show relatively close agreement between average CFS and CIC rates for the upper part of all cores (fig. 22 and table 7). In five cores, there is agreement between rates based on all three models (fig. 22). In the other six cores, however, CRS rates are higher than those based on CFS and CIC. In addition, there is disagreement between the CFS- and CRS-derived sedimentation trends for earlier and later periods. For example, unlike the CFS model, which indicates lower rates after 1930, CRS rates for some cores increased after 1930 (fig. 23).

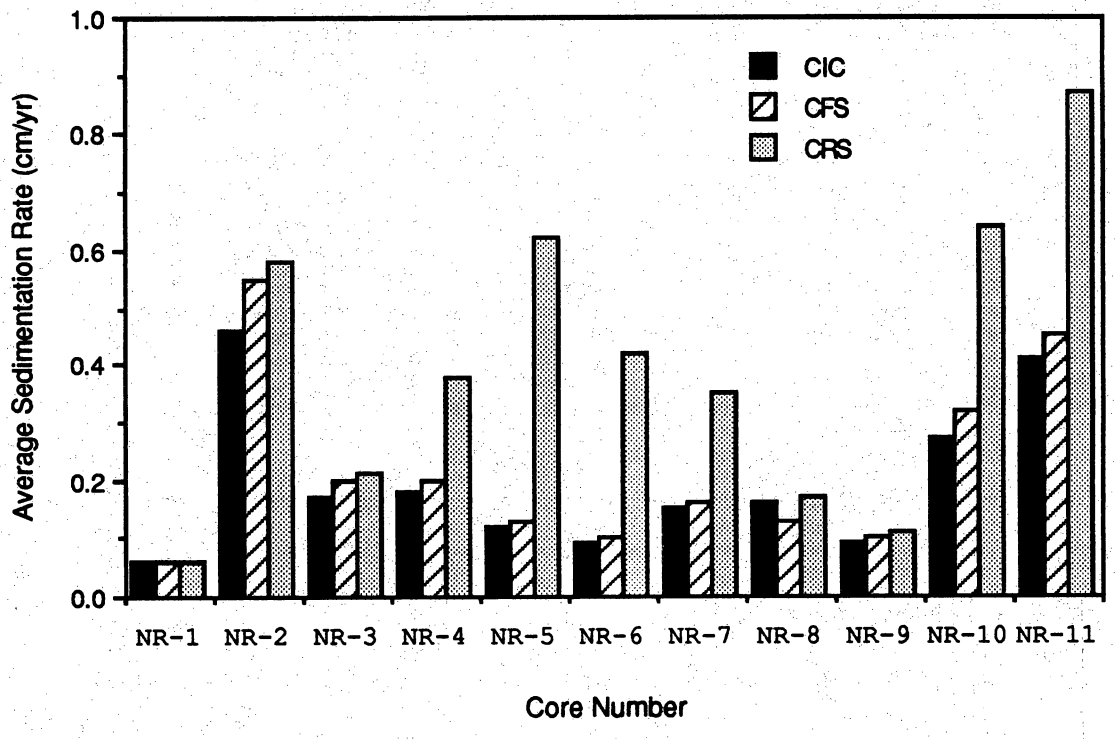


Figure 22. Comparison of sedimentation rates derived from the CFS, CRS, and CIC models. There is relatively close agreement between CFS and CIC rates in all cores and between CFS, CIC, and CRS rates in five cores. See table 7 for core depths on which rates are based.

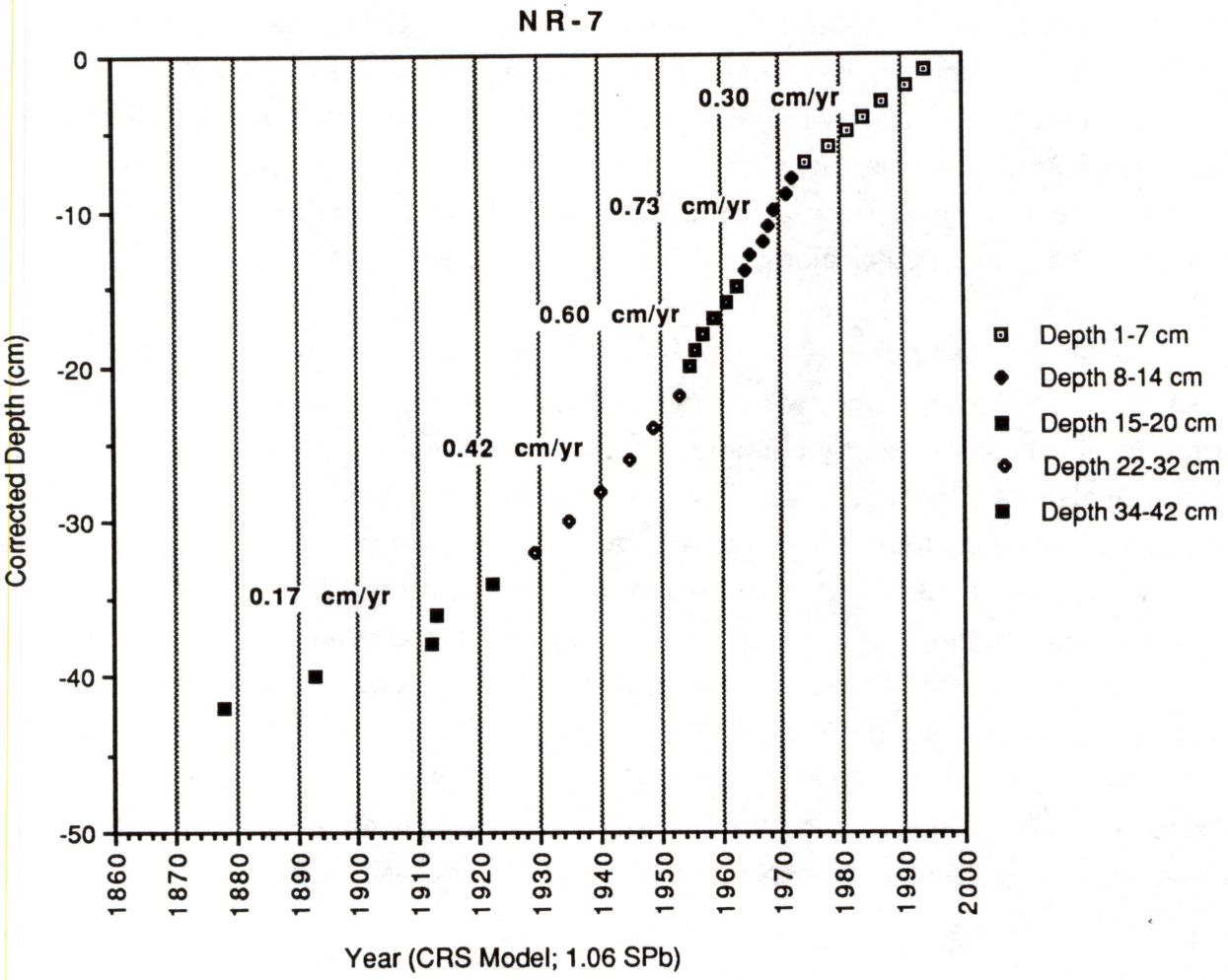


Figure 23. Changes in sedimentation rates through time at core site NR-7, based on the CRS model. Note that rates appear to increase after the 1930s until 1975. The CFS model indicates that rates decreased after 1930 at this site (fig. 20).

The CRS model helps define more recent trends, for example, from the 1950s to present. Changes in relative sea-level (RSL) rise over the past five decades may have influenced sedimentation at some sites. At NR-11, an intertidal site, rates of sedimentation appear to have been highest during the period from 1964 to 1975, when the rate of RSL rise was the highest, and lower from 1975 to the 1990s, when the rate of RSL rise was lower (fig. 24). A few other coring sites also indicate a decline in sedimentation rates during these periods, but these trends can be related to suspended load changes along the Nueces River (figs. 25 and 26).

Although sedimentation can be influenced by changes in streamflow or relative sea-level rise, these two processes are sometimes related. Secular variations in sea level can be caused by climatic factors, such as droughts and periods of higher than normal precipitation and riverine discharge. These short-term sea-level variations produce temporary adjustments in the longer term trends related to eustatic sea-level rise and subsidence. Such variations can apparently affect sedimentation rates as illustrated by the positive correlation between changes in RSL rise rates, streamflow (and suspended sediment load), and sedimentation at least in some cores for the period 1961–1975 (fig. 27). It is possible that Hurricanes Carla (1961), Beulah (1967), and Fern (1971) affected the sedimentation rates for the period 1961–1975. Hurricanes Beulah and Fern caused abnormally high rainfall, which was reflected in high streamflow (and sediment load) along the Nueces River in 1967 and 1971 (fig. 27).

Table 7. Average rates of sedimentation for selected depths in Nueces River cores based on CFS, CIC, and CRS models.

| Core no. | CFS rate (cm/yr) | CRS rate (cm/yr) | CIC rate (cm/yr) | Corrected (cm) | Anomalies excluded |
|---|---|---|---|---|---|
| NR-1 | 0.06 | 0.06 | 0.06 | 1-10 | |
| NR-2 | 0.55 | 0.58 | 0.46 | 1-29 | |
| NR-3 | 0.20 | 0.21 | 0.17 | 1-10 | |
| NR-4 | 0.20 | 0.38 | 0.18 | 1-15 | 1 |
| NR-5 | 0.13 | 0.62 | 0.12 | 1-6 | |
| NR-6 | 0.10 | 0.42 | 0.09 | 1-6; 1-12 CRS | |
| NR-7 | 0.16 | 0.35 | 0.15 | 1-12; 1-7 CRS | |
| NR-8 | 0.13 | 0.17 | 0.16 | 1-13 | 1 |
| NR-9 | 0.08 | 0.10 | 0.07 | 1-8; CRS | |
| NR-10 | 0.32 | 0.64 | 0.27 | 1-20; 1-11 CRS | 3 |
| NR-11 | 0.45 | 0.87 | 0.41 | 2-25; 1-18 CRS | 3 |

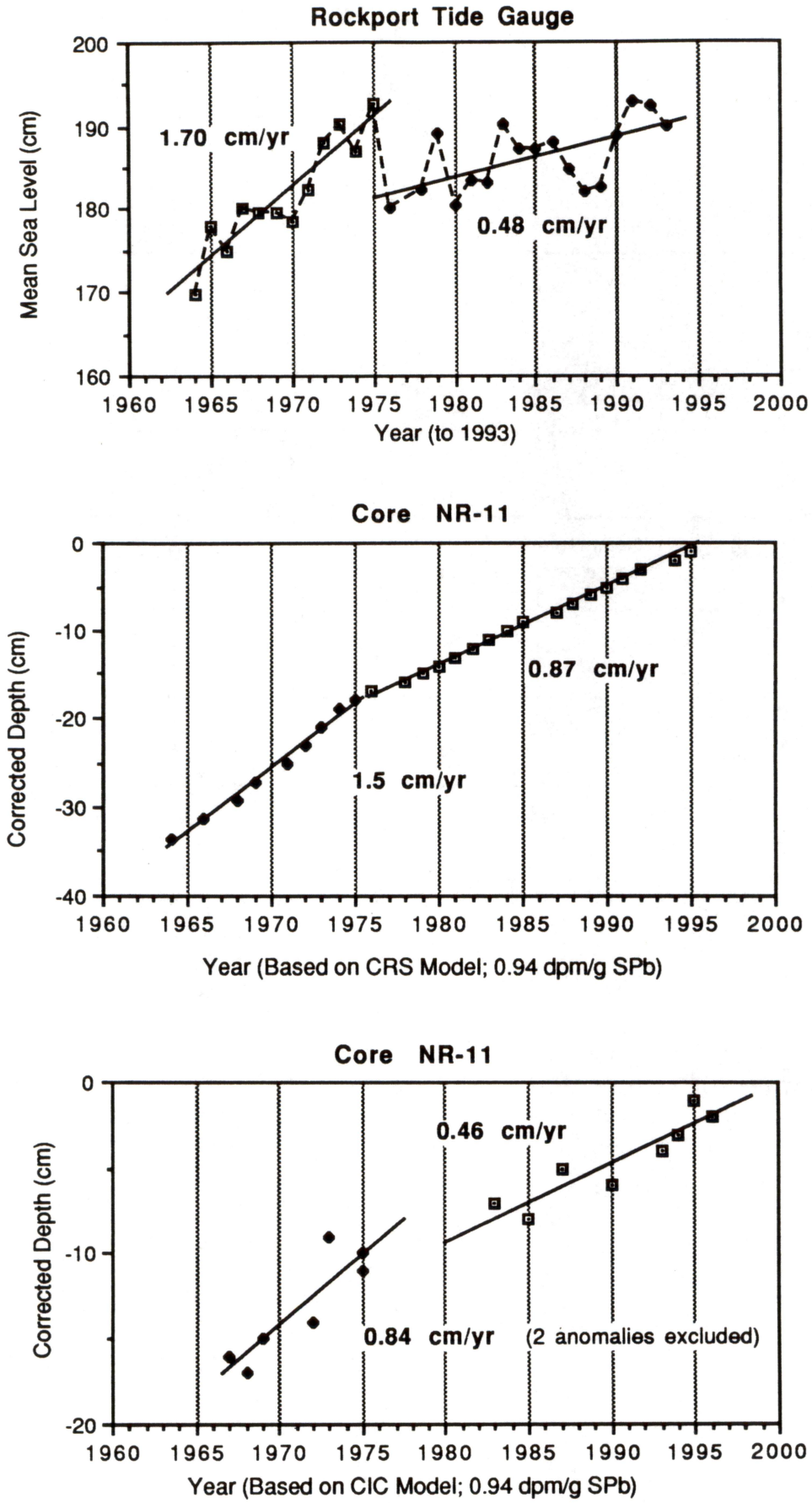


Figure 24. Comparison of changes in rates of relative sea-level rise at the Rockport tide gauge with changes in sedimentation rates at core site NR-11. Tide data from NOAA.

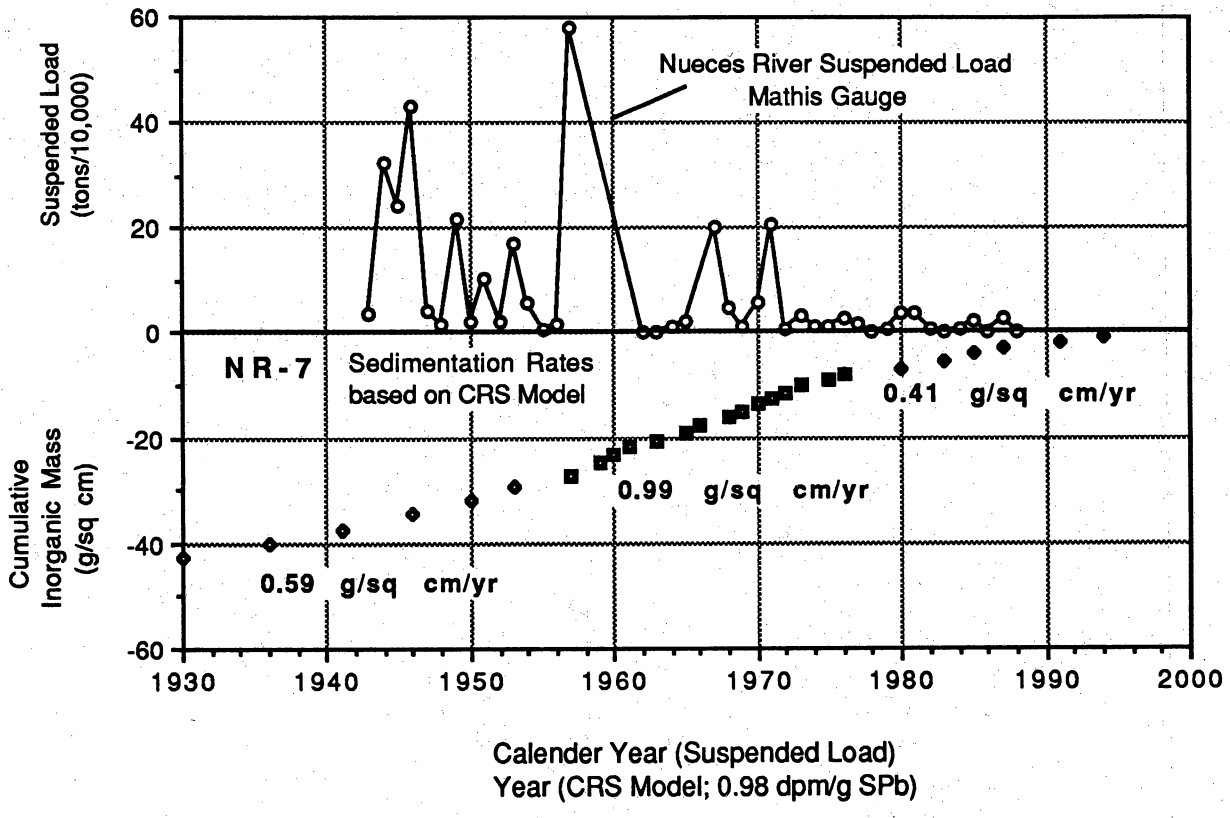


Figure 25. Comparison of changes in suspended load of the Nueces River with changes in sedimentation at core site NR-7. The sedimentation rate decreased in the mid 1970s, which corresponds with a decrease in suspended load. Suspended load data from the Texas Water Development Board (TWDB).

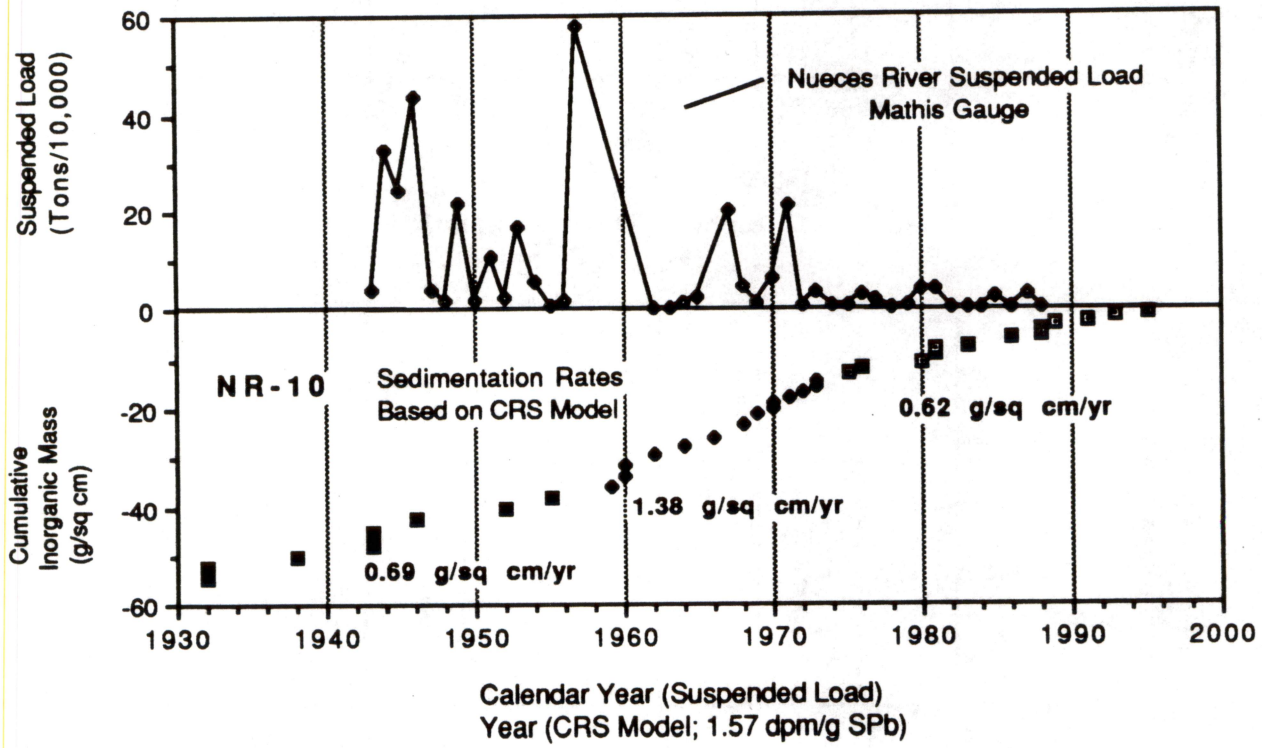


Figure 26. Comparison of decreasing rates of sedimentation at core site NR-10 with a decreasing sediment load along the Nueces River. The rate decreased after the mid-1970s as at core site NR-7 (fig. 25). Suspended load data from TWDB.

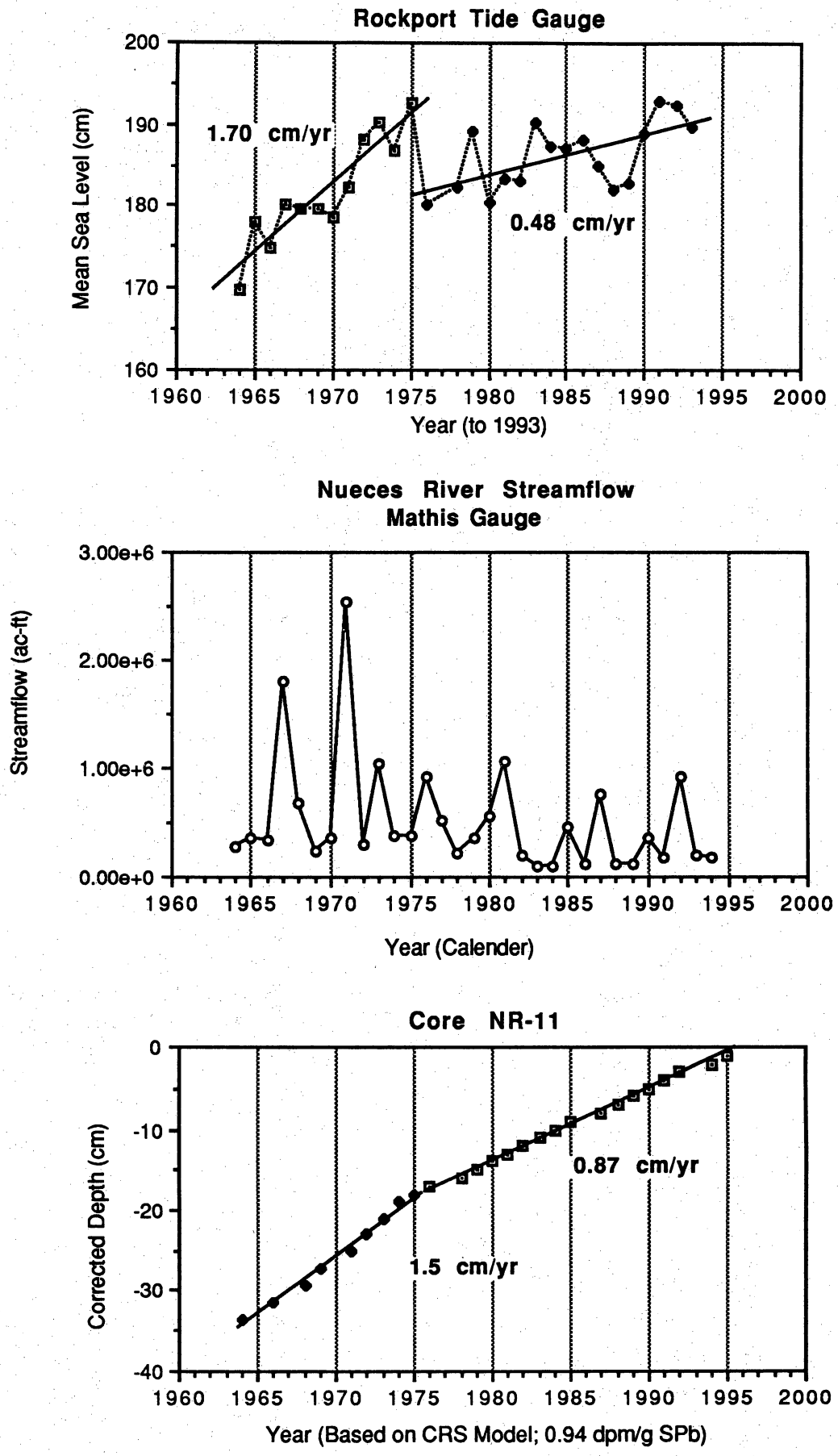


Figure 27. Comparison of rates of sea-level rise at the Rockport gauge, streamflow at the Mathis station, and sedimentation at core site NR-11. Tide data from NOAA and streamflow data from TWDB.

## Annotated Plots of Probable Causes for Variance in $^{210}Pb$ Activity

Depth plots of total $^{210}Pb$ activity (figs. 28 to 38) are annotated to indicate probable causes of local variations in excess $^{210}Pb$ activity. The plots were compared with the actual cores, core descriptions, x-radiographs, organic matter (LOI), and textural properties in an effort to explain some of the variations in $^{210}Pb$ activity. Note that depths used in these illustrations are actual core depths and are not corrected for shortening.

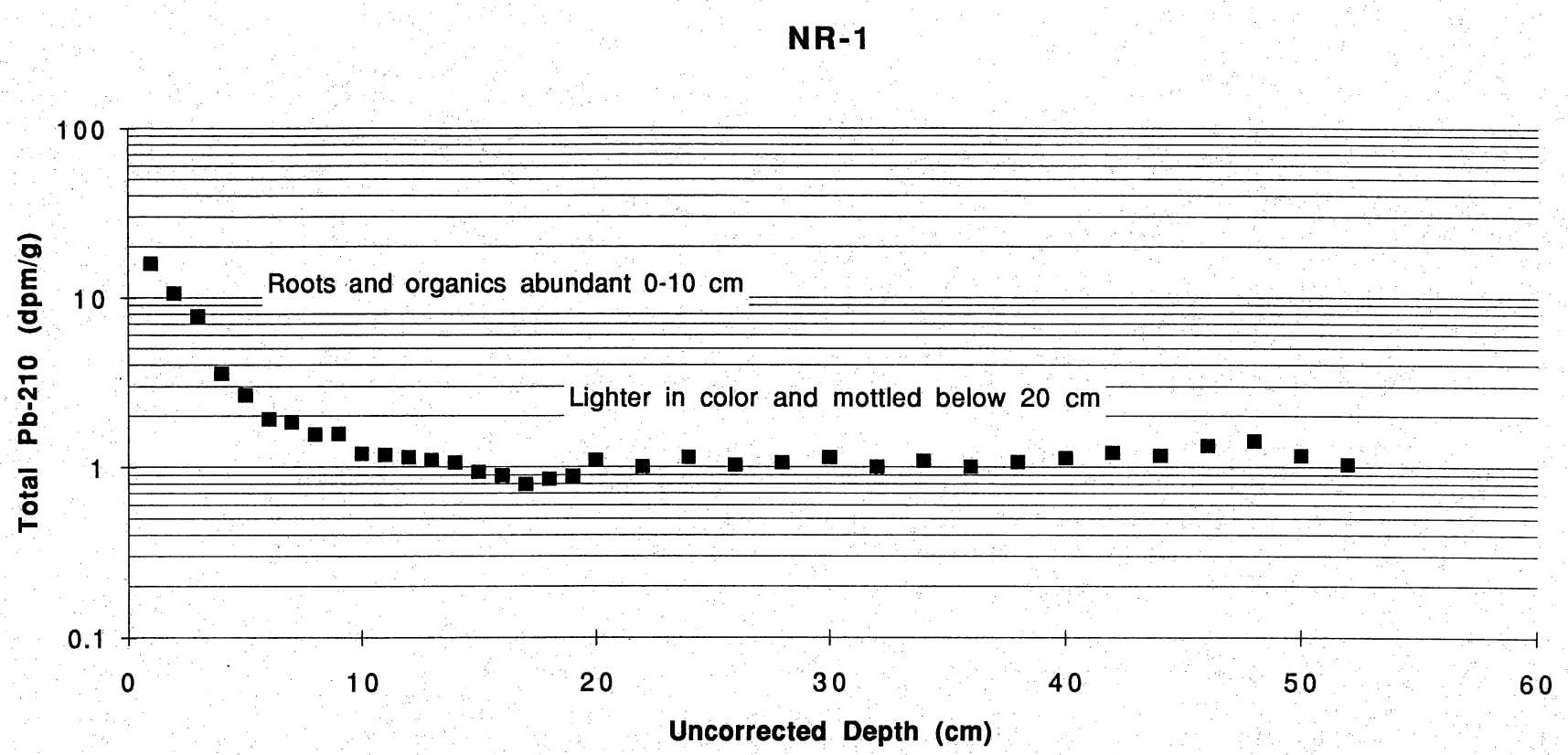


Figure 28. Core NR-1 annotated profile.

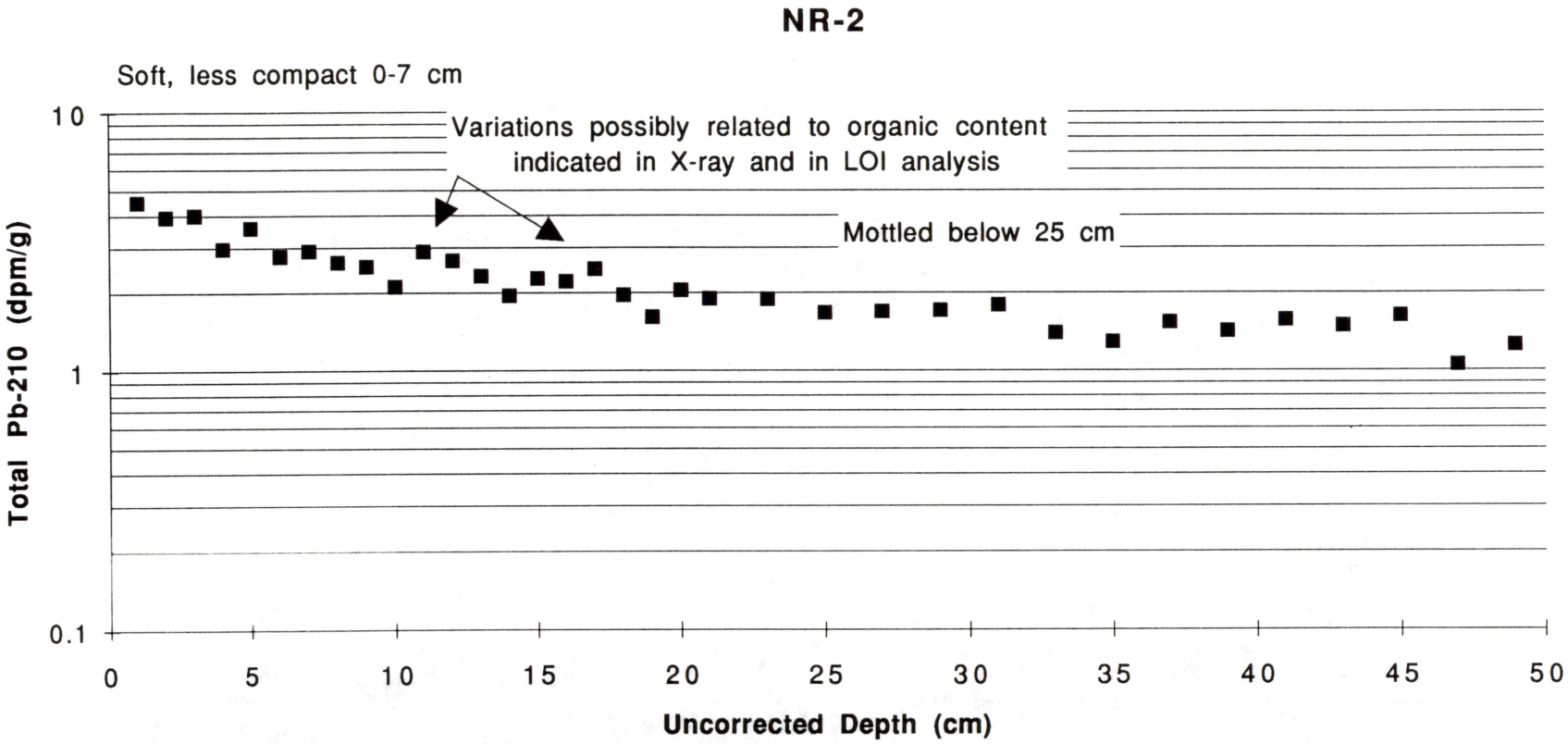


Figure 29. Core NR-2 annotated profile.

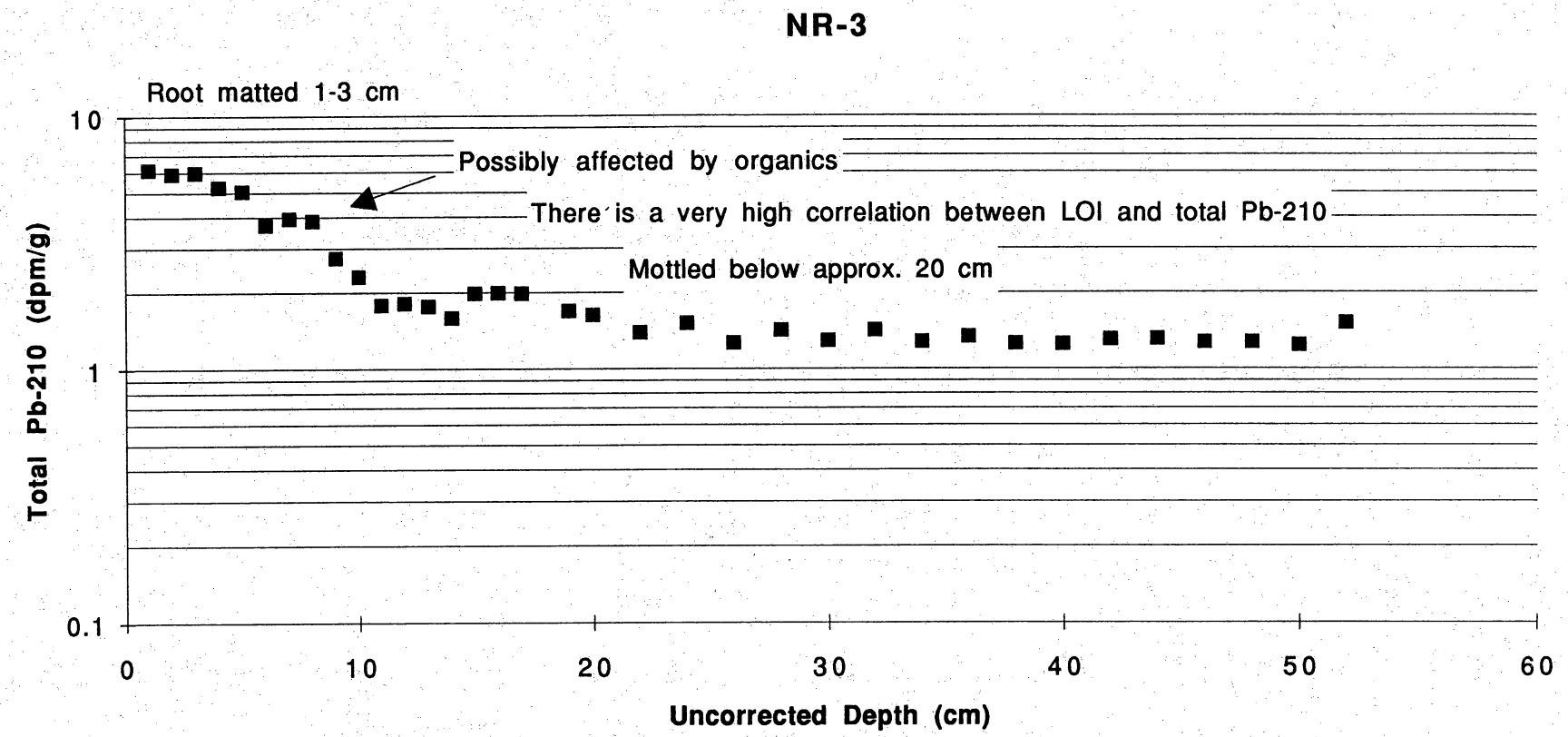


Figure 30. Core NR-3 annotated profile.

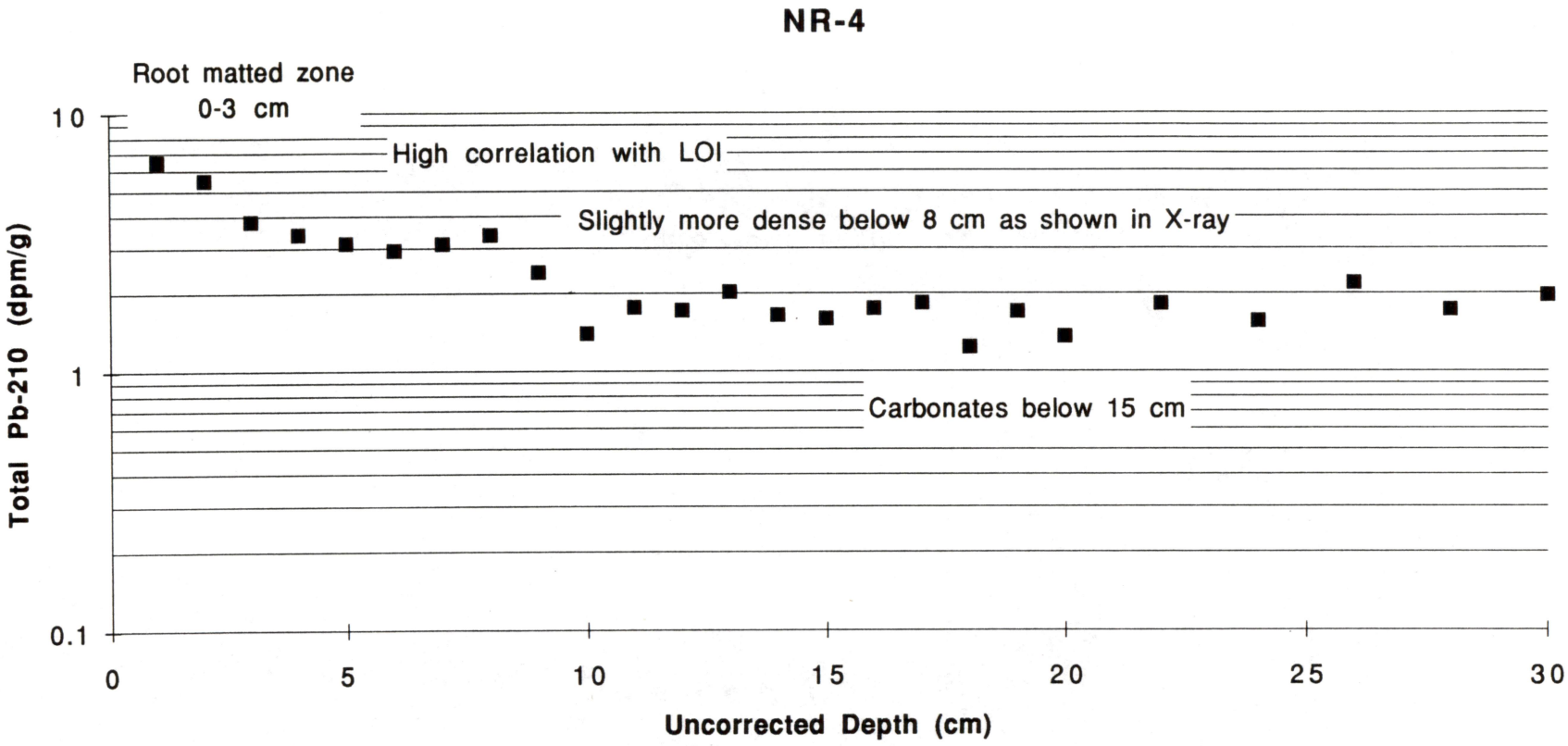


Figure 31. Core NR-4 annotated profile.

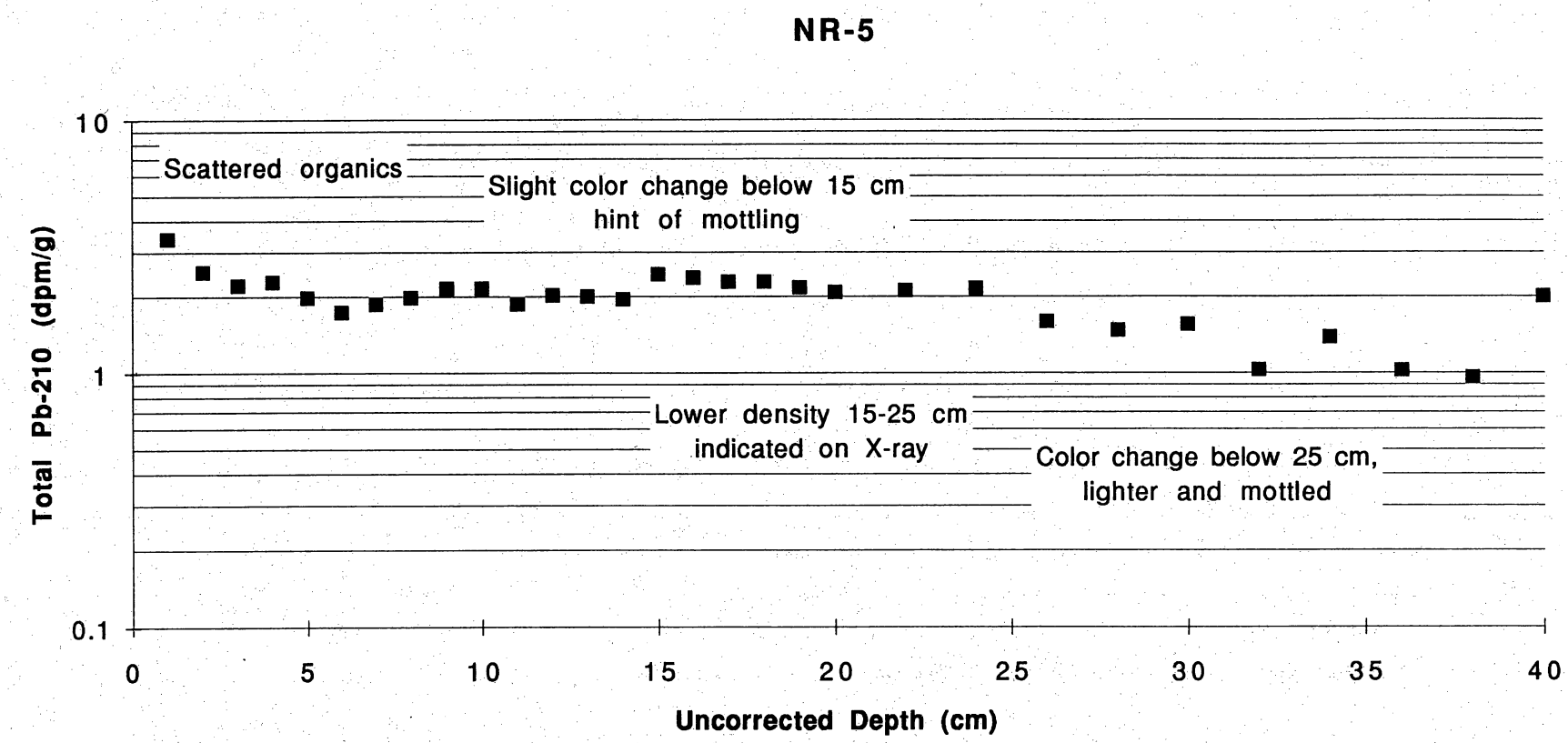


Figure 32. Core NR-5 annotated profile.

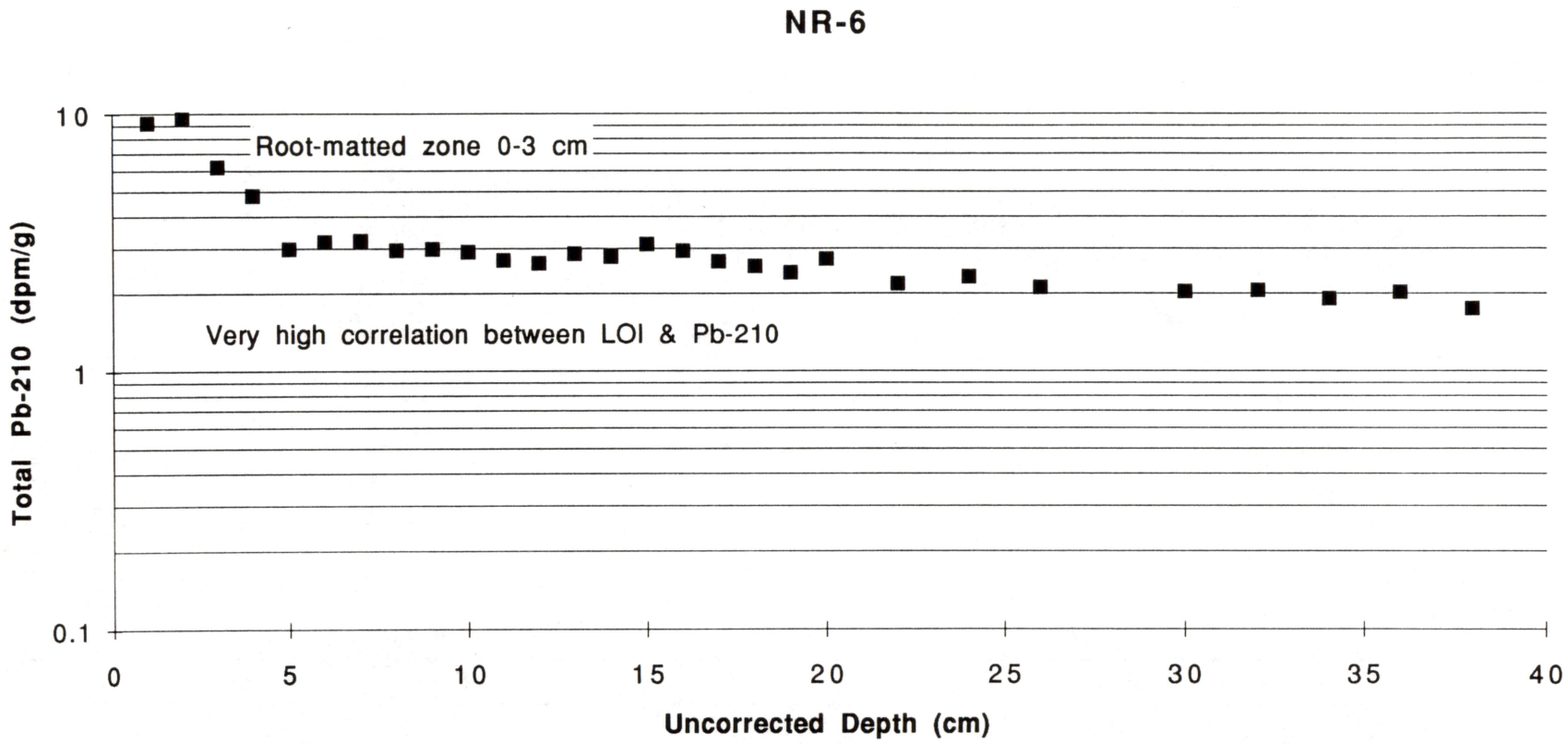


Figure 33. Core NR-6 annotated profile.

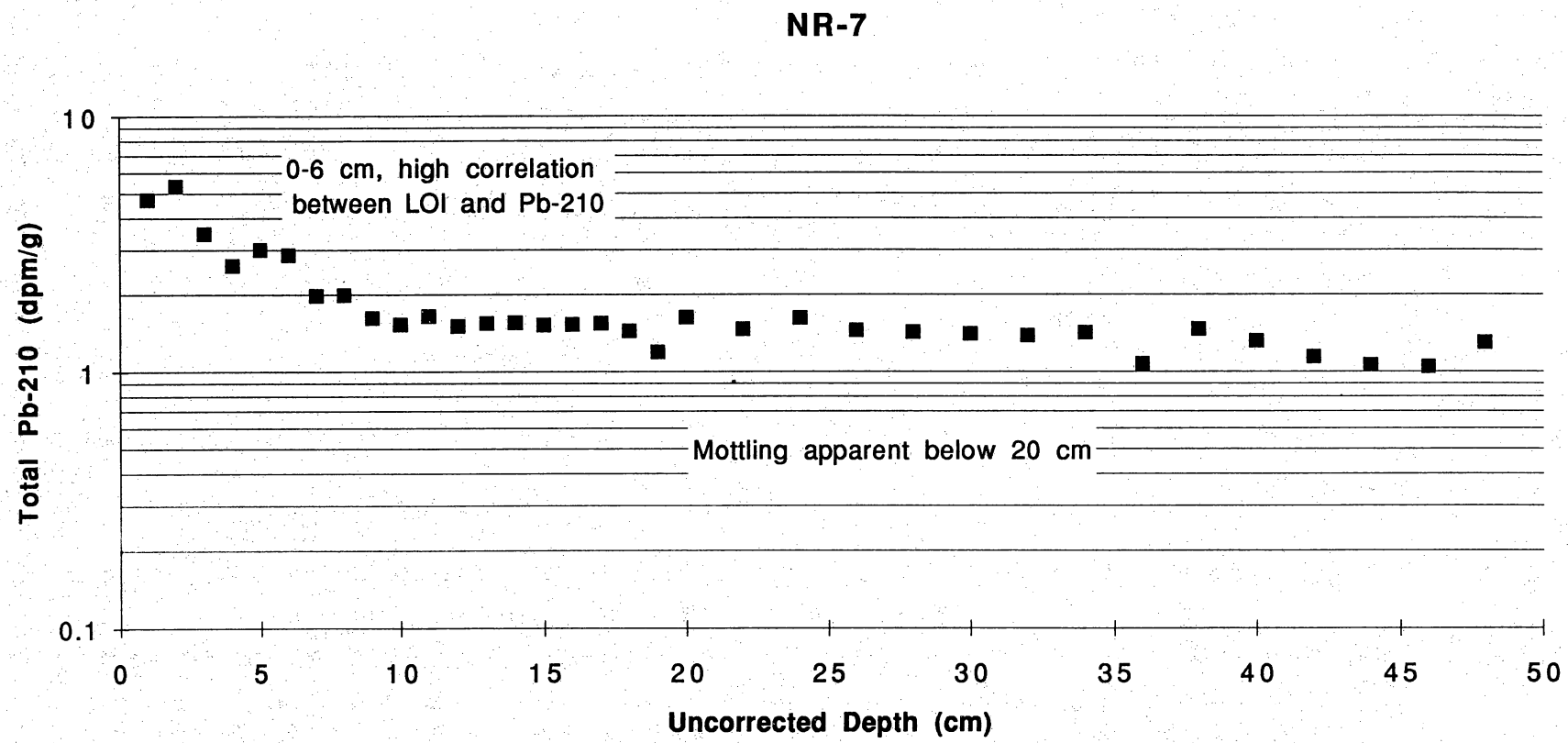


Figure 34. Core NR-7 annotated profile.

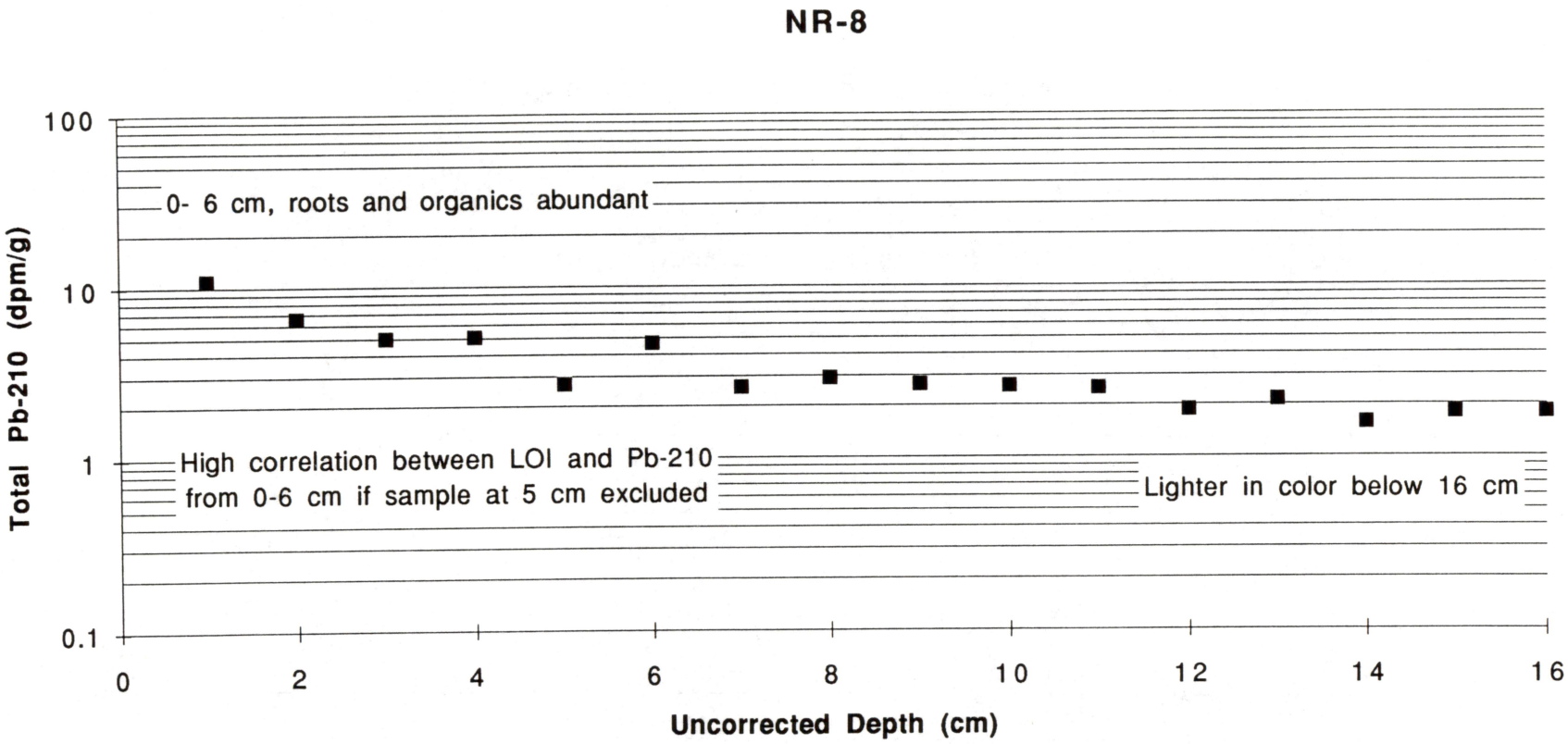


Figure 35. Core NR-8 annotated profile.

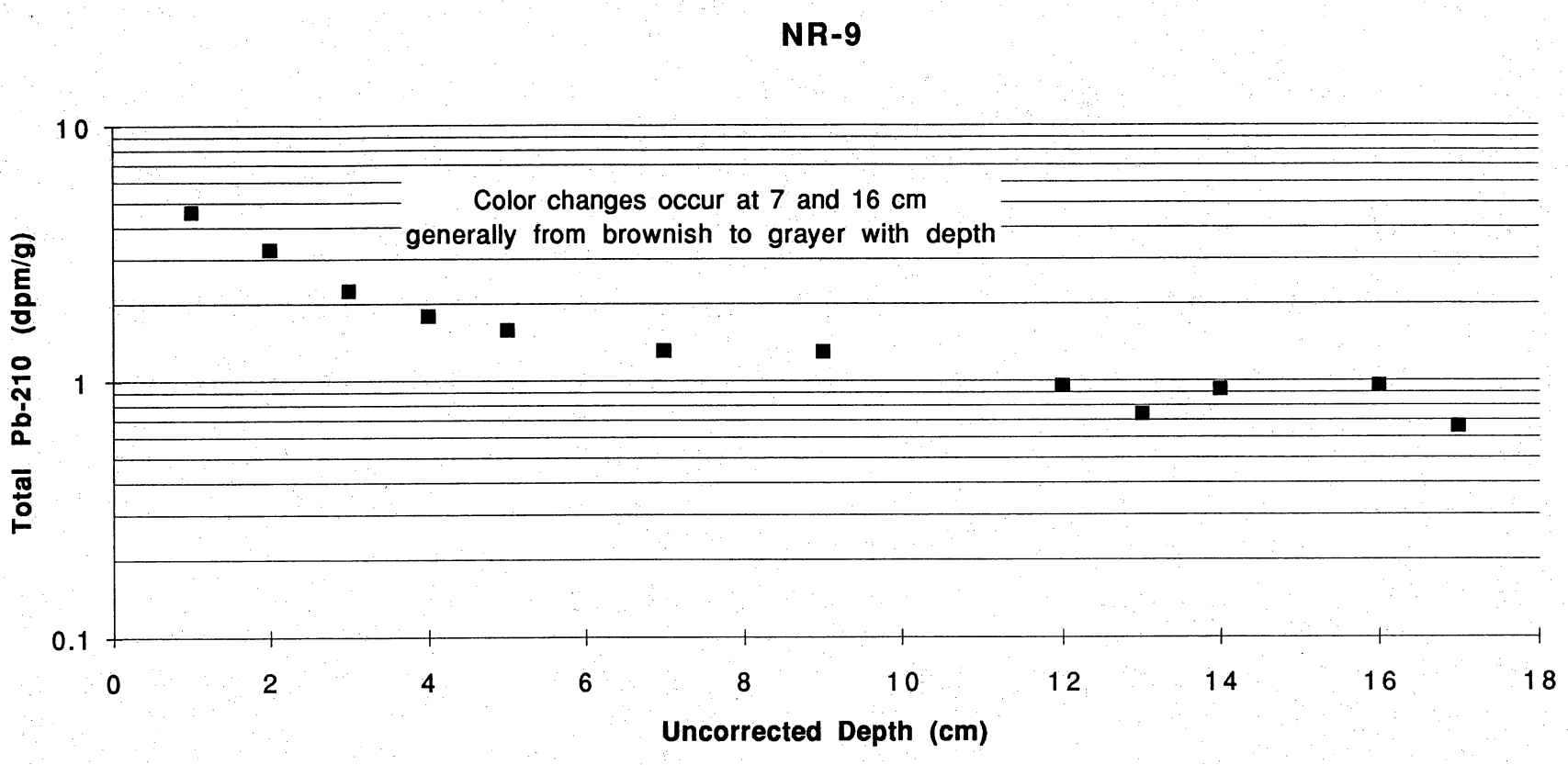


Figure 36. Core NR-9 annotated profile.

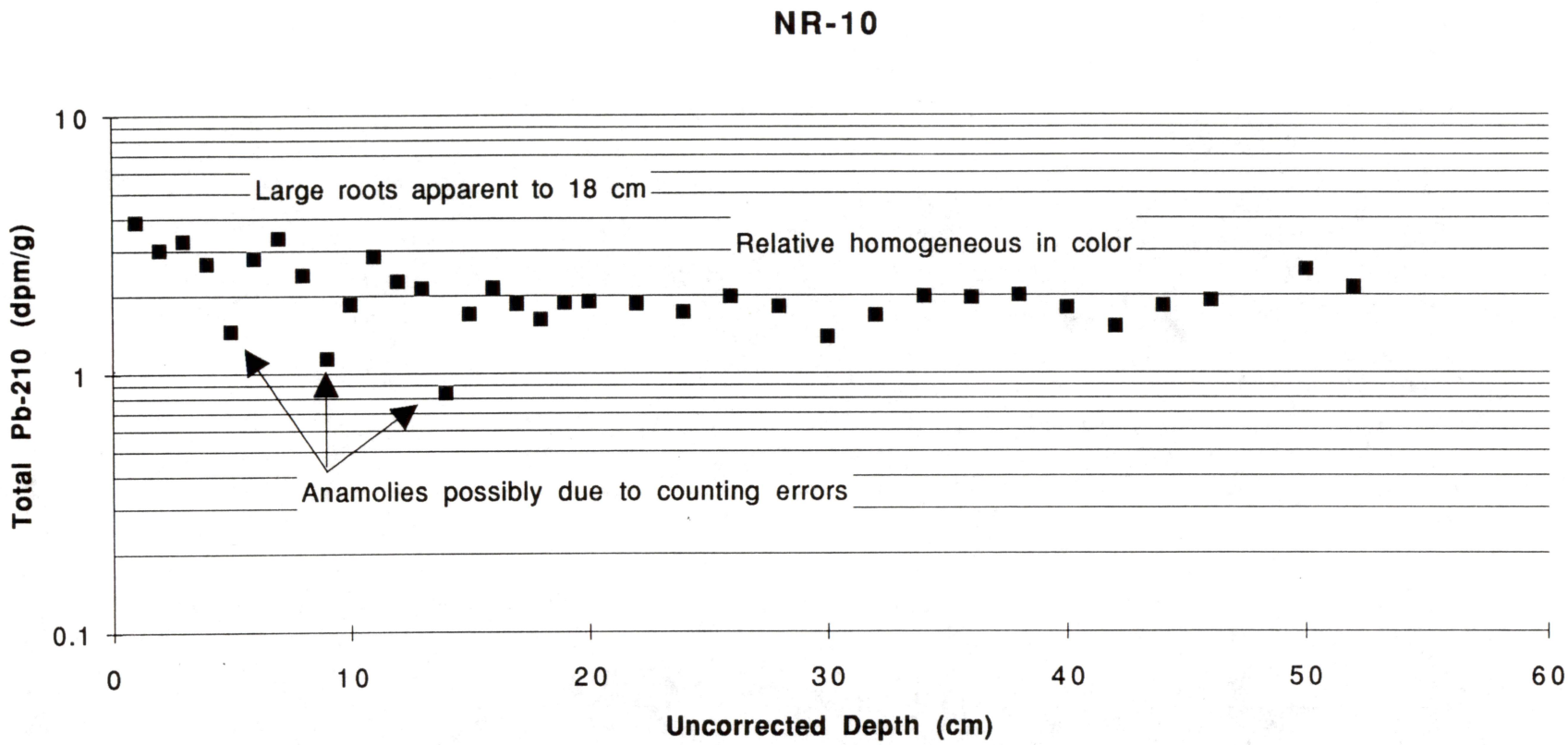


Figure 37. Core NR-10 annotated profile.

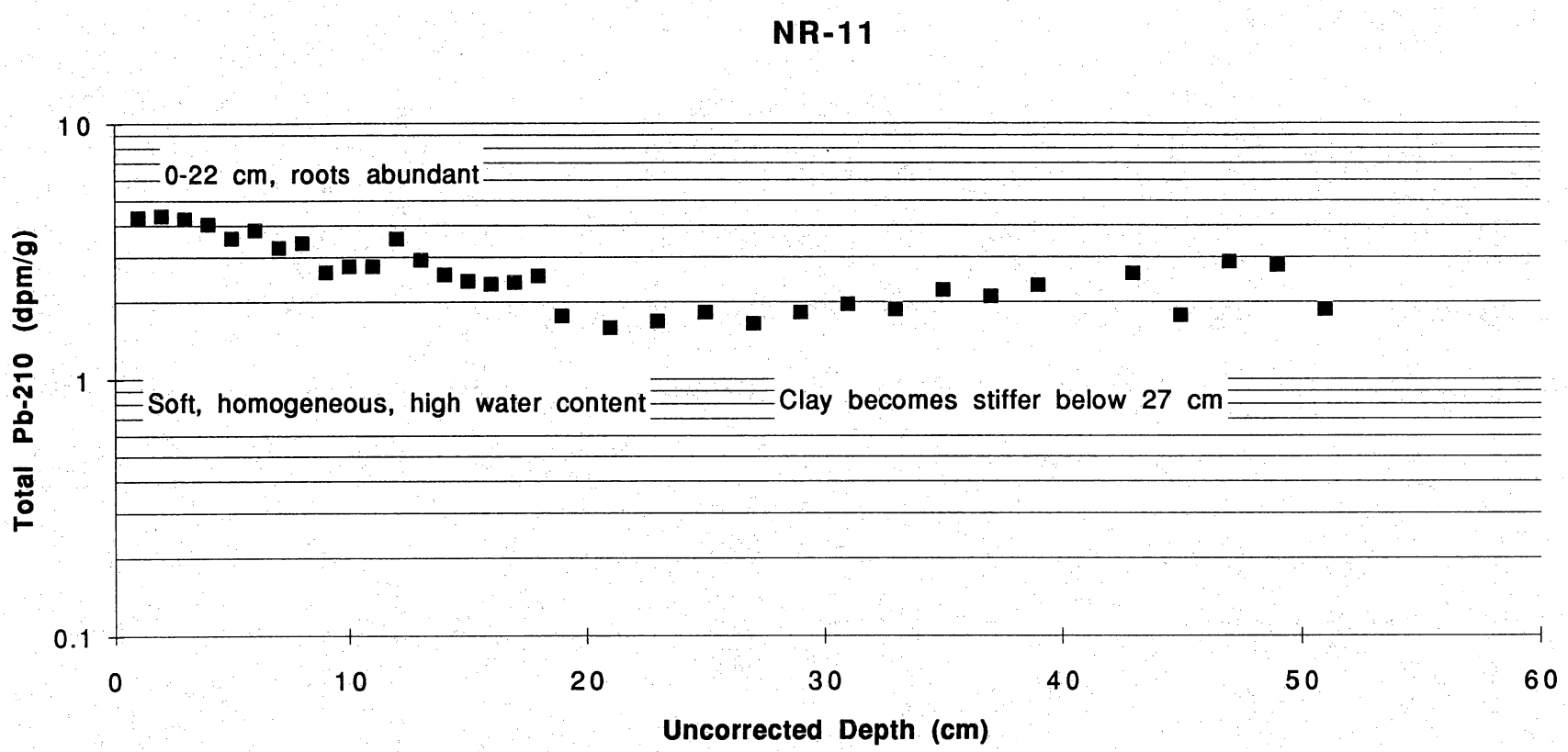


Figure 38. Core NR-11 annotated profile.

## RELATIVE SEA-LEVEL RISE

Relative sea-level rise as used here is the relative vertical rise in water level with respect to a datum at the land surface, whether it is caused by a rise in mean-water level or subsidence of the land surface. Along the Texas coast both processes eustatic sea-level rise and subsidence, are part of the relative sea-level rise equation. Subsidence, especially associated with pumpage of ground water and oil and gas, is the overriding component. As defined in this report, relative sea-level rise does not include the offsetting effects of vertical accretion.

### Eustatic Sea-Level Rise and Subsidence

Over the past century, sea level has been rising on a worldwide (eustatic) basis at a rate of about 1.2 mm/yr, with a rate in the Gulf of Mexico and Caribbean region of 2.4 mm/yr (Gornitz and others, 1982; Gornitz and Lebedeff, 1987). Adding compactional subsidence to these rates yields a relative sea-level rise that locally exceeds 10 mm/yr (Swanson and Thurlow, 1973; Penland and others, 1988).

Rates of "natural" compactional subsidence and eustatic sea-level rise, which together may range up to 12 mm/yr in the Galveston area (Swanson and Thurlow, 1973; Gornitz and Lebedeff, 1987; Penland and others, 1988), are locally dwarfed by human-induced subsidence, for example in the Houston area, where subsidence rates at some locations exceed 100 mm/yr (Gabrysch and Coplin, 1990). The major cause of human-induced subsidence is the withdrawal of underground fluids, principally ground water, oil, and gas (Pratt and Johnson, 1926; Winslow and Doyel, 1954; Gabrysch, 1969, 1984; Gabrysch and Bonnet, 1975; Kreitler, 1977; Verbeek and Clanton, 1981; Kreitler and others, 1988).

### Relative Sea-Level Rise in the Study Area

Tide gauge records and benchmark releveling surveys from the National Oceanic and Atmospheric Administration (NOAA) National Geodetic Survey (NGS) provide data for determining rates of relative sea-level rise in the Nueces River valley near Odem. Paine (1993) compiled data on vertical movement using regional first-order levelings conducted by NGS in the 1950s, late 1970s, and early

1980s. Vertical movement at each benchmark in the network was determined with reference to an arbitrarily chosen benchmark, F46 at Sinton (Paine, 1993). The geodetic network was referenced to sea level through leveling lines to tide gauge stations at Galveston, Rockport, and Port Isabel (fig. 39). These data provide relative sea-rise rates at benchmarks along the main leveling line that crosses the Nueces River valley south of Odem (fig. 40).

Rates of relative sea-level rise in millimeters per year for the period 1951–1982 were determined for five benchmarks along the MOPAC railroad that crosses the Nueces River valley just east of U.S. Highway 77, between Odem and Calallen (fig. 41 and table 8). Rates of relative sea-level rise were estimated relative to the tide gauge at Port Isabel because dates of leveling surveys between Algoa and Harlingen and Harlingen and Port Isabel were in close agreement, and use of the Port Isabel gauge did not require extrapolation from a benchmark several kilometers away as was necessary for the Rockport gauge (Paine, 1993). Rates of relative sea-level rise are also relative to the reference benchmark F46. Movement of tide gauges relative to F46 are shown in table 9.

Table 8. Rate of vertical movement relative to BM F46 (Sinton) for selected benchmarks along a leveling line that crosses the Nueces River valley at the Missouri-Pacific Railroad between Odem and Calallen just east of U.S. Highway 77. Positive change is upward relative to BM F46. Data from National Geodetic Survey as compiled by Paine (1993).

| NGS Benchmark | Rate of vertical movement of BM (mm/yr) 1951–1978 |
|---|---|
| Z175 | +7.10 |
| V175 | +0.80 |
| K46 | +1.63 |
| P176 | +0.71 |
| R176 | +16.73 |

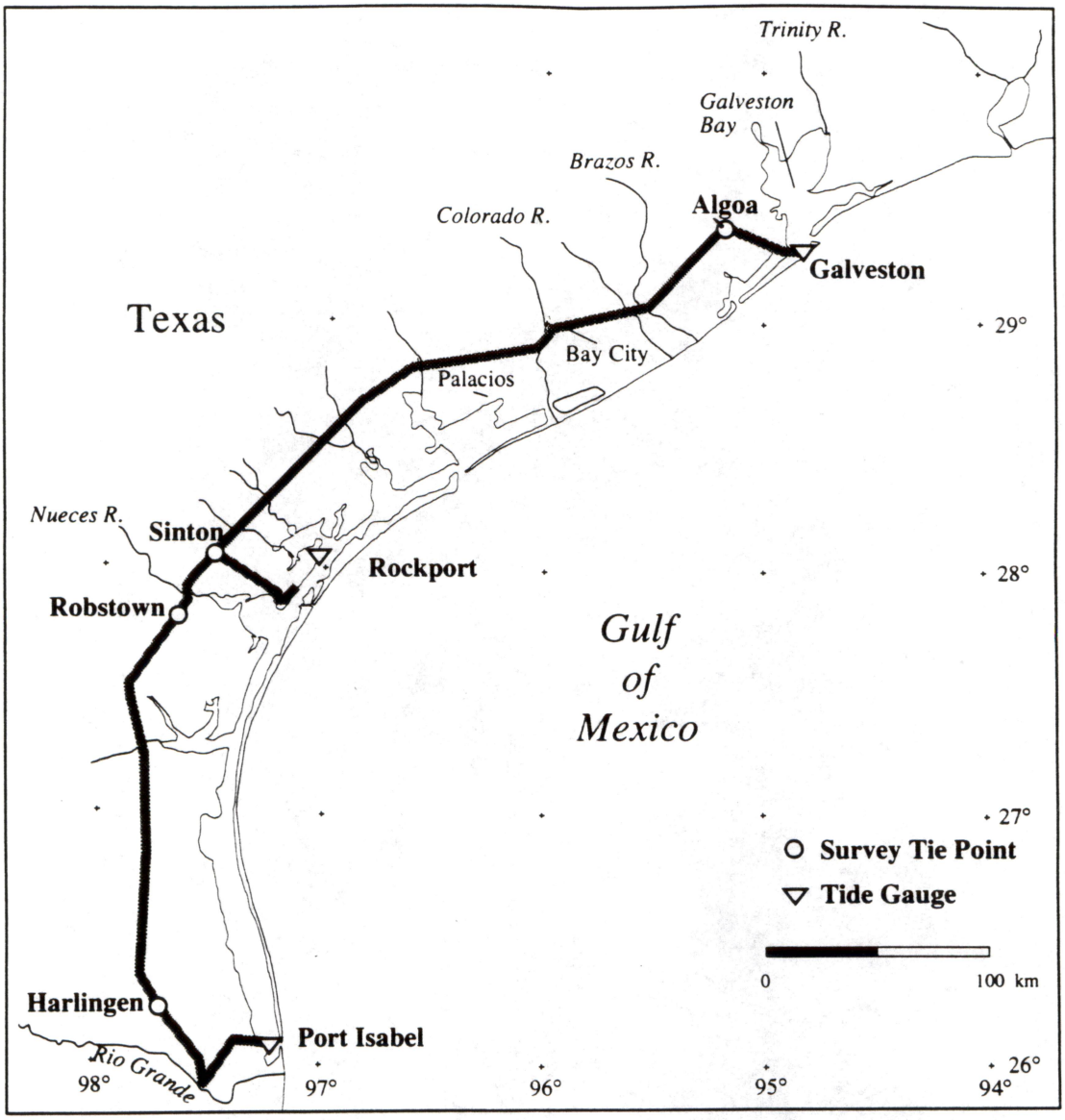


Figure 39. Location of National Geodetic Survey leveling lines and National Ocean Survey tide gauges. From Paine (1993).

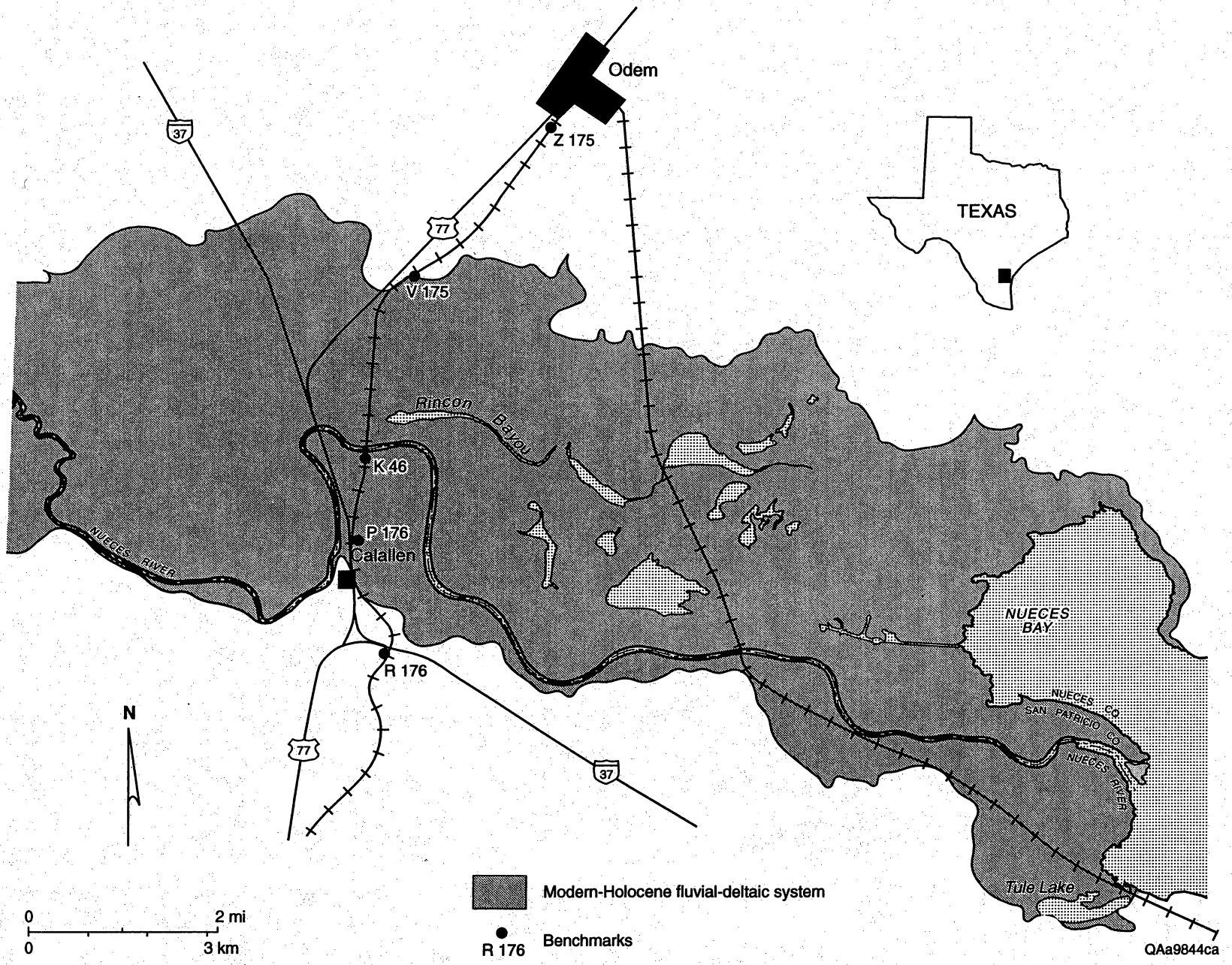


Figure 40. Location of benchmarks along leveling line across the Nueces River south of Odem.

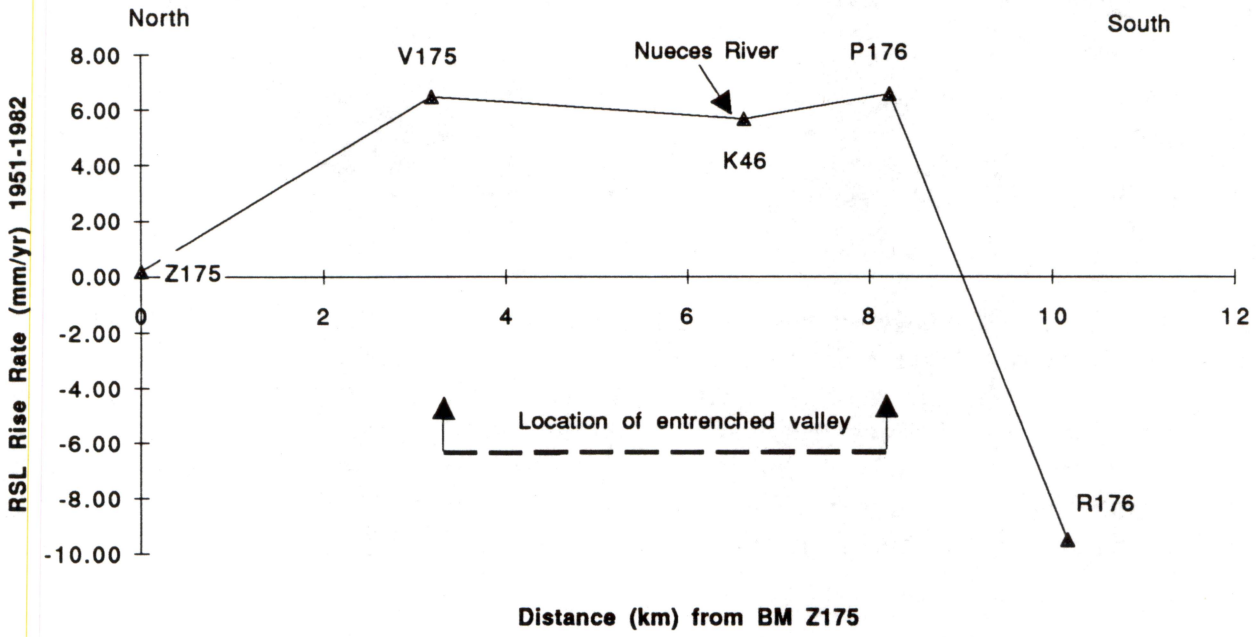


Figure 41. Rates of relative sea-level rise between 1951 and 1978 to 1982 along a line crossing the Nueces River valley south of Odem. Based on data from Paine (1993).

Table 9. Rates of vertical movement relative to NGS benchmark F46 and rates of relative sea-level rise at the Port Isabel, Rockport, and Galveston Pier 21 gauges. From Paine (1993).

| Tide gauge | Vertical movement relative to F46 (mm/yr) | Relative sea-level rise rate 1951 to 1982 (mm/yr) | Relative sea-level rise rate relative to F46 (mm/yr) |
|---|---|---|---|
| Port Isabel | +2.7 | 4.6 | 7.3 |
| Rockport | +2.2 | 5.4 | 7.6 |
| Galveston Pier 21 | -2.3 | 8.2 | 5.9 |

Table 10. Relative sea-level rise rates for selected benchmarks along a line that crosses the Nueces River valley between Odem and Calallen. Rates are relative to the Port Isabel tide gauge and benchmark F46 (Sinton) and were determined by adding the relative sea-level rise rate (equivalent to a negative vertical movement of the land surface) at the Port Isabel gauge (table 9) with the vertical movement of benchmarks shown in table 8. These data are from Paine (1993). See figure 40 for location of benchmarks and figure 41 for plot of rates of relative sea-level rise.

| NGS benchmark | RSL rate (mm/yr) 1951-1982 |
|---|---|
| Z175 | 0.2 |
| V175 | 6.5 |
| K46 | 5.7 |
| P176 | 6.6 |
| R176 | -9.4 |

For the period of 1951 to 1982, rates at benchmarks on the north and south edges of the Nueces River valley were about 6.5 mm/yr (table 10 and fig. 41). Rates are considerably lower at benchmarks further north and south, and, in fact, BM R176 to the south moved upward relative to BM F46 and the Port Isabel tide gauge; the relative rate of sea-level rise at this benchmark is –9.4 mm/yr, indicating a rise in the land surface relative to sea level (table 10).

The rate of 5.7 mm/yr at benchmark K46 on the south bank of the Nueces River is similar to the RSL rate of 5.4 mm/yr for the Rockport tide gauge for the period 1951–1982. This rate (5.7 mm/yr) exceeds the Gulf of Mexico mean sea-level rise rate by a factor of about 2 to 5, based on the regional Gulf of Mexico rate of 2.4 mm/yr and the eustatic rate of 1.2 mm/yr, respectively (Gornitz and Lebedeff, 1987). The accelerated rates of sea-level rise are apparently related to subsidence, much of which may be the result of regional oil and gas production and depressurization (Paine, 1993). Subsidence and faulting associated with the Saxet oil and gas field west of Corpus Christi are well documented (Gustavson and Kreitler, 1976; Hillenbrand, 1985). NGS benchmark releveling data reported by Brown and others (1976) show subsidence of approximately 6.7 mm/yr from 1942 to 1951, encompassing an area of 389 $km^2$ north and northeast of Corpus Christi, an area that includes the Nueces River alluvial valley and delta south of U.S. Highway 77 (fig. 42).

### Relative Sea-Level Rise at Coring Sites

Because rates of relative sea-level rise can be locally affected by subsidence associated with oil and gas production, it is difficult to determine with certainty the rates at locations away from the benchmark releveling line. Historically, wetland loss has been most extensive near the bayward reaches of the Nueces River delta (White and Calnan, 1990). Between the 1930s and 1979, approximately 130 ha of emergent vegetation was converted to open water and barren flats. Progradation of the Nueces River delta into Nueces Bay ended sometime between 1930 and 1959 (Morton and Paine, 1984). Subsidence and reductions in the volume of fluvial sediments delivered by the Nueces River as a result of upstream dams may account for the retreating shoreline and loss of interior emergent vegetation (White and Calnan, 1990). Still, without benchmark releveling data down the valley, it is not possible to determine if subsidence is occurring at a higher rate nearer to Nueces Bay. As mentioned, the closest tide gauge station with a sufficient period of record is at Rockport, where the relative sea-level rise rate for the period 1951–1982 is 5.4 mm/yr (Paine, 1993) and from the 1940s to 1980s, 4.5 mm/yr (fig. 15).

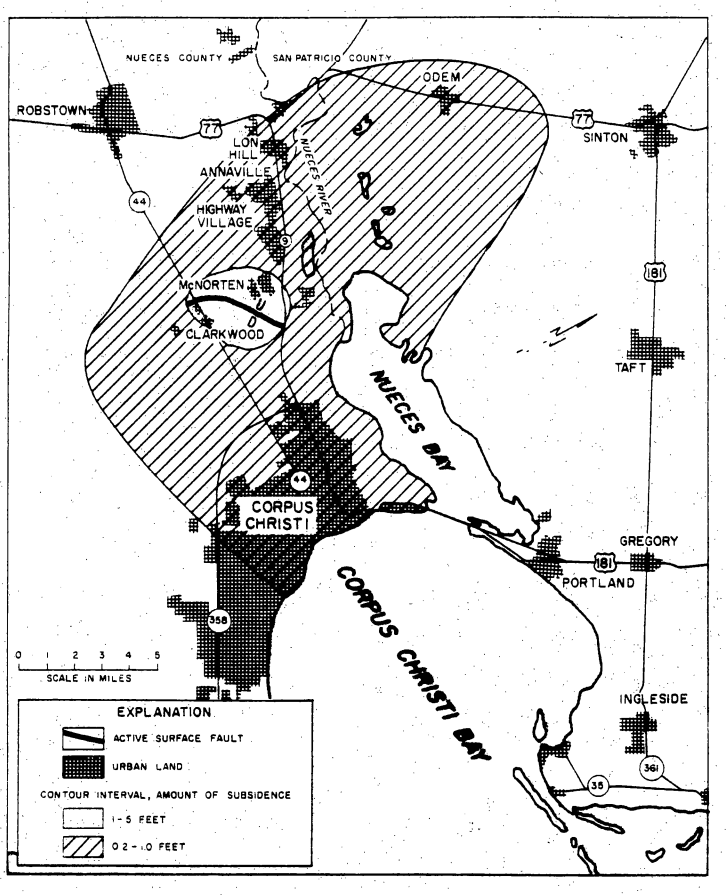


Figure 42. Land-surface subsidence in the Corpus Christi area (1942–1951). Level data from NOAA. After Brown and others (1976). Subsidence probably caused by oil and gas production.

Our best information on rates of relative sea-level rise are provided by the benchmark releveling surveys and tide gauges, which indicate that rates near U.S. Highway 77 are about 6 mm/yr in the Nueces River valley and about 6.5 mm/yr on the valley margins. This releveling line is closest to coring sites NR-6, NR-7, and NR-10 (fig. 1); however, we suggest that a relative sea-level rise rate of at least 6.5 mm/yr be used for all sites in the study area.

## CONCLUSIONS

Excess $^{210}Pb$ activity decreases exponentially with depth. Most of the profiles of log normal activity versus depth exhibit few departures from linear relationships. A "flattening" of the $^{210}Pb$ profile occurs in most cores where background activities (supported $^{210}Pb$) are reached at depths typically below 20 cm. Some variations in excess $^{210}Pb$ activity appear to correspond to physical or chemical variations in the sediments such as changes in organic and textural content. Isolated samples that plot considerably outside linear trends of other samples (possibly as a result of counting errors) should be examined individually for possible exclusion from calculations. Subtle variations in excess $^{210}Pb$ activity may signify a relationship between flooding and sedimentation, which hopefully can be defined by the Texas Water Board's model (Longley, 1992b). Because most cores from the Nueces River underwent some shortening during coring, corrected depths should be used in determining sedimentation rates unless rates are based on cumulative inorganic mass.

Preliminary analysis of excess $^{210}Pb$ activities, including cumulative inventories, indicates that these data should provide useable dates and sedimentation rates for comparison with river discharge information. Preliminary estimates of dates and sedimentation rates in several cores indicate some interesting trends. For example, in core NR-1, different models (CFS, CRS, and CIC) yield equivalent sedimentation rates of 0.06 cm/yr. This is the lowest measured rate in all cores and is supported by archeological evidence collected near the site. One of the highest rates of sedimentation was at core site NR-11, an intertidal *Spartina alterniflora* marsh on the edge of Nueces Bay and the Nueces River. The average

rate of sedimentation at this site is 0.45 cm/yr, which is equivalent to the rate of relative sea-level rise for a similar period (1940s to 1990s) at the Rockport tide gauge. Average rates of sedimentation based on CFS and CIC models are in agreement in all cores. Average sedimentation rates based on all three models—CFS, CIC, and CRS—are in agreement in five cores.

Using the CFS model, the calculated rate of sediment accumulation in all cores decreases after about 1930, suggesting that impoundment of Lake Corpus Christi in 1929 was responsible. The CRS model flags more recent events in several cores, indicating a period of higher sedimentation from 1960 to 1975 and a lower rate (50 percent lower) after 1975. This decreasing rate correlates with decreasing sediment load along the Nueces River and a lower rate of relative sea-level rise as documented by the Rockport tide gauge. The period 1960 to 1975 was influenced by three hurricanes that impacted the area, Hurricanes Carla (1961), Beulah (1967), and Fern (1971). Hurricane Carla was characterized by high storm surge that flooded the Nueces River valley and all coring sites, and Hurricane Beulah was characterized by high rainfall and extensive fresh-water flooding. Streamflow peaks recorded at the Mathis stream-gauging station in 1967 and 1971 documented the high rainfall that occurred during these years.

Supported $^{210}Pb$ levels vary from core to core and in a single core depending on whether average activities of $^{226}Ra$ or constant activities of $^{210}Pb$ at depth are used to determine the level of supported $^{210}Pb$. The supported $^{210}Pb$ levels determined by both methods should be considered.

Benchmark releveling lines indicate that the lower Nueces River valley is subsiding. For the purpose of determining offsetting sedimentation rates, it is recommended that a relative sea-level rise rate of at least 6.5 mm/yr be used for all coring sites.

## ACKNOWLEDGMENTS

Funding for this study was provided by the Texas Water Development Board under Research and Planning Fund Grant Contract No. 95-483-075. Cores were analyzed for isotopic elements, weight loss-on-ignition, water content, mineral matter, bulk density, and texture by Dr. Charles Holmes of the U.S. Geological Survey, Denver. Bulk density and sediment salinities were analyzed by Steve Tweedy, Chemist in Charge of the BEG Mineral Studies Laboratory. Word processing was by Susan Lloyd, and proofreading and editing were by Jeannette Miether. Pasteup of figures was by Susan Lloyd. Drafted figures were by Nancy Cottington under the direction of Chief Cartographer, Richard L. Dillon. Others providing assistance in the Bureau's Core Research Center included George Bush, Alex Colunga, James Donnelly, and Robert Sanchez. Bill Longley (TWDB) provided data on river flow and sediment load of the Nueces River. The authors are especially grateful to numerous landowners in the study area who gave permission to enter their property and take cores. Michael Irlbeck, Bureau of Reclamation, and James Dodson, City of Corpus Christi, were very helpful in providing names of landowners and maps of their properties.

## REFERENCES

Appleby, P. G., Nolan, P. J., Oldfield, F., Richardson, N., and Higgitt, S. R., 1988, $^{210}Pb$ dating of lake sediments and ombrotrophic peats by gamma essay: The science of the total environment, special issue, v. 69, p. 157–177.

Brenner, M., Peplow, A. J., and Schelske, C. L., 1994, Disequilibrium between $^{226}Ra$ and supported $^{210}Pb$ in a sediment core from a shallow Florida Lake: Limnology and Oceanography, v. 39, no. 5, p. 1222–1227.

Brown, L. F., Jr., Brewton, J. L., McGowen, J. H., Evans, T. J., Fisher, W. L., and Groat, C. G., 1976, Environmental geologic atlas of the Texas Coastal Zone—Corpus Christi area: The University of Texas at Austin, Bureau of Economic Geology, 123 p., 9 maps.

Brune, G. M., 1953, Trap efficiency of reservoirs: Transactions of the American Geophysical Union, v. 34, p. 407-418.

Church, T. M., Lord, C. J., III, and Somayajulu, B. L. K., 1981, Uranium, thorium, lead nuclides in a Delaware salt marsh sediment: Estuarine, Coastal and Shelf Science, v. 13, p. 267–275.

Duxbury, A. C., 1971, The earth and its oceans: Reading, Massachusetts, Addison-Wesley Publishing Company, 381 p.

Flynn, W. W., 1968, The determination of low levels of polonium-210 in environmental materials: Analytica Chimica Acta, v. 43, p. 221–227.

Gabrysch, R. K., 1969, Land-surface subsidence in the Houston–Galveston region, Texas: United Nations Educational, Scientific and Cultural Organization (UNESCO), Studies and Reports in Hydrology, Land Subsidence Symposium, v. 1, p. 43–54.

_____ 1984, Ground-water withdrawals and land-surface subsidence in the Houston–Galveston region, Texas, 1906–1980: Texas Department of Water Resources Report 287, 64 p.

Gabrysch, R. K., and Bonnet, C. W., 1975, Land-surface subsidence in the Houston–Galveston region, Texas: Texas Water Development Board, Report 188, 19 p.

Gabrysch, R. K., and Coplin, L. S., 1990, Land-surface subsidence resulting from ground-water withdrawals in the Houston–Galveston region, Texas, through 1987: U.S. Geological Survey Report of Investigations No. 90-01, 53 p.

Gornitz, V., and Lebedeff, S., 1987, Global sea-level changes during the past century: Society of Economic Paleontologists and Mineralogists, Special Publication No. 41, p. 3–16.

Gornitz, V., Lebedeff, S., and Hansen, J., 1982, Global sea level trend in the past century: Science, v. 215, p. 1611–1614.

Gustavson, T. C., and Kreitler, C. W., 1976, Geothermal resources of the Texas Gulf coast—environmental concerns arising from the production and disposal of geothermal waters: The University of Texas at Austin, Bureau of Economic Geology Geological Circular 76-7, 35 p.

Hillenbrand, C. J., 1985, Subsidence and fault activation related to fluid extraction Saxet Field, Nueces County, Texas: University of Houston, Master's thesis, 144 p.

Holland, J. S., Maciolek, N. J., Kalke, R. D., and Oppenheimer, C. H., 1975, A benthos and plankton study of the Corpus Christi, Copano, and Aransas Bay systems: report on data collected during the period July 1974–May 1975 and summary of the three-year project: The University of Texas at Port Aransas Marine Science Institute, Final report to the Texas Water Development Board, 171 p.

Holmes, C. W., and Martin, E. A., 1976, Rates of sedimentation, *in* Holmes, C. W., and others, Environmental studies, South Texas Outer Continental Shelf, 1976, Geology report for the Bureau of Land Management prepared by the U.S. Geological Survey, 626 p.

Kreitler, C. W., 1977, Faulting and land subsidence from ground-water and hydrocarbon production, Houston–Galveston, Texas: The University of Texas at Austin, Bureau of Economic Geology Research Note 8, 22 p.

Kreitler, C. W., White, W. A., and Akhter, M. S., 1988, Land subsidence associated with hydrocarbon production, Texas Gulf Coast (abs.): American Association of Petroleum Geologists Bulletin, v. 72, no. 2, p. 208.

Liebbrand, N. F., 1987, Estimated sediment deposition in Lake Corpus Christi, Texas, 1972–1985: U.S. Geological Survey Open-File Report 87-239, 26 p.

Longley, W. L., 1992a, Freshwater inflow to Texas bays and estuaries: ecological relationships and methods for determining needs: Texas Water Development Board and Texas Parks and Wildlife Department, 366 p.

_____ 1992b, Analytical approach to determine sediment requirements for maintenance of the Trinity River delta: Texas Water Development Board proposal document, 5 p.

Martin, E. A., and Rice, C. A., 1981, $^{210}Pb$ geochronology and trace metal concentrations of sediments from Upper Klamath Lake and Lake Euwana, Oregon: Northwest Science, v. 55, no. 4, p. 269–280.

McCaffrey, R. J., 1977, A record of the accumulation of sediment and trace metals in a Connecticut, U.S.A., salt marsh: Yale University, Ph.D. dissertation, 156 p.

Morton, R. A., and Paine, J. G., 1984, Historical shoreline changes in Corpus Christi, Oso, and Nueces Bays, Texas Gulf Coast: The University of Texas at Austin, Bureau of Economic Geology Geological Circular 84-6, 66 p.

Nicolau, B. A., 1995, Estuarine faunal use in a mitigation project, Nueces River delta, Texas: year five: Texas A&M University–Corpus Christi, Center for Coastal Studies, 107 p.

Nicolau, B. A., and Adams, J. S., 1993, Estuarine faunal use in a mitigation project, Nueces River delta, Texas: years two and three: Texas A&M University–Corpus Christi, Center for Coastal Studies, 114 p.

Nittrouer, C. A., Sternberg, R. W., Carpenter, R., and Bennett, J. T., 1979, The use of Pb-210 geochronology as a sedimentological tool: application to the Washington continental shelf: Marine Geology, v. 31, p. 297–316.

Oldfield, F., and Appleby, P. G., 1984, Empirical testing of $^{210}$Pb-dating models for lake sediments, *in* Haworth, E. Y., and Lund, J. W. G., eds., Lake sediments and environmental history: Minneapolis, Minnesota, University of Minnesota Press, p. 93–124.

Paine, J. G., 1993, Subsidence in the Texas coast: inferences from historical and late Pleistocene sea levels: Tectonophysics, v. 222, p. 445–458.

Penland, Shea, Ramsey, K. E., McBride, R. A., Mestayer, J. T., and Westphal, K. A., 1988, Relative sea level rise and delta-plain development in the Terrebone Parish region: Baton Rouge, Louisiana Geological Survey, Coastal Geology Technical Report No. 4, 121 p.

Pratt, W. E., and Johnson, D. W., 1926, Local subsidence of the Goose Creek oil field: Journal of Geology, v. 34, p. 577–590.

Robbins, J. A., 1978, Geochemical and geophysical applications of radioactive lead, *in* Nriagu, J. O., ed., The biogeochemistry of lead in the environment, Part A. Ecological cycles: New York, Elsevier/North-Holland Biomedical Press, chap. 9, p. 285–393.

Robbins, J. A., Edgington, D. N., and Kemp, A. L. W., 1978, Comparative $^{210}$Pb, $^{137}$Cs, and pollen geochronologies of sediments from Lakes Ontario and Erie: Quaternary Research, v. 10, p. 256–278.

Ruth, B. F., 1990, Establishment of estuarine faunal use in a salt marsh creation project, Nueces River delta, Texas: Texas A&M University-Corpus Christi, Center for Coastal Studies, 51 p.

Starkey, H. C., Blackmon, P. D., and Hauff, P. L., 1984, The routine mineralogical analysis of clay-bearing samples: U.S. Geological Survey Bulletin 1563, 32 p.

Swanson, R. L., and Thurlow, C. I., 1973, Recent subsidence rates along the Texas and Louisiana coasts as determined from tide measurements: Journal of Geophysical Research, v. 78, no. 5, p. 2665–2671.

Texas Department of Water Resources, 1981, Nueces and Mission-Aransas estuaries: a study of the influence of freshwater inflows: Texas Department of Water Resources, LP-108, 308p.

Verbeek, E. R., and Clanton, U. S., 1981, Historically active faults in the Houston metropolitan area, Texas, *in* Etter, E. M., ed., Houston area environmental geology: surface faulting, ground subsidence, hazard liability: Houston Geological Society, p. 28–68.

White, W. A., and Calnan, T. C., 1990, Sedimentation and historical changes in fluvial-deltaic wetlands along the Texas Gulf Coast with emphasis on the Colorado and Trinity River deltas: The University of Texas at Austin, Bureau of Economic Geology, report prepared for the Texas Parks and Wildlife Department and Texas Water Development Board under interagency contract (88-89) 1423, 124 p., 6 appendices.

White, W. A., and Calnan, T. C., 1991, Submergence of vegetated wetlands in fluvial-deltaic areas, Texas Gulf Coast, *in* Coastal depositional systems in the Gulf of Mexico: Quaternary framework and environmental issues: 12th Annual Research Conference, Society of Economic Paleontologists and Mineralogists, Gulf Coast Section, Houston, Texas, p. 278–279.

White, W. A., Calnan, T. C., Morton, R. A., Kimble, R. S., Littleton, T. G., McGowen, J. H., Nance, H. S., and Schmedes, K. S., 1983, Submerged lands of Texas, Corpus Christi area: sediments, geochemistry, benthic macroinvertebrates, and associated wetlands: The University of Texas at Austin, Bureau of Economic Geology Special Publication, 154 p.

White, W. A., and Morton, R. A., 1993, Determining recent sedimentation rates of the Trinity River, Texas: The University of Texas at Austin, Bureau of

Economic Geology, report prepared for the Texas Water Development Board under interagency contract no. 93-483-356, 50 p., 3 appendices.

White, W. A., and Morton, R. A., 1995, Determining recent sedimentation rates of the Lavaca-Navidad River System, Texas: The University of Texas at Austin, Bureau of Economic Geology, report prepared for the Texas Water Development Board under interagency contract no. 93-483-013, 76 p., 5 appendices.

Winslow, A. G., and Doyel, W. W., 1954, Land-surface subsidence and its relation to the withdrawal of ground water in the Houston–Galveston region, Texas: Economic Geology, v. 49, no. 4, p. 413–422.

# APPENDIX A

## Core Shortening Analysis

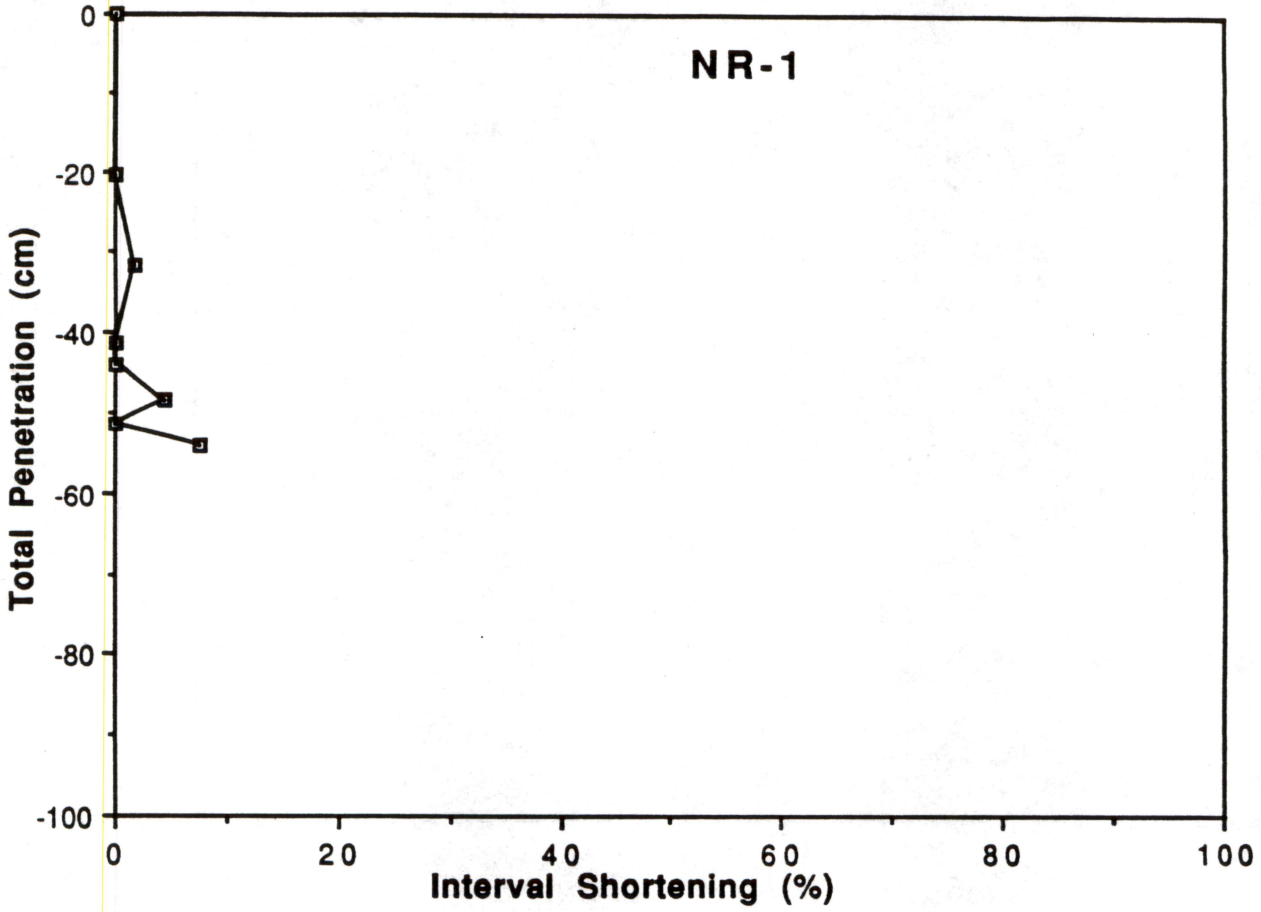
NR-1
Total Penetration (cm)
0
-20
-40
-60
-80
-100
0
20
40
60
80
100
Interval Shortening (%)

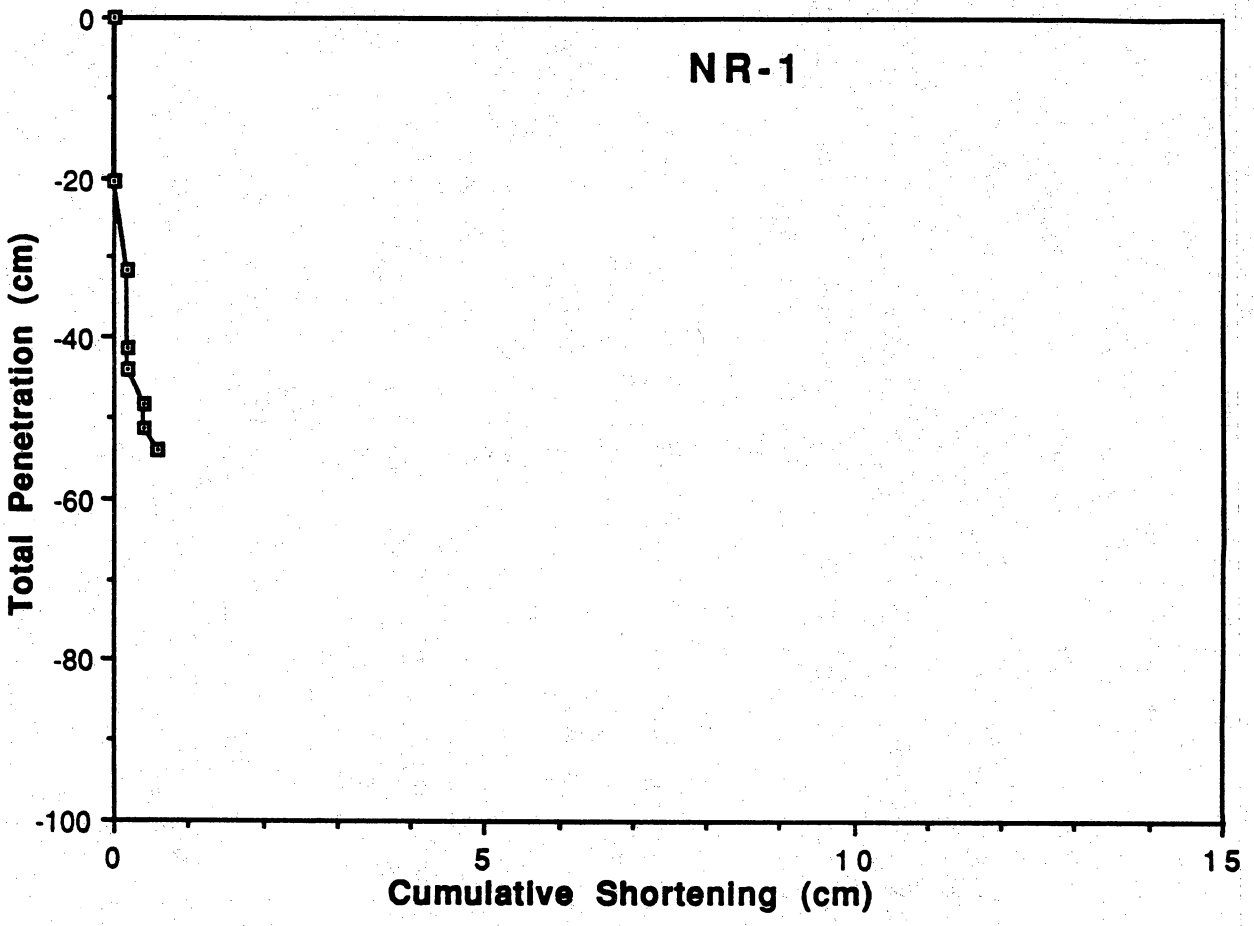
NR-1
0
-20
-40
-60
-80
-100
Total Penetration (cm)
0
5
10
15
Cumulative Shortening (cm)

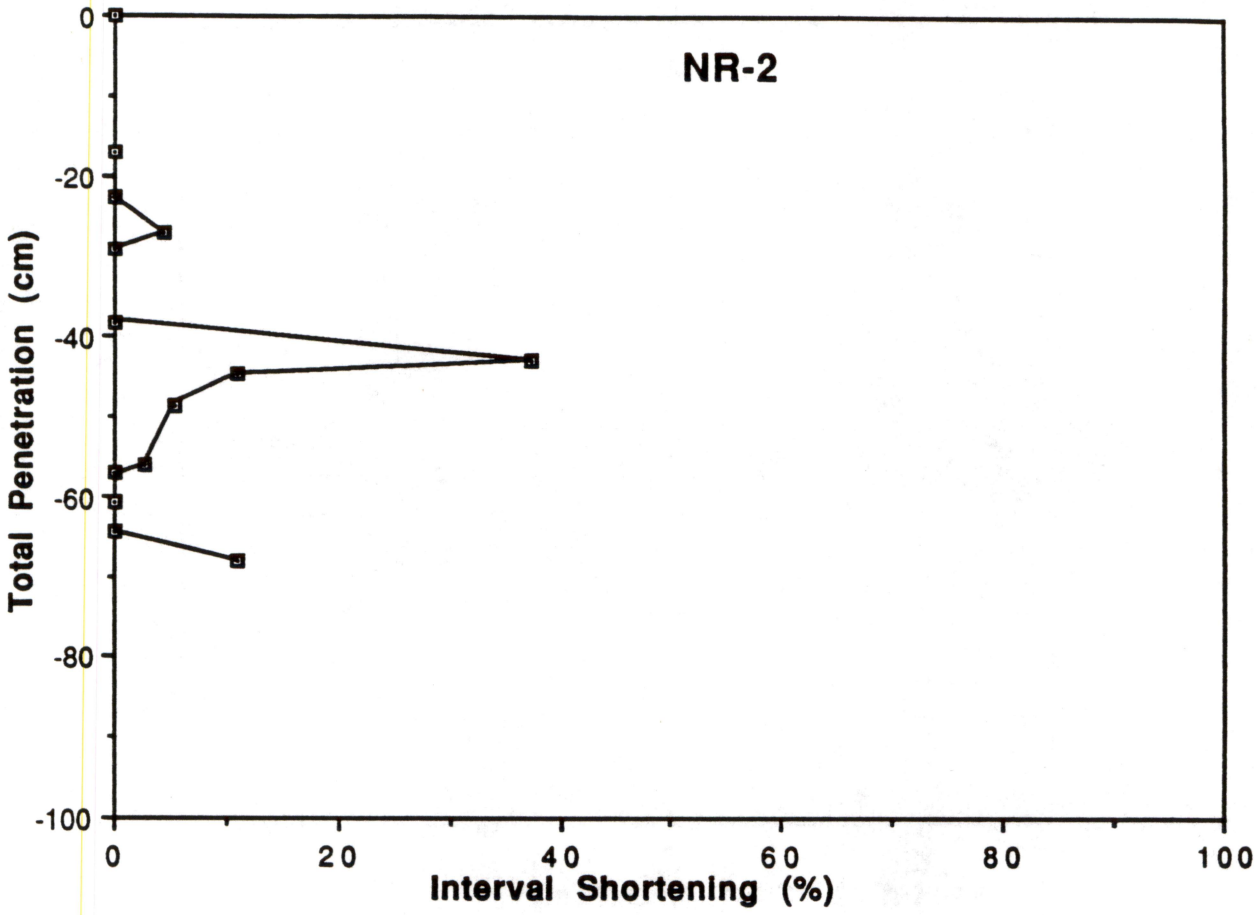
NR-2
Total Penetration (cm)
0
-20
-40
-60
-80
-100
0
20
40
60
80
100
Interval Shortening (%)

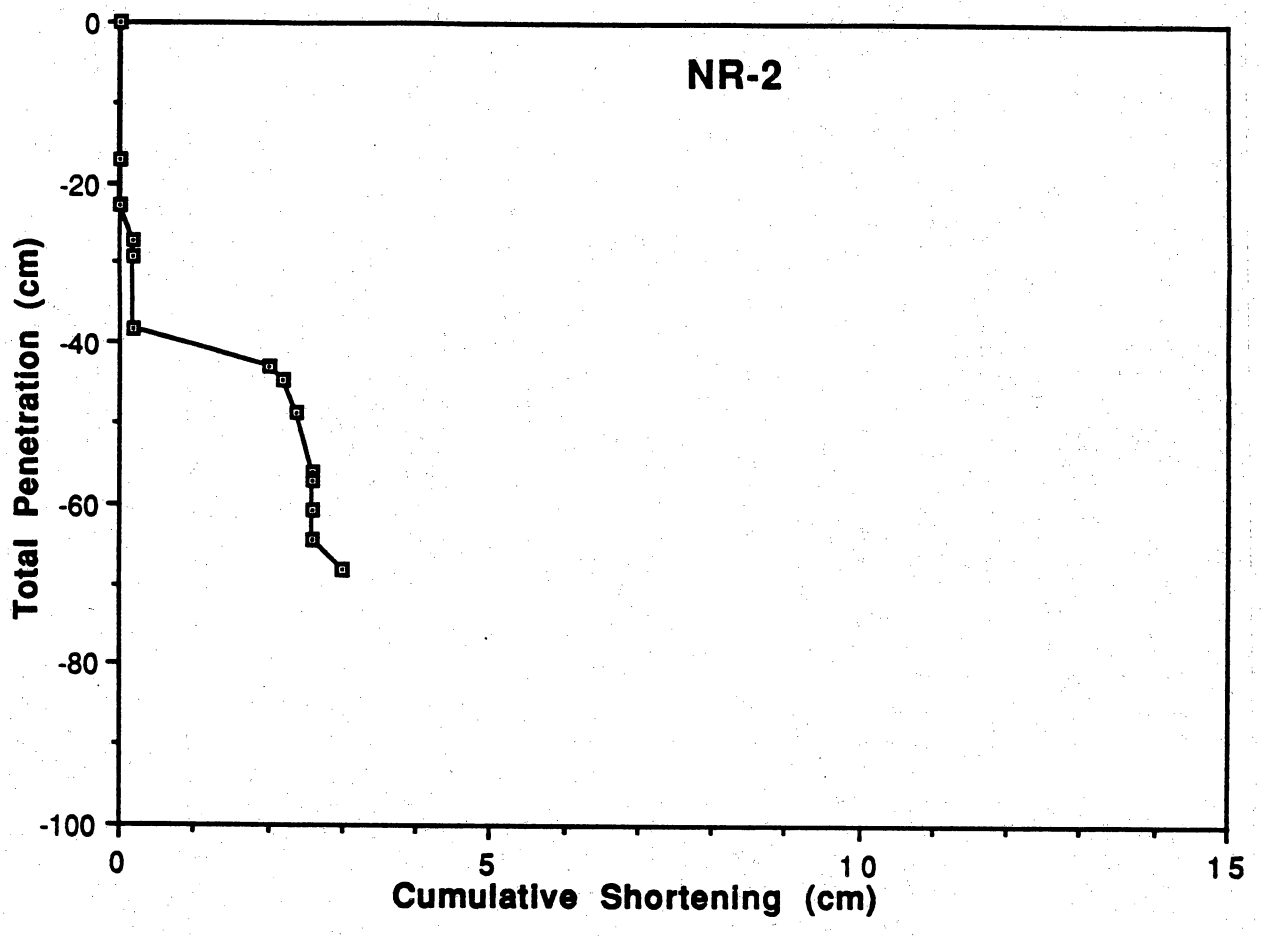
NR-2
0
-20
-40
-60
-80
-100
Total Penetration (cm)
0
5
10
15
Cumulative Shortening (cm)

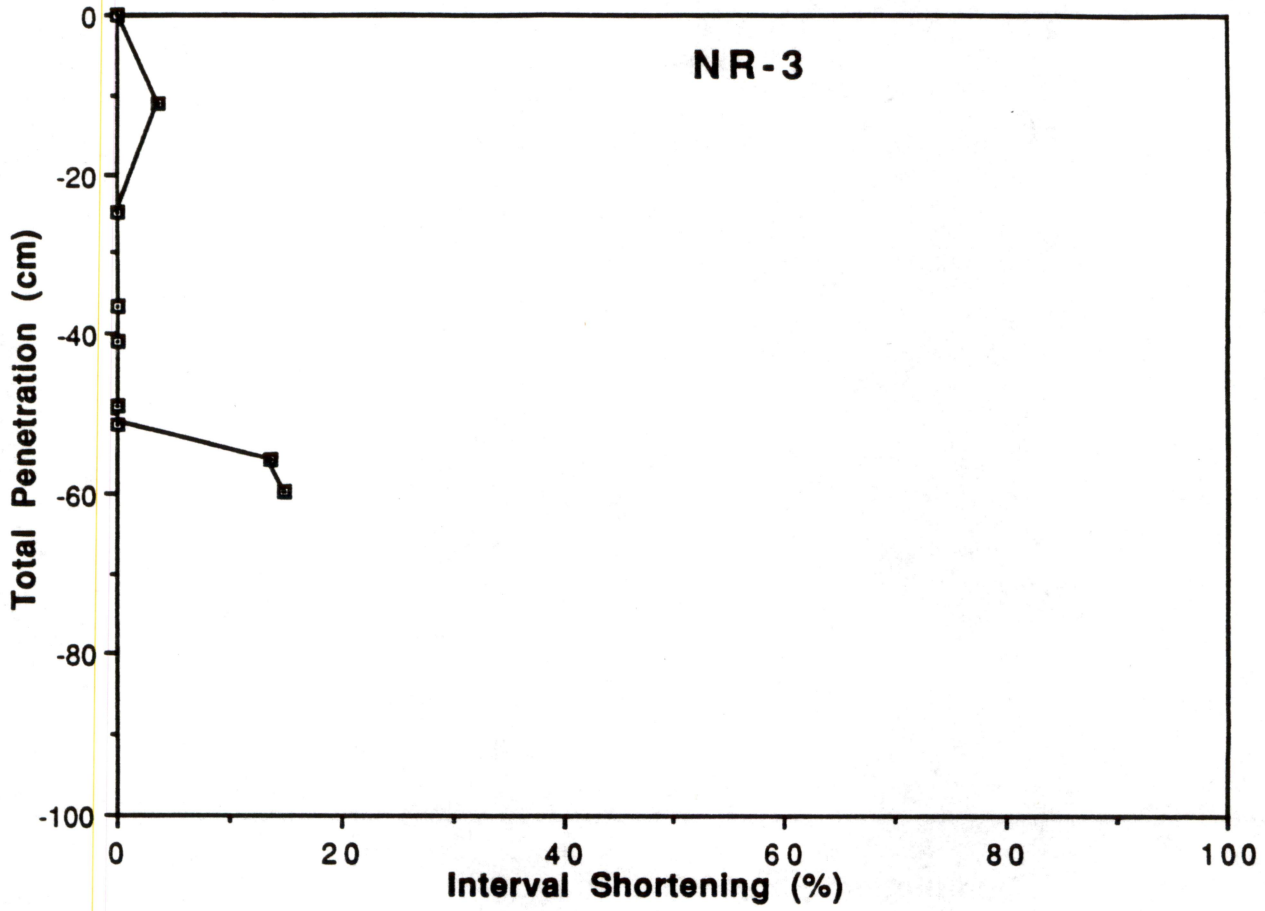
NR-3
Total Penetration (cm)
0
-20
-40
-60
-80
-100
0
20
40
60
80
100
Interval Shortening (%)

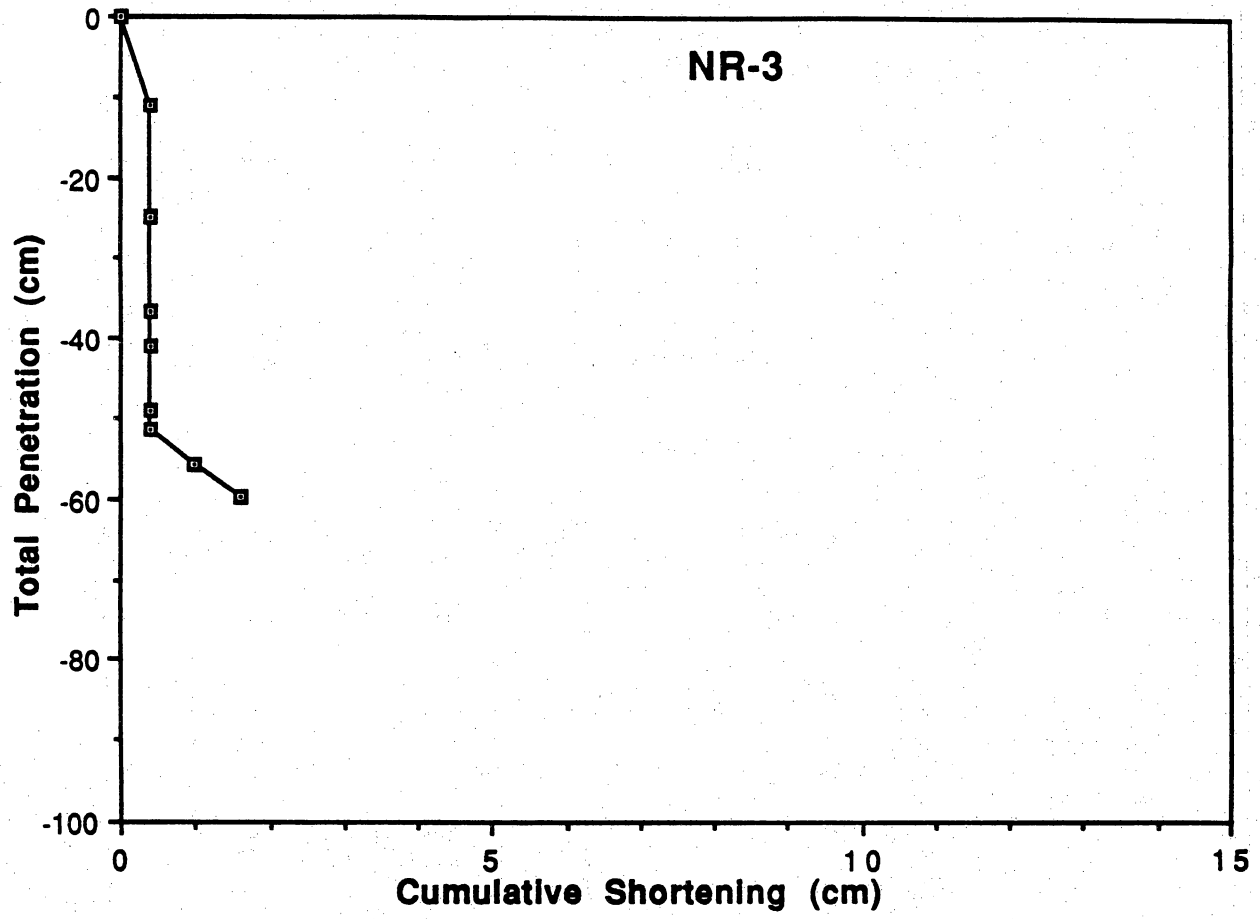
NR-3
0
-20
-40
-60
-80
-100
Total Penetration (cm)
0
5
10
15
Cumulative Shortening (cm)

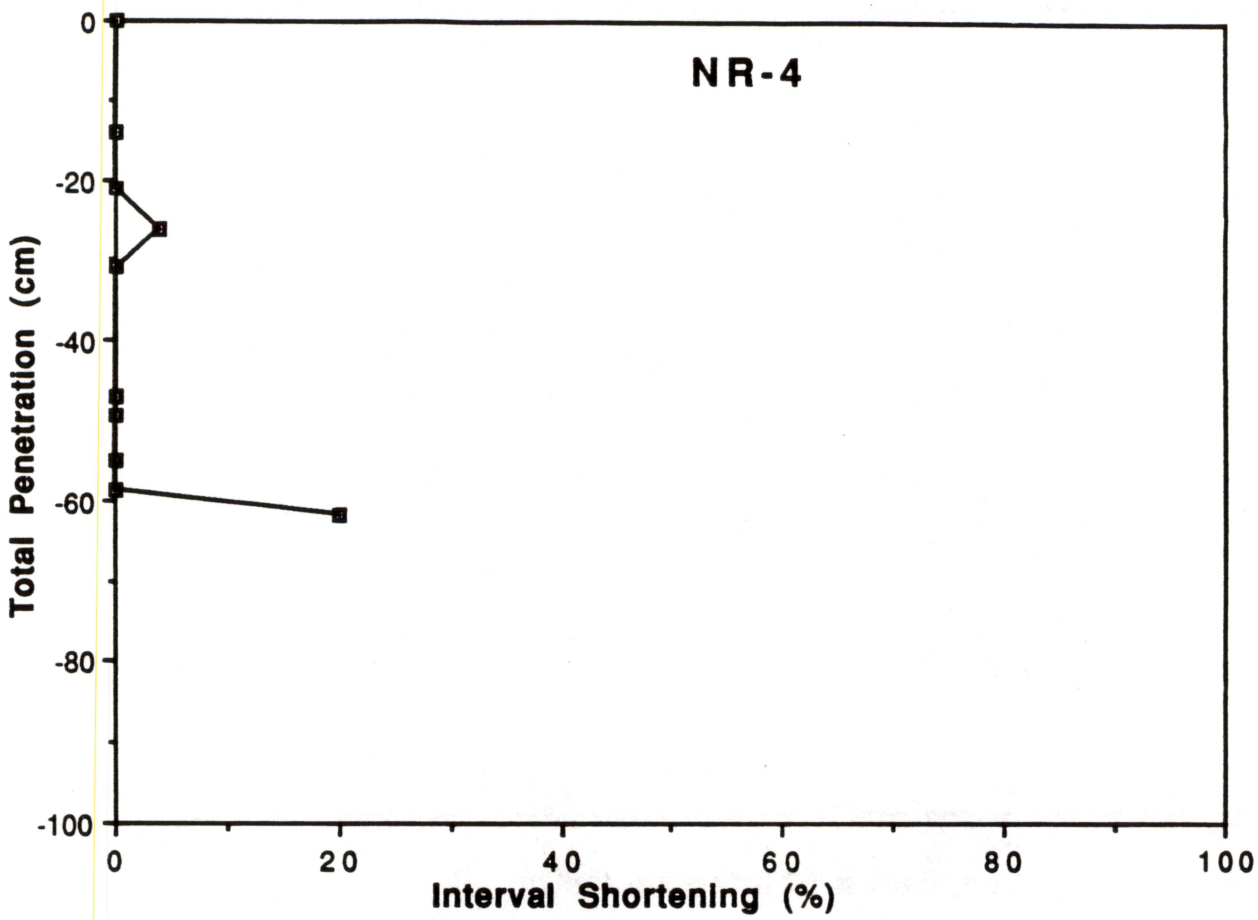
NR-4
0
-20
-40
-60
-80
-100
Total Penetration (cm)
0
20
40
60
80
100
Interval Shortening (%)

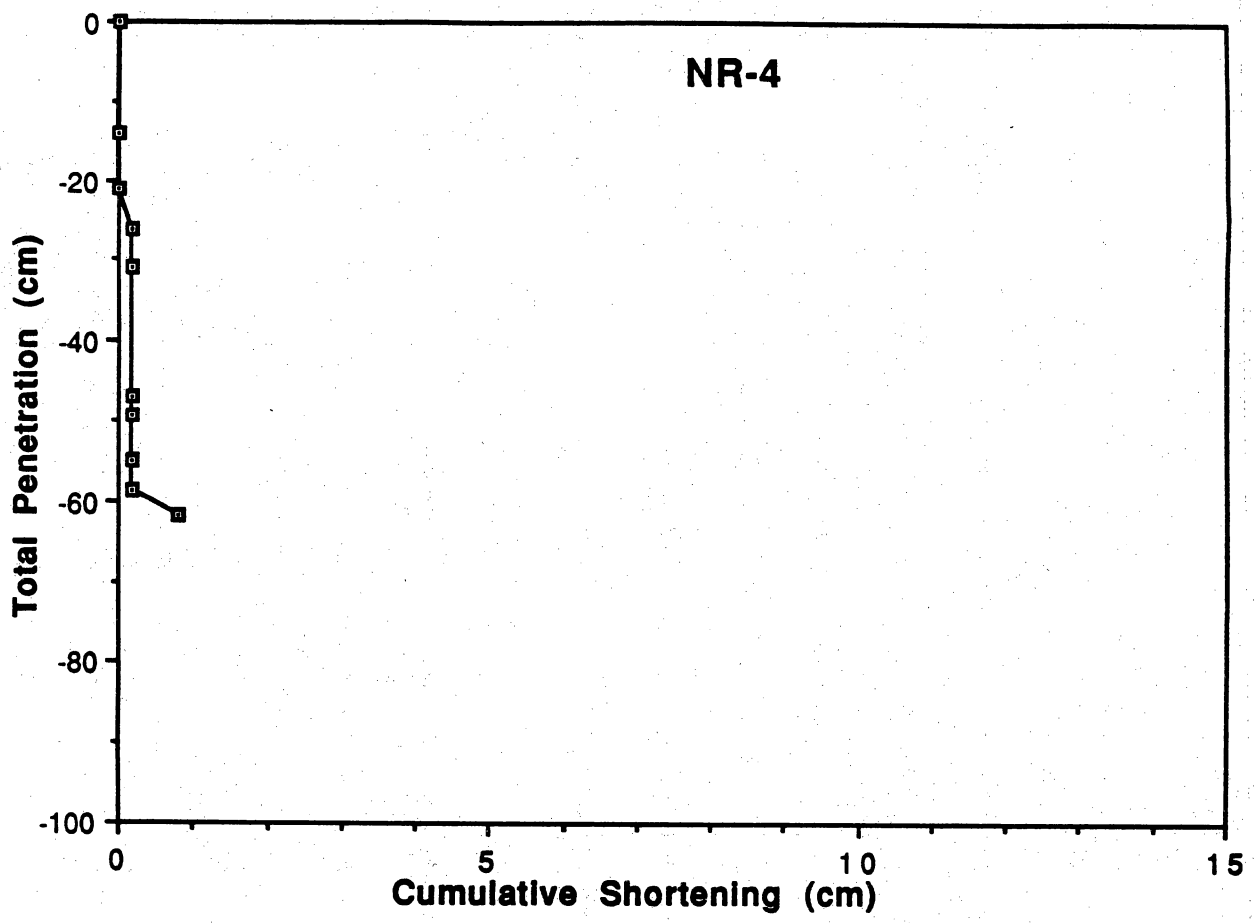
NR-4
0
-20
-40
-60
-80
-100
Total Penetration (cm)
0
5
10
15
Cumulative Shortening (cm)

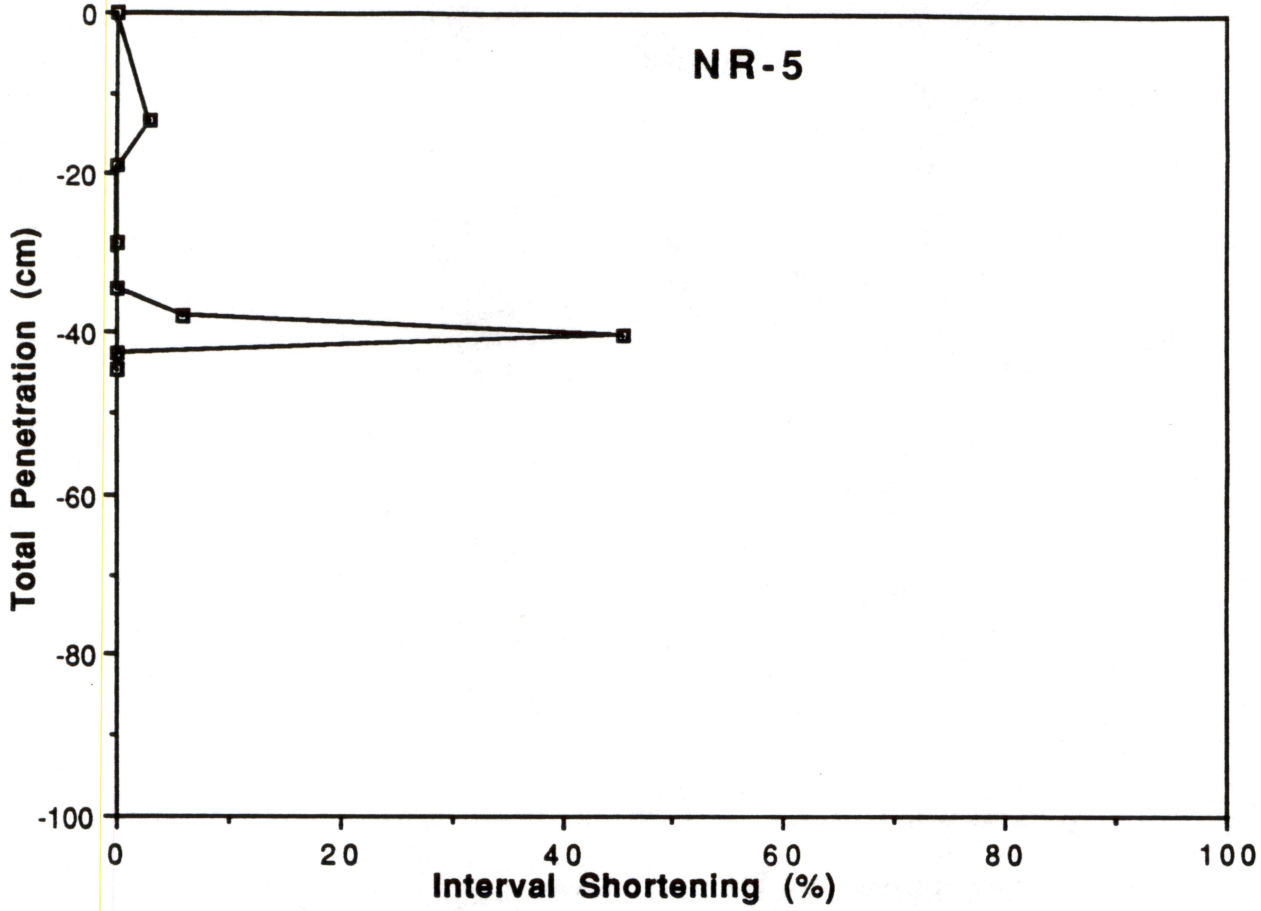
NR-5
0
-20
-40
-60
-80
-100
Total Penetration (cm)
0
20
40
60
80
100
Interval Shortening (%)

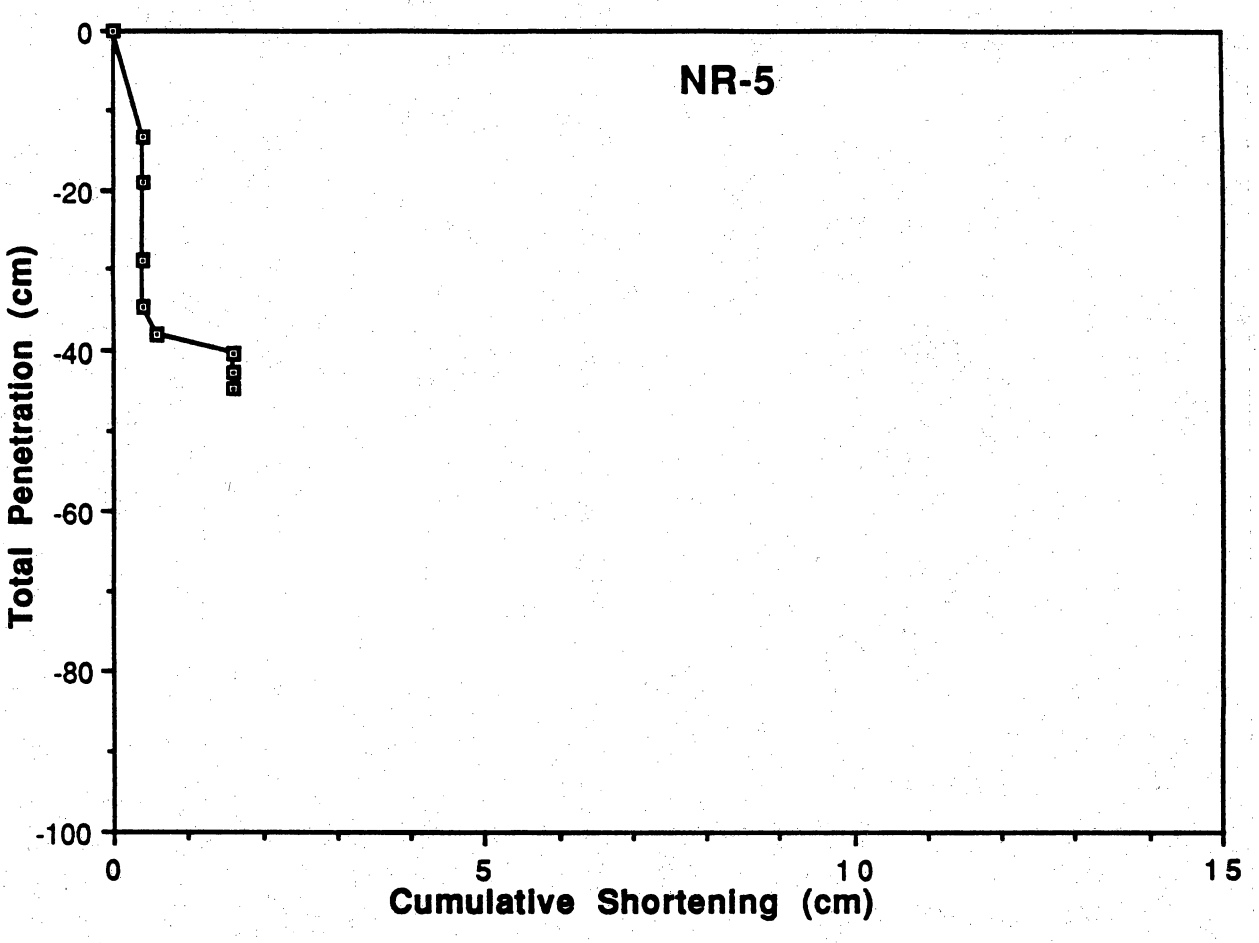
NR-5
0
-20
-40
-60
-80
-100
Total Penetration (cm)
0
5
10
15
Cumulative Shortening (cm)

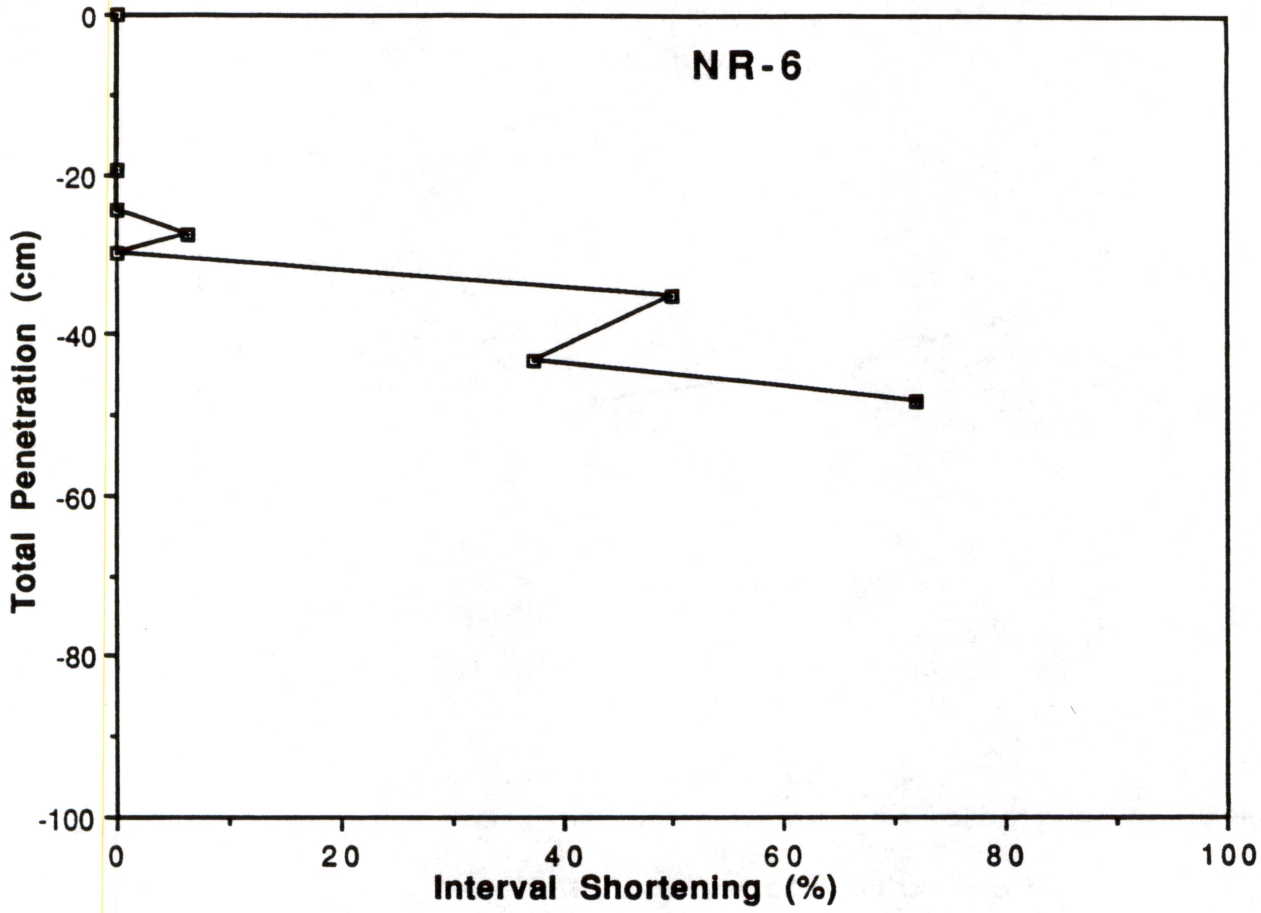
NR-6
0
-20
-40
-60
-80
-100
Total Penetration (cm)
0
20
40
60
80
100
Interval Shortening (%)

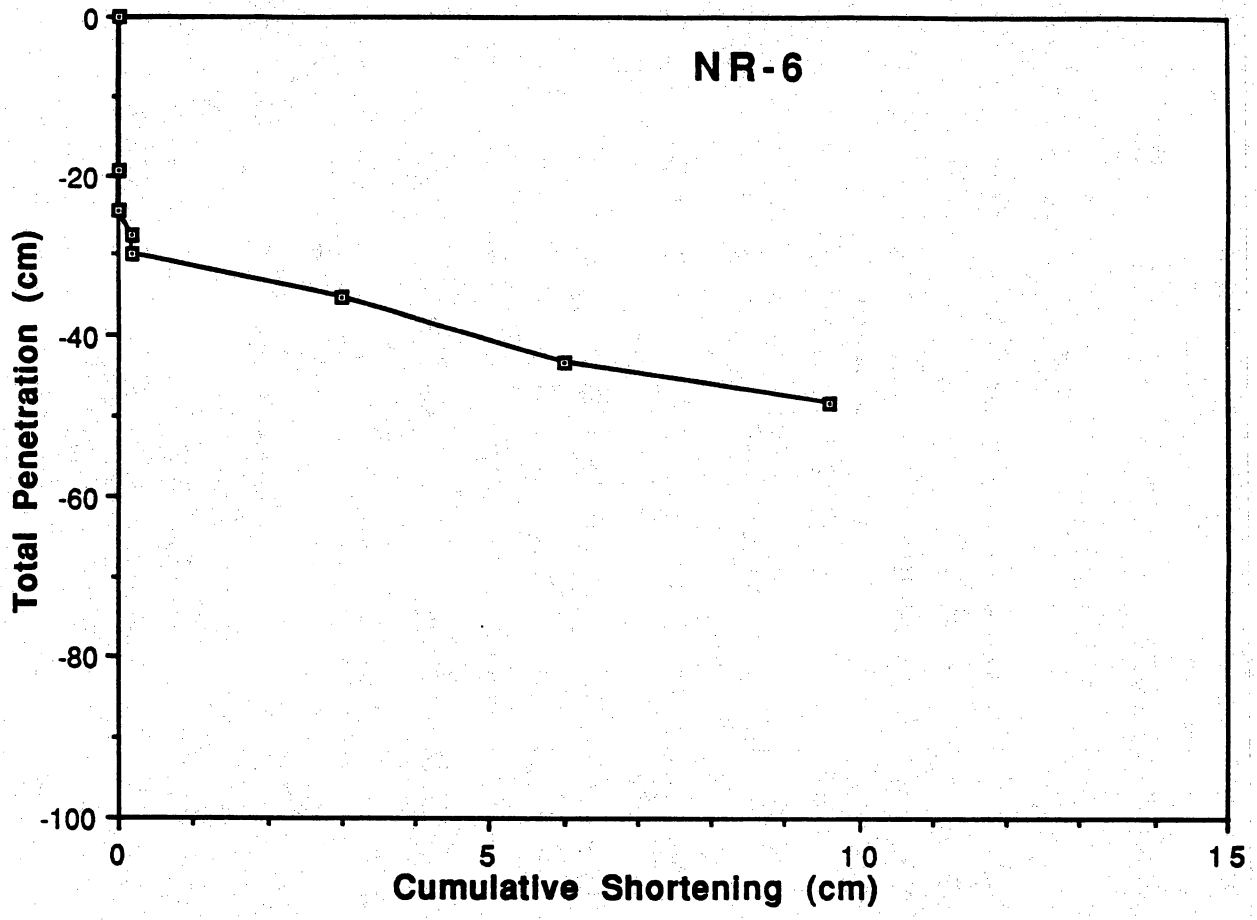
NR-6
0
-20
-40
-60
-80
-100
Total Penetration (cm)
0
5
10
15
Cumulative Shortening (cm)

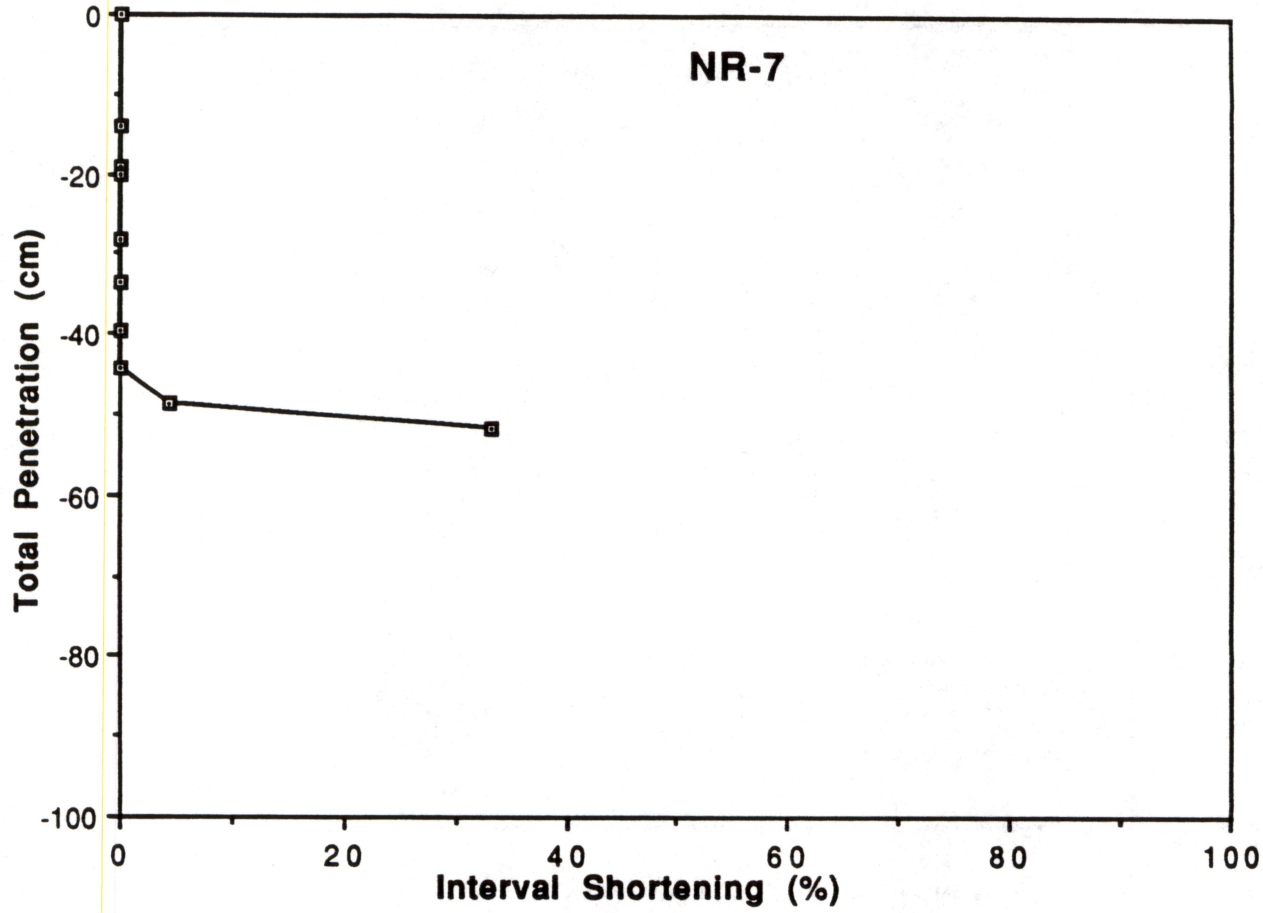
NR-7
Total Penetration (cm)
0
-20
-40
-60
-80
-100
0
20
40
60
80
100
Interval Shortening (%)

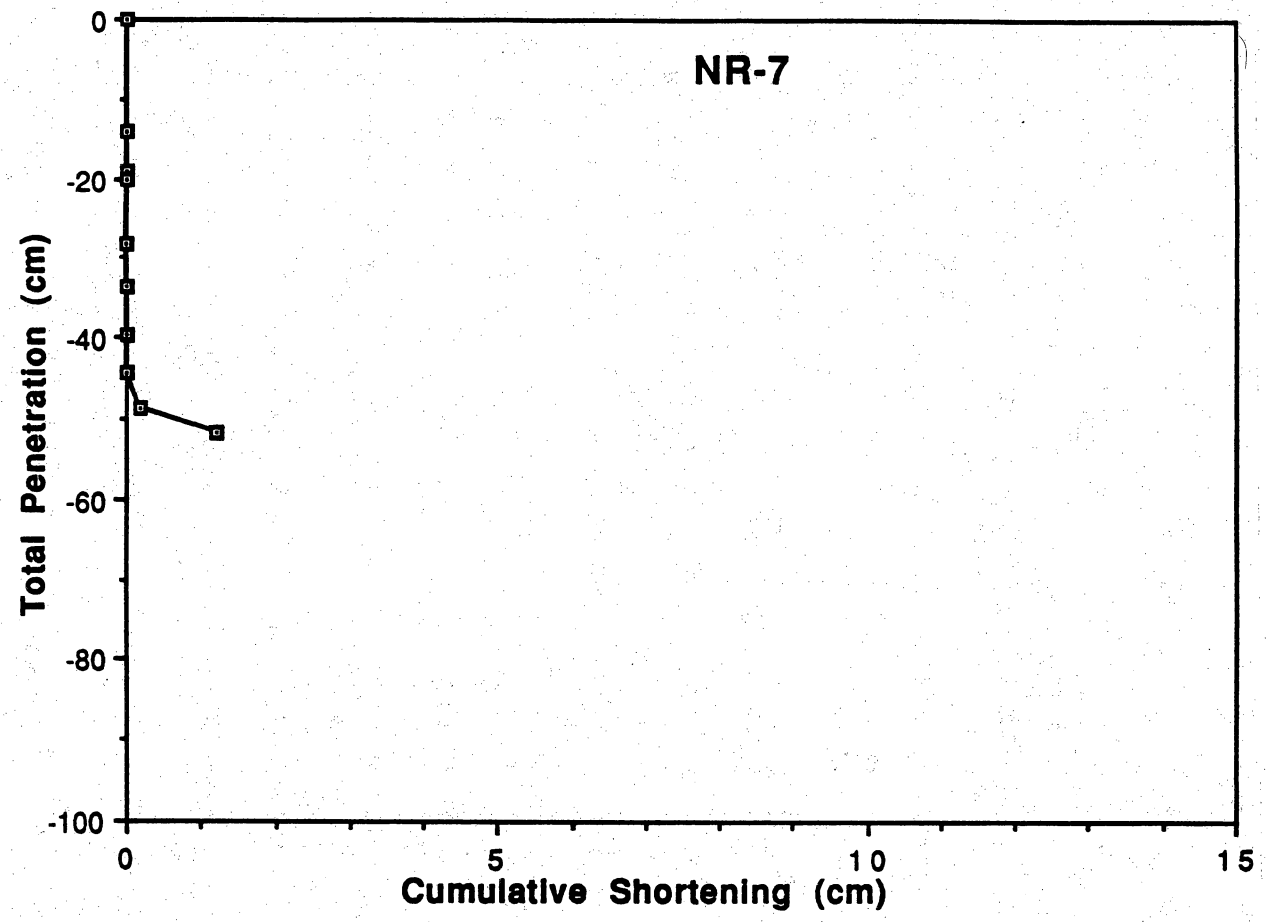
NR-7
0
-20
-40
-60
-80
-100
Total Penetration (cm)
0
5
10
15
Cumulative Shortening (cm)

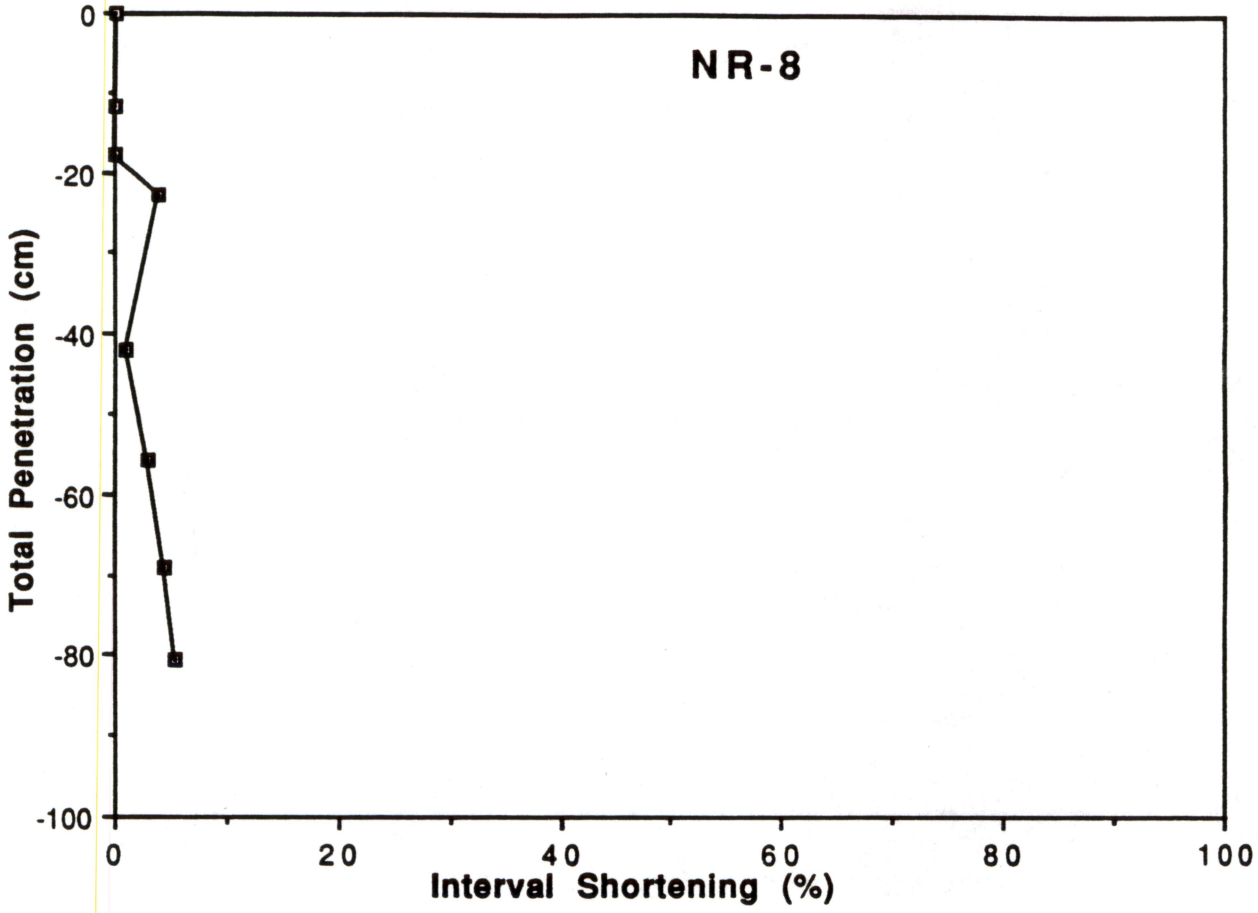
NR-8
0
-20
-40
-60
-80
-100
Total Penetration (cm)
0
20
40
60
80
100
Interval Shortening (%)

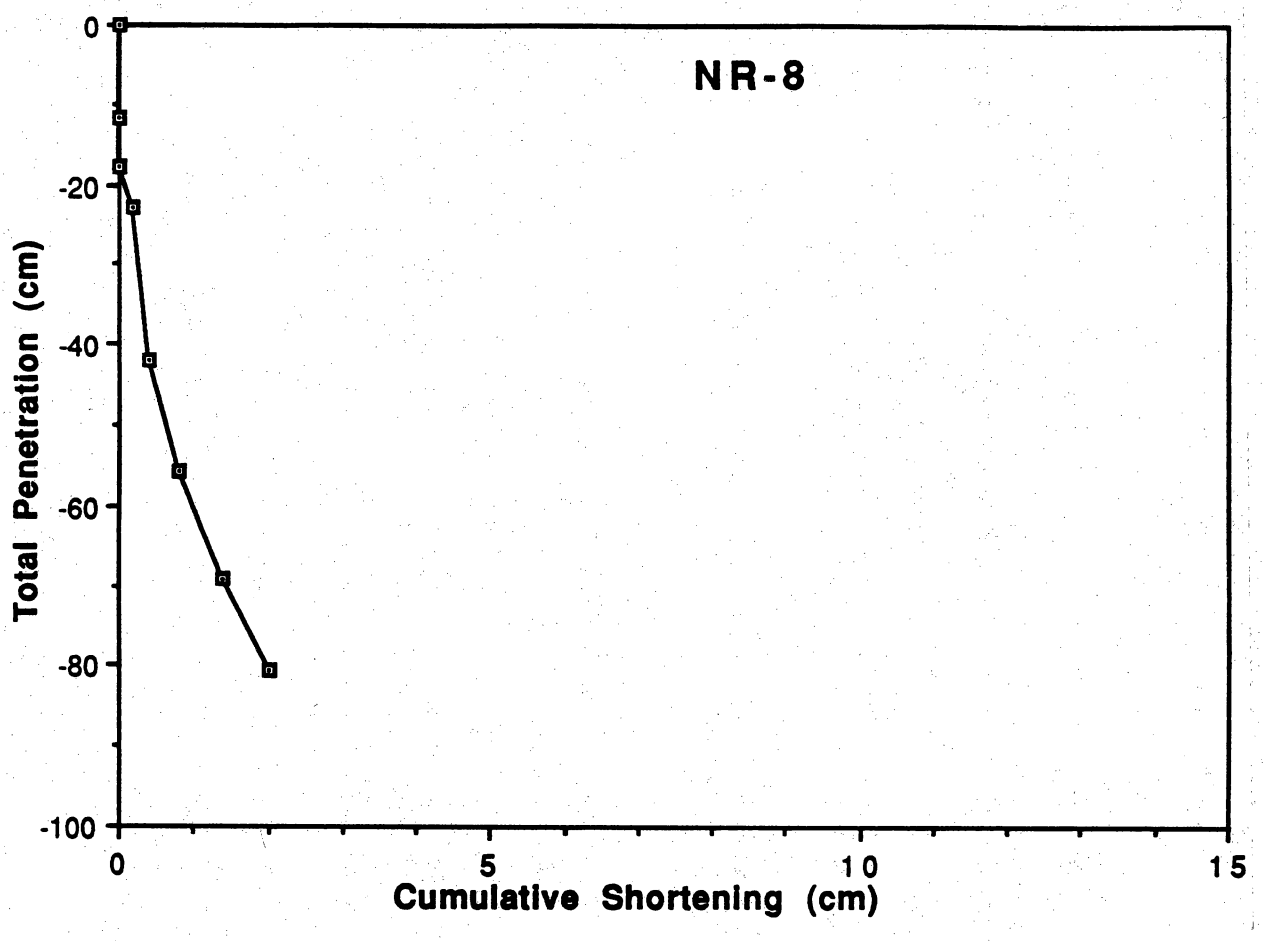
NR-8
0
-20
-40
-60
-80
-100
Total Penetration (cm)
0
5
10
15
Cumulative Shortening (cm)

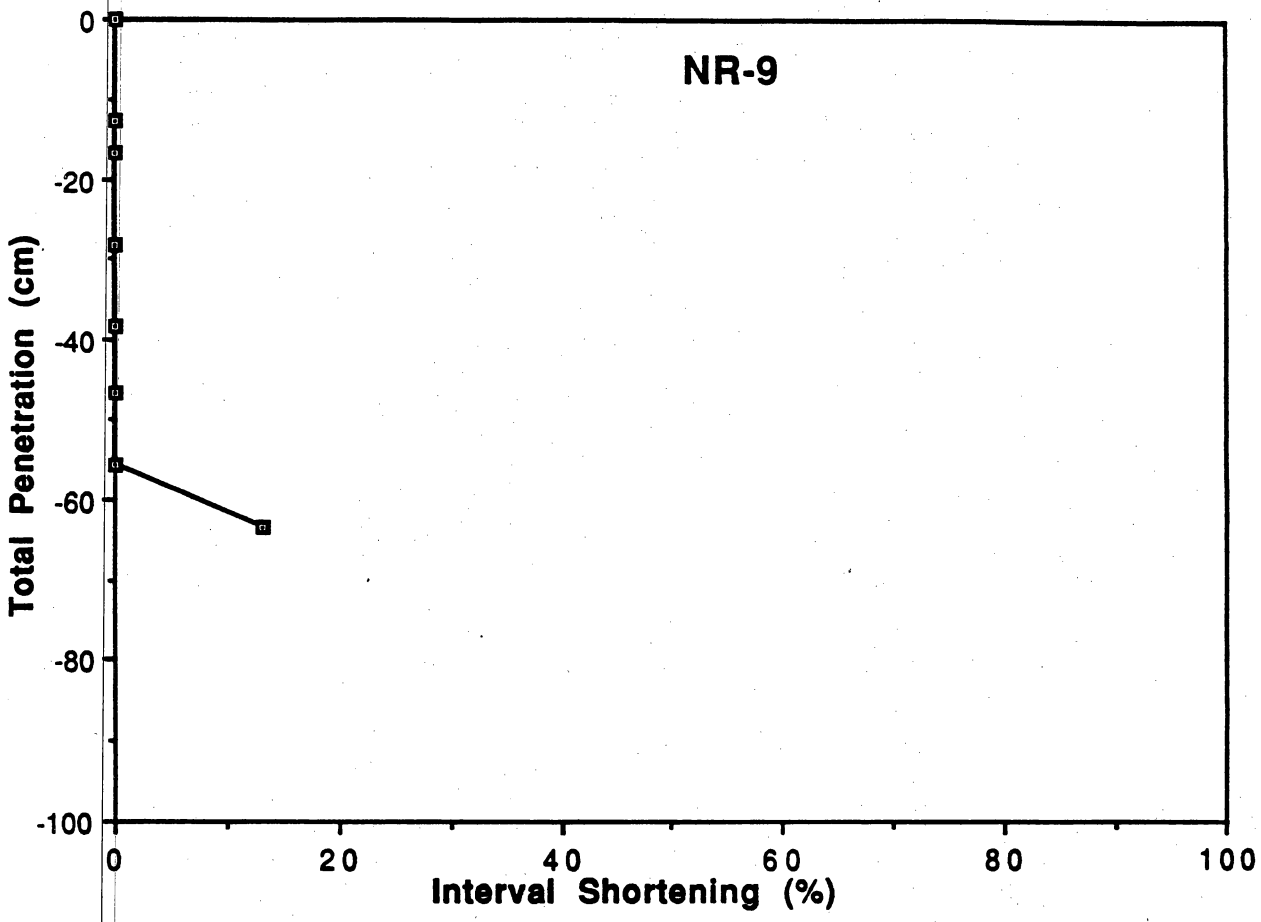
NR-9
0
-20
-40
-60
-80
-100
Total Penetration (cm)
0
20
40
60
80
100
Interval Shortening (%)

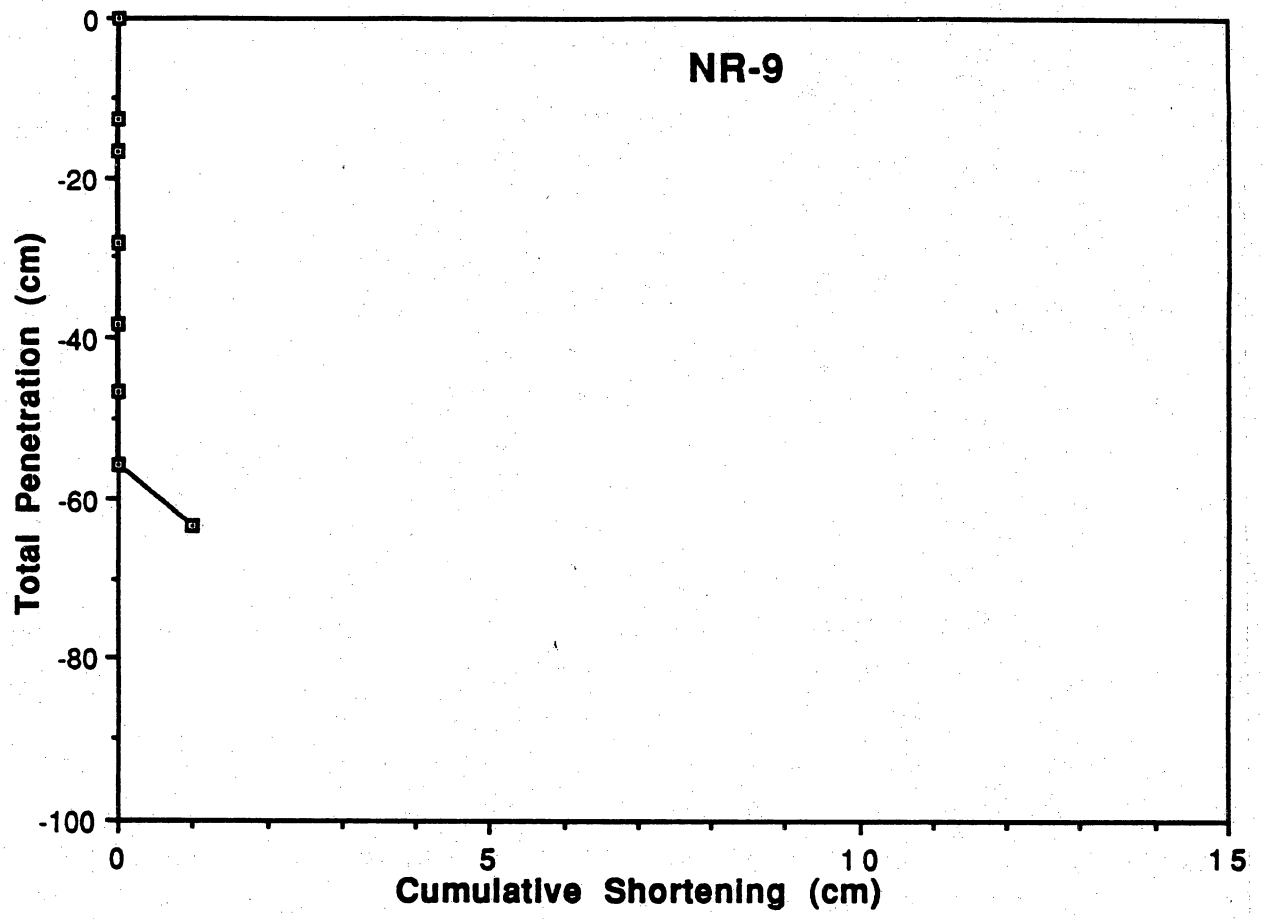
NR-9
0
-20
-40
-60
-80
-100
Total Penetration (cm)
0
5
10
15
Cumulative Shortening (cm)

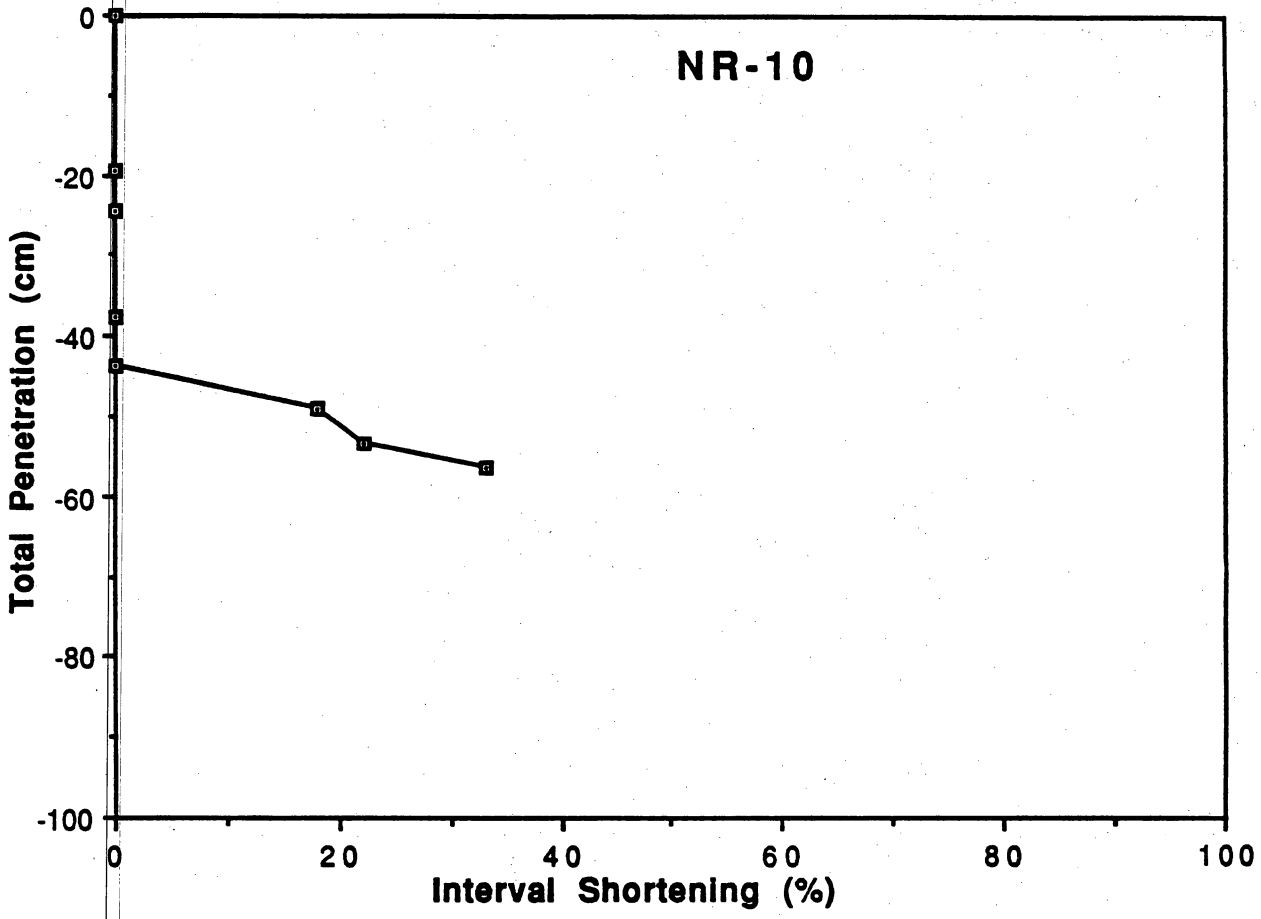
NR-10
0
-20
-40
-60
-80
-100
Total Penetration (cm)
0
20
40
60
80
100
Interval Shortening (%)

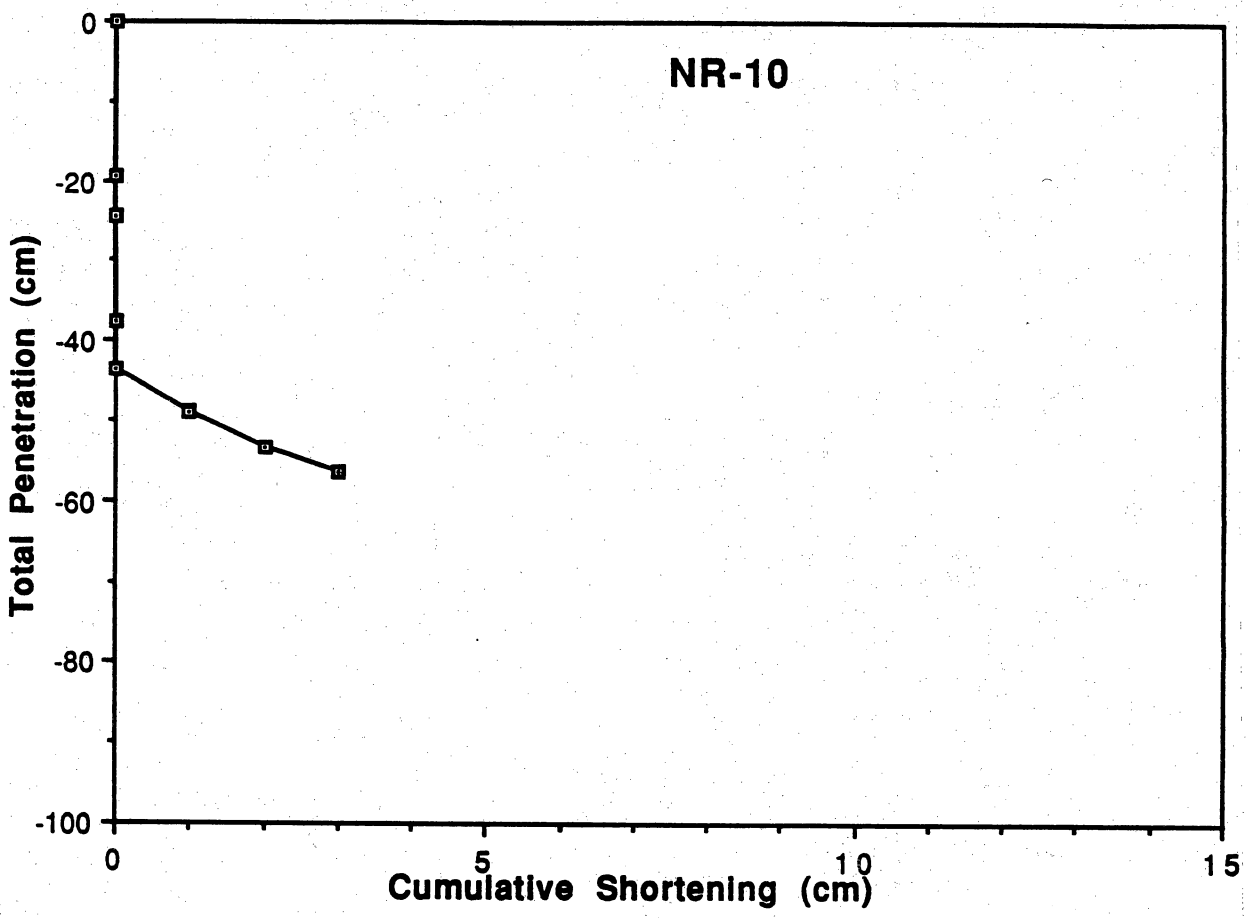
NR-10
0
-20
-40
-60
-80
-100
Total Penetration (cm)
0
5
10
15
Cumulative Shortening (cm)

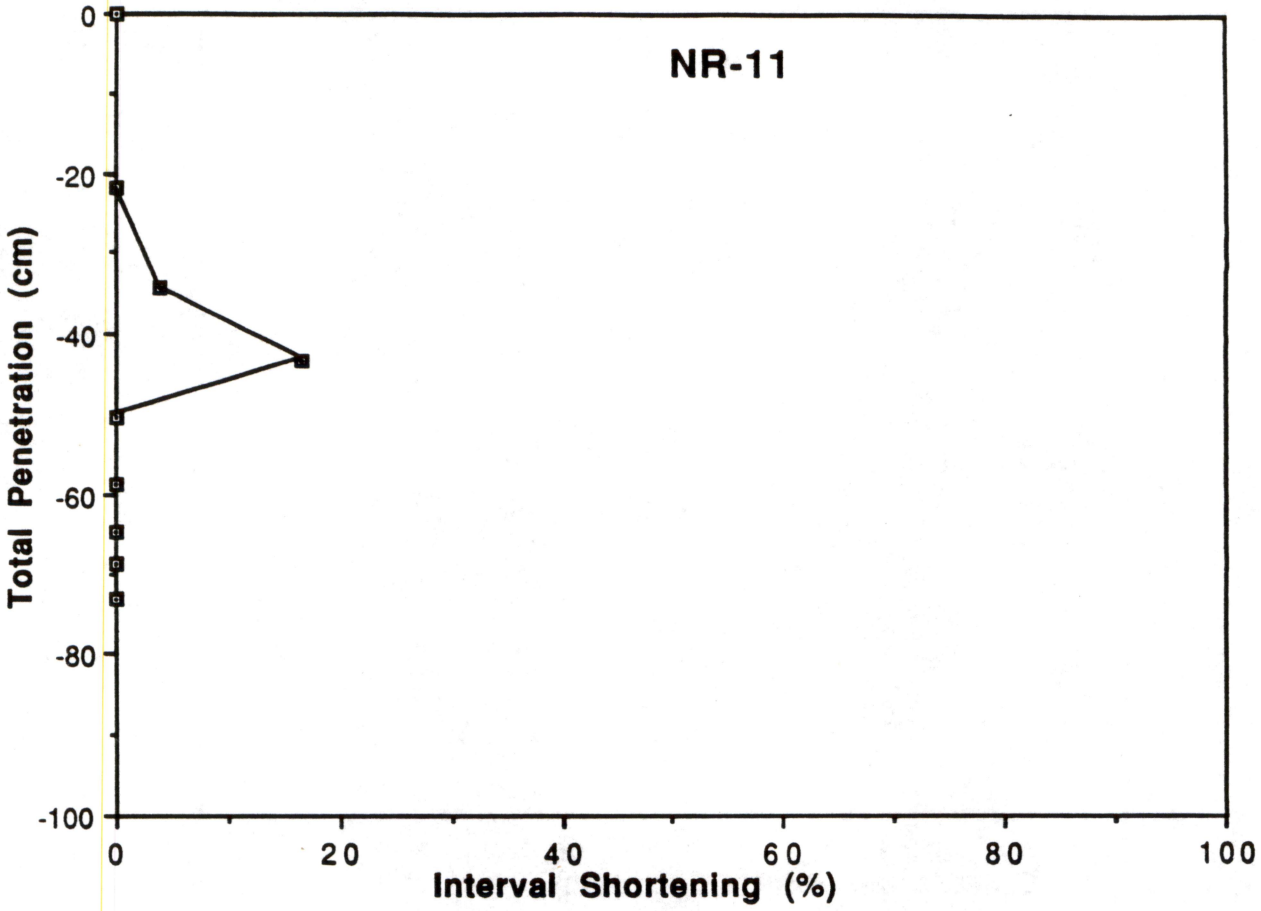
NR-11
0
-20
-40
-60
-80
-100
Total Penetration (cm)
0
20
40
60
80
100
Interval Shortening (%)

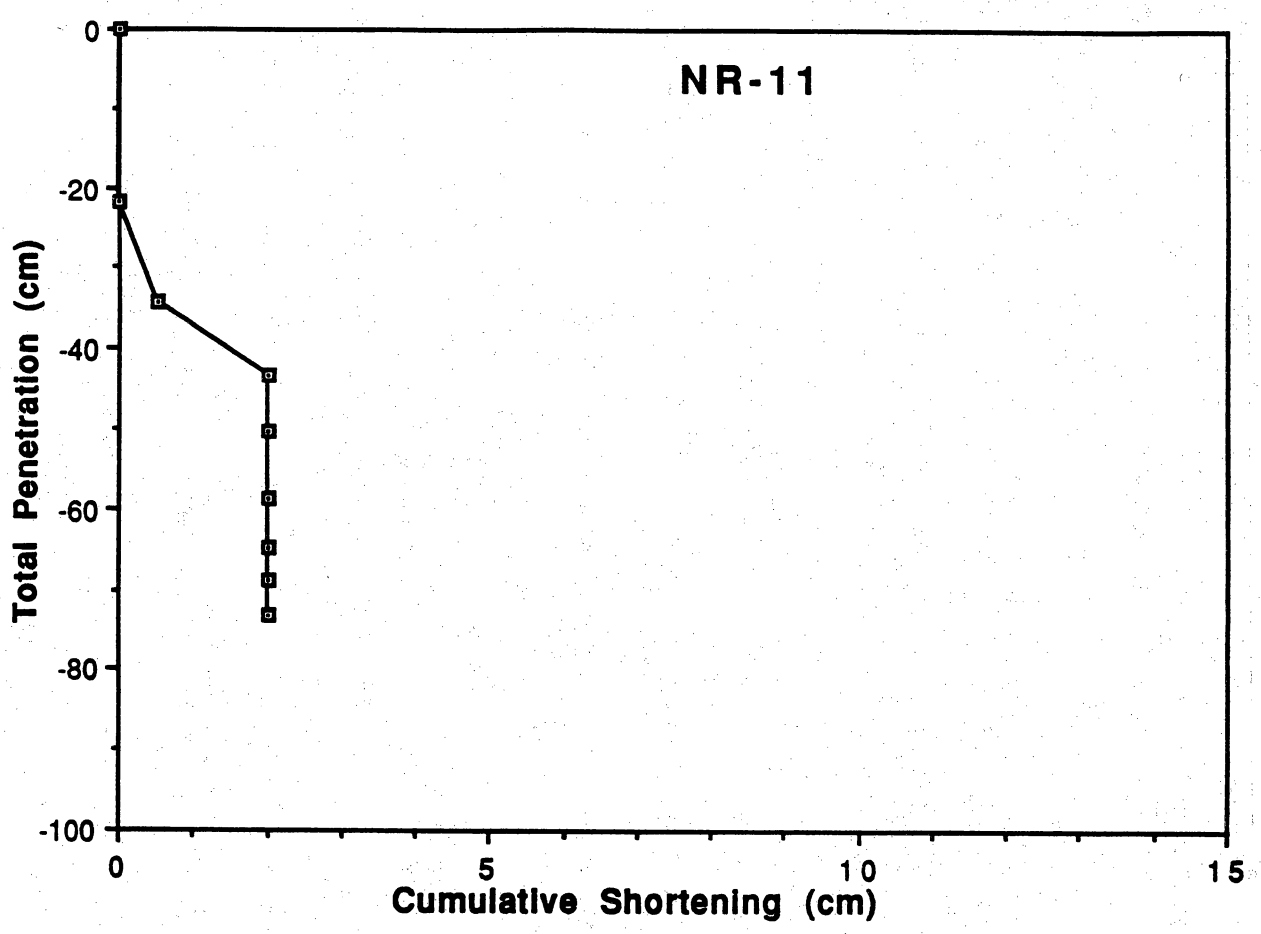
NR-11
0
-20
-40
-60
-80
-100
Total Penetration (cm)
0
5
10
15
Cumulative Shortening (cm)

# APPENDIX B

## $^{210}Pb$, $^{226}Ra$, Water Content, LOI, Bulk Density, Texture, and Depth Corrections from Shortening

| Core No. | Sample No. | Uncorr. Depth (cm) | Corr. Depth (cm) | Wt. Wet Sample (g) | Wt. Dry Sample (g) | Water (%) | LOI (%) | Mineral (%) | Coarse Fraction (%) | Silt Fraction (%) | Clay Fraction (%) | Wet Bulk Dens (g/cc) | Dry Bulk Dens (g/cc) | Total Pb-210 (dpm/g) | Ra-226 (dpm/g) | USGS Excess Pb-210 (dpm/g) | +/- |
|---|---|---|---|---|---|---|---|---|---|---|---|---|---|---|---|---|---|
| NR 1 | 1 | 1 | 1.0000 | 25.8 | 21.9 | 15.1 | 11.26 | 73.62 | 67.2 | 29.7 | 3.1 | 0.54 | 0.46 | 16.0603 | | 15.1703 | 0.054 |
| NR 1 | 2 | 2 | 2.0000 | 32.8 | 25.5 | 22.3 | 9.74 | 68.00 | 35.6 | 47.7 | 16.7 | 0.69 | 0.54 | 10.6574 | | 9.7674 | 0.035 |
| NR 1 | 3 | 3 | 3.0000 | 45.8 | 33.5 | 26.9 | 9.49 | 63.66 | 21.7 | 39.9 | 38.4 | 0.96 | 0.71 | 7.8611 | | 6.9711 | 0.029 |
| NR 1 | 4 | 4 | 4.0000 | 66.4 | 48.9 | 26.4 | 7.86 | 65.79 | 17.2 | 39.1 | 43.7 | 1.40 | 1.03 | 3.5928 | | 2.7028 | 0.020 |
| NR 1 | 5 | 5 | 5.0000 | 70.5 | 53 | 24.8 | 6.35 | 68.83 | 15.2 | 37.9 | 46.9 | 1.48 | 1.12 | 2.6808 | | 1.7908 | 0.020 |
| NR 1 | 6 | 6 | 6.0000 | 66.5 | 50.4 | 24.2 | 6.16 | 69.63 | 14.5 | 41.8 | 43.6 | 1.40 | 1.06 | 1.9271 | | 1.0371 | 0.013 |
| NR 1 | 7 | 7 | 7.0000 | 61.2 | 46.5 | 24.0 | 6.55 | 69.43 | 14.7 | 41.6 | 43.7 | 1.29 | 0.98 | 1.8586 | | 0.9686 | 0.012 |
| NR 1 | 8 | 8 | 8.0000 | 70.3 | 52.8 | 24.9 | 6.59 | 68.52 | 13.4 | 39.3 | 47.2 | 1.48 | 1.11 | 1.5629 | | 0.6729 | 0.010 |
| NR 1 | 9 | 9 | 9.0000 | 60.7 | 45.3 | 25.4 | 6.52 | 68.11 | 10.1 | 42.4 | 47.5 | 1.28 | 0.95 | 1.5851 | | 0.6951 | 0.017 |
| NR 1 | 10 | 10 | 10.0000 | 72.0 | 53.2 | 26.1 | 5.91 | 67.98 | 8.8 | 36.6 | 54.6 | 1.52 | 1.12 | 1.2063 | | 0.3163 | 0.015 |
| NR 1 | 11 | 11 | 11.0000 | 70.6 | 52.1 | 26.2 | 6.37 | 67.42 | 12.2 | 36.1 | 51.7 | 1.49 | 1.10 | 1.1901 | | 0.3001 | 0.003 |
| NR 1 | 12 | 12 | 12.0000 | 61.9 | 45.4 | 26.7 | 6.56 | 66.78 | 12.9 | 38.6 | 48.6 | 1.30 | 0.96 | 1.1498 | | 0.2598 | 0.009 |
| NR 1 | 13 | 13 | 13.0000 | 68.3 | 50.1 | 26.6 | 6.29 | 67.07 | 13.0 | 36.6 | 50.3 | 1.44 | 1.05 | 1.1083 | 0.85 | 0.2183 | 0.010 |
| NR 1 | 14 | 14 | 14.0000 | 67.9 | 49.7 | 26.8 | 5.92 | 67.28 | 11.4 | 38.1 | 50.5 | 1.43 | 1.05 | 1.0665 | | 0.1765 | 0.010 |
| NR 1 | 15 | 15 | 15.0000 | 75.6 | 54.6 | 27.8 | 5.70 | 66.52 | 11.2 | 40.2 | 48.6 | 1.59 | 1.15 | 0.9453 | | 0.0553 | 0.010 |
| NR 1 | 16 | 16 | 16.0000 | 63.3 | 45.9 | 27.5 | 5.30 | 67.21 | 12.5 | 43.7 | 43.7 | 1.33 | 0.97 | 0.8999 | | 0.0099 | 0.004 |
| NR 1 | 17 | 17 | 17.0000 | 66.3 | 47.9 | 27.8 | 5.52 | 66.72 | 12.8 | 44.1 | 43.1 | 1.40 | 1.01 | 0.7955 | | -0.0945 | 0.004 |
| NR 1 | 18 | 18 | 18.0000 | 75.2 | 54.2 | 27.9 | 5.39 | 66.69 | 13.0 | 50.3 | 36.6 | 1.58 | 1.14 | 0.8546 | | -0.0354 | 0.006 |
| NR 1 | 19 | 19 | 19.0000 | 63.3 | 45.4 | 28.3 | 4.55 | 67.17 | 9.0 | 45.2 | 45.9 | 1.33 | 0.96 | 0.8929 | | 0.0029 | 0.004 |
| NR 1 | 20 | 20 | 20.0000 | 73.8 | 52.5 | 28.9 | 5.54 | 65.59 | 10.4 | 37.0 | 52.6 | 1.55 | 1.10 | 1.1022 | | 0.2122 | 0.004 |
| NR 1 | 21 | 22 | 22.0275 | 125.8 | 88.7 | 29.5 | 4.97 | 65.54 | 11.1 | 34.8 | 54.1 | 2.65 | 1.87 | 1.0145 | 0.92 | 0.1245 | 0.004 |
| NR 1 | 22 | 24 | 24.0642 | 147.7 | 104.3 | 29.4 | 5.17 | 65.45 | 14.4 | 38.9 | 46.6 | 3.11 | 2.20 | 1.1480 | | 0.2580 | 0.007 |
| NR 1 | 23 | 26 | 26.1009 | 120.1 | 85.2 | 29.1 | 4.57 | 66.37 | 14.0 | 32.6 | 53.3 | 2.53 | 1.79 | 1.0396 | | 0.1496 | 0.004 |
| NR 1 | 24 | 28 | 28.1376 | 141.8 | 100.4 | 29.2 | 4.55 | 66.26 | 12.0 | 42.8 | 45.2 | 2.98 | 2.11 | 1.0746 | | 0.1846 | 0.002 |
| NR 1 | 25 | 30 | 30.1743 | 132.4 | 94.6 | 28.5 | 5.15 | 66.30 | 10.9 | 34.5 | 54.6 | 2.79 | 1.99 | 1.1502 | | 0.2602 | 0.004 |
| NR 1 | 26 | 32 | 32.2000 | 121.1 | 87.5 | 27.7 | 4.79 | 67.46 | 10.7 | 37.3 | 52.0 | 2.55 | 1.84 | 1.0131 | | 0.1231 | 0.002 |
| NR 1 | 27 | 34 | 34.2000 | 111.0 | 80.1 | 27.8 | 4.36 | 67.81 | 13.3 | 32.1 | 54.6 | 2.34 | 1.69 | 1.0996 | | 0.2096 | 0.004 |
| NR 1 | 28 | 36 | 36.2000 | 134.5 | 97.7 | 27.4 | 3.98 | 68.66 | 16.4 | 31.4 | 52.2 | 2.83 | 2.06 | 1.0143 | | 0.1243 | 0.004 |
| NR 1 | 29 | 38 | 38.2000 | 147.5 | 106.4 | 27.9 | 3.78 | 68.35 | 12.7 | 36.0 | 51.4 | 3.10 | 2.24 | 1.0773 | | 0.1873 | 0.006 |
| NR 1 | 30 | 40 | 40.2000 | 170.8 | 122.4 | 28.3 | 3.78 | 67.88 | 11.7 | 34.7 | 53.6 | 3.59 | 2.58 | 1.1381 | | 0.2481 | 0.003 |
| NR 1 | 31 | 42 | 42.2000 | 154.8 | 111.9 | 27.7 | 3.74 | 68.55 | 16.6 | 23.1 | 60.3 | 3.26 | 2.35 | 1.2238 | | 0.3338 | 0.003 |
| NR 1 | 32 | 44 | 44.2182 | 132.0 | 95.4 | 27.7 | 3.38 | 68.89 | 12.7 | 41.2 | 46.1 | 2.78 | 2.01 | 1.1720 | | 0.2820 | 0.006 |
| NR 1 | 33 | 46 | 46.3091 | 159.5 | 114.4 | 28.3 | 3.17 | 68.56 | 19.2 | 34.3 | 46.5 | 3.36 | 2.41 | 1.3485 | | 0.4585 | 0.013 |
| NR 1 | 34 | 48 | 48.4000 | 160.8 | 114.8 | 28.6 | 2.77 | 68.62 | 17.3 | 42.5 | 40.3 | 3.38 | 2.42 | 1.4318 | | 0.5418 | 0.009 |
| NR 1 | 35 | 50 | 50.4000 | 140.9 | 100.4 | 28.7 | 2.95 | 68.30 | 13.7 | 25.4 | 61.0 | 2.97 | 2.11 | 1.1731 | | 0.2831 | 0.006 |
| NR 1 | 36 | 52 | 52.4833 | 108.2 | 77.9 | 28.0 | 4.35 | 67.65 | 11.3 | 37.9 | 50.8 | 2.28 | 1.64 | 1.0436 | | 0.1536 | 0.004 |
| | | | | | | | | | | | | | | | Avg = 0.89 | | |

Sup, Pb 0.89

| Core No. | Sample No. | Uncorr. Depth (cm) | Corrected Depth (cm) | Wt. Wet Sample (g) | Wt. Dry Sample (g) | Water (%) | LOI (%) | Mineral (%) | Coarse Fraction (%) | Silt Fraction (%) | Clay Fraction (%) | Wet Bulk Dens (g/cc) | Dry Bulk Dens (g/cc) | Total Pb-210 (dpm/g) | Ra-226 (dpm/g) | USGS Excess Pb-210 (dpm/g) | +/- |
|---|---|---|---|---|---|---|---|---|---|---|---|---|---|---|---|---|---|
| NR 2 | 1 | 1 | 1.0000 | 80.1 | 45.1 | 43.7 | 11.13 | 45.17 | 19.3 | 37.9 | 42.8 | 1.69 | 0.95 | 4.5069 | | 3.4669 | 0.063 |
| NR 2 | 2 | 2 | 2.0000 | 57.9 | 30.2 | 47.8 | 11.93 | 40.23 | 26.1 | 46.2 | 27.7 | 1.22 | 0.64 | 3.9605 | | 2.9205 | 0.049 |
| NR 2 | 3 | 3 | 3.0000 | 54.0 | 25.2 | 53.3 | 11.61 | 35.05 | 41.2 | 34.7 | 24.1 | 1.14 | 0.53 | 4.0195 | 0.98 | 2.9795 | 0.028 |
| NR 2 | 4 | 4 | 4.0000 | 66.5 | 33.3 | 49.9 | 11.49 | 38.59 | 28.1 | 37.5 | 34.5 | 1.40 | 0.70 | 2.9792 | | 1.9392 | 0.043 |
| NR 2 | 5 | 5 | 5.0000 | 60.0 | 32.7 | 45.5 | 10.58 | 43.92 | 19.2 | 33.5 | 47.4 | 1.26 | 0.69 | 3.5858 | | 2.5458 | 0.040 |
| NR 2 | 6 | 6 | 6.0000 | 72.5 | 41.7 | 42.5 | 10.74 | 46.78 | 12.4 | 31.6 | 56.0 | 1.53 | 0.88 | 2.7763 | | 1.7363 | 0.040 |
| NR 2 | 7 | 7 | 7.0000 | 83.5 | 46.5 | 44.3 | 10.66 | 45.03 | 10.9 | 40.1 | 49.0 | 1.76 | 0.98 | 2.9144 | | 1.8744 | 0.020 |
| NR 2 | 8 | 8 | 8.0000 | 70.7 | 41.4 | 41.4 | 11.05 | 47.51 | 9.5 | 39.7 | 50.8 | 1.49 | 0.87 | 2.6387 | | 1.5987 | 0.036 |
| NR 2 | 9 | 9 | 9.0000 | 96.4 | 52.8 | 45.2 | 11.20 | 43.57 | 13.5 | 32.3 | 54.3 | 2.03 | 1.11 | 2.5477 | | 1.5077 | 0.017 |
| NR 2 | 10 | 10 | 10.0000 | 53.2 | 31.2 | 41.4 | 11.78 | 46.87 | 12.1 | 33.7 | 54.2 | 1.12 | 0.66 | 2.1241 | | 1.0841 | 0.022 |
| NR 2 | 11 | 11 | 11.0000 | 74.9 | 43.6 | 41.8 | 11.03 | 47.18 | 13.9 | 36.5 | 49.6 | 1.58 | 0.92 | 2.8992 | | 1.8592 | 0.077 |
| NR 2 | 12 | 12 | 12.0000 | 91.1 | 54.8 | 39.8 | 12.01 | 48.15 | 14.6 | 31.5 | 53.9 | 1.92 | 1.15 | 2.6874 | | 1.6474 | 0.025 |
| NR 2 | 13 | 13 | 13.0000 | 71.4 | 44.0 | 38.4 | 12.03 | 49.59 | 8.5 | 22.7 | 68.8 | 1.50 | 0.93 | 2.3386 | 1.03 | 1.2986 | 0.024 |
| NR 2 | 14 | 14 | 14.0000 | 62.2 | 39.0 | 37.3 | 11.73 | 50.97 | 8.5 | 30.9 | 60.7 | 1.31 | 0.82 | 1.9561 | | 0.9161 | 0.005 |
| NR 2 | 15 | 15 | 15.0000 | 79.8 | 48.6 | 39.1 | 11.58 | 49.32 | 7.9 | 28.8 | 63.3 | 1.68 | 1.02 | 2.2852 | | 1.2452 | 0.021 |
| NR 2 | 16 | 16 | 16.0000 | 72.6 | 43.9 | 39.5 | 11.51 | 48.96 | 7.0 | 29.5 | 63.5 | 1.53 | 0.92 | 2.2232 | | 1.1832 | 0.012 |
| NR 2 | 17 | 17 | 17.0000 | 72.4 | 43.7 | 39.6 | 11.68 | 48.68 | 5.0 | 31.3 | 63.7 | 1.52 | 0.92 | 2.4936 | | 1.4536 | 0.017 |
| NR 2 | 18 | 18 | 18.0000 | 68.4 | 42.0 | 38.6 | 11.75 | 49.65 | 7.4 | 24.1 | 68.5 | 1.44 | 0.88 | 1.9715 | | 0.9315 | 0.034 |
| NR 2 | 19 | 19 | 19.0000 | 69.5 | 43.1 | 38.0 | 11.46 | 50.55 | 6.0 | 25.4 | 68.7 | 1.46 | 0.91 | 1.6210 | | 0.5810 | 0.062 |
| NR 2 | 20 | 20 | 20.0000 | 77.0 | 47.8 | 37.9 | 10.52 | 51.56 | 9.2 | 25.0 | 65.8 | 1.62 | 1.01 | 2.0540 | | 1.0140 | 0.007 |
| NR 2 | 21 | 21 | 21.0000 | 67.7 | 43.6 | 35.6 | 10.93 | 53.47 | 7.1 | 21.2 | 71.7 | 0.71 | 0.46 | 1.9139 | | 0.8739 | 0.009 |
| NR 2 | 22 | 23 | 23.0143 | 98.7 | 62.9 | 36.3 | 9.98 | 53.75 | 7.5 | 27.4 | 65.0 | 1.04 | 0.66 | 1.8961 | 1.13 | 0.8561 | 0.006 |
| NR 2 | 23 | 25 | 25.1095 | 118.4 | 74.5 | 37.1 | 10.22 | 52.71 | 10.6 | 35.7 | 53.7 | 1.25 | 0.78 | 1.6829 | | 0.6429 | 0.005 |
| NR 2 | 24 | 27 | 27.2001 | 133.8 | 85.3 | 36.2 | 9.29 | 54.46 | 11.0 | 36.0 | 53.0 | 1.41 | 0.90 | 1.6961 | | 0.6561 | 0.004 |
| NR 2 | 25 | 29 | 29.2000 | 138.3 | 88.3 | 36.2 | 9.16 | 54.68 | 9.9 | 40.1 | 50.0 | 1.46 | 0.93 | 1.7178 | | 0.6778 | 0.006 |
| NR 2 | 26 | 31 | 31.2000 | 126.5 | 80.9 | 36.0 | 8.70 | 55.26 | 16.4 | 34.1 | 49.5 | 1.33 | 0.85 | 1.7964 | | 0.7564 | 0.005 |
| NR 2 | 27 | 33 | 33.2000 | 129.0 | 83.7 | 35.1 | 8.51 | 56.37 | 10.3 | 31.6 | 58.2 | 1.36 | 0.88 | 1.4069 | | 0.3669 | 0.011 |
| NR 2 | 28 | 35 | 35.2000 | 146.6 | 95.9 | 34.6 | 8.00 | 57.42 | 9.3 | 32.7 | 58.0 | 1.54 | 1.01 | 1.2958 | | 0.2558 | 0.006 |
| NR 2 | 29 | 37 | 37.2000 | 143.0 | 92.6 | 35.2 | 7.66 | 57.09 | 9.9 | 30.5 | 59.6 | 1.50 | 0.97 | 1.5441 | | 0.5041 | 0.010 |
| NR 2 | 30 | 39 | 39.8600 | 157.5 | 102.8 | 34.7 | 6.89 | 58.38 | 9.4 | 27.5 | 63.1 | 1.66 | 1.08 | 1.4255 | | 0.3855 | 0.003 |
| NR 2 | 31 | 41 | 43.0125 | 132.4 | 85.9 | 35.1 | 6.78 | 58.10 | 9.2 | 28.7 | 62.1 | 1.39 | 0.90 | 1.5811 | | 0.5411 | 0.004 |
| NR 2 | 32 | 43 | 45.2278 | 141.1 | 92.5 | 34.4 | 6.89 | 58.67 | 8.2 | 23.2 | 68.6 | 1.48 | 0.97 | 1.4937 | | 0.4537 | 0.012 |
| NR 2 | 33 | 45 | 47.3389 | 155.3 | 101.7 | 34.5 | 5.04 | 60.45 | 8.5 | 29.6 | 61.9 | 1.63 | 1.07 | 1.6379 | | 0.5979 | 0.014 |
| NR 2 | 34 | 47 | 49.4243 | 132.0 | 87.2 | 33.9 | 3.04 | 63.02 | 10.9 | 27.2 | 62.0 | 1.39 | 0.92 | 1.0531 | | 0.0131 | 0.011 |
| NR 2 | 35 | 49 | 51.4784 | 151.2 | 100.6 | 33.5 | 4.67 | 61.86 | 13.1 | 13.5 | 73.5 | 1.59 | 1.06 | 1.2580 | | 0.2180 | 0.024 |
| NR 2 | 36 | 51 | 53.5324 | 146.3 | 95.2 | 34.9 | na | | 10.0 | 26.3 | 63.7 | 1.54 | 1.00 | na | na | na | na |
| NR 2 | 37 | 53 | 55.5865 | 142.5 | 93.8 | 34.2 | na | | 11.6 | 23.2 | 65.3 | 1.50 | 0.99 | na | na | na | na |
| NR 2 | 38 | 55 | 57.6000 | 151.9 | 102.2 | 32.7 | na | | 16.1 | 27.1 | 56.8 | 1.60 | 1.08 | na | na | na | na |
| NR 2 | 39 | 57 | 59.6000 | 155.6 | 109.1 | 29.9 | na | | 25.9 | 33.3 | 40.8 | 1.64 | 1.15 | na | na | na | na |
| NR 2 | 40 | 61 | 63.6000 | 153.4 | 106.9 | 30.3 | na | | 26.4 | 34.5 | 39.1 | 1.61 | 1.12 | na | na | na | na |
| NR 2 | 41 | 63 | 65.7370 | 164.9 | 119.1 | 27.8 | na | | 34.5 | 31.7 | 33.9 | 1.74 | 1.25 | na | na | na | na |
| NR 2 | 42 | 65 | 67.9875 | 168.3 | 123.0 | 26.9 | na | | 46.8 | 23.1 | 30.1 | 1.77 | 1.29 | na | na | na | na |
| NR 2 | 43 | 67 | | 179.8 | 130.3 | 27.5 | na | | 41.0 | 28.9 | 30.1 | 1.89 | 1.37 | na | na | na | na |
| | | | | | | | | | | | | | | Avg = 1.04 | | | |

| Core No. | Sample No. | Uncorr. Depth (cm) | Corr. Depth (cm) | Wt. Wet Sample (g) | Wt. Dry Sample (g) | Water (%) | LOI (%) | Mineral (%) | Coarse Fraction (%) | Silt Fraction (%) | Clay Fraction (%) | Wet Bulk Dens (g/cc) | Dry Bulk Dens (g/cc) | Total Pb-210 (dpm/g) | Ra-226 (dpm/g) | USGS Excess Pb-210 (dpm/g) | +/- |
|---|---|---|---|---|---|---|---|---|---|---|---|---|---|---|---|---|---|
| NR3 | 1 | 1 | 1.0374 | 69.3 | 25.5 | 63.2 | 10.80 | 47.60 | 24.2 | 41.2 | 34.6 | 1.46 | 0.54 | 6.1770 | | 4.8870 | 0.024 |
| NR3 | 2 | 2 | 2.0748 | 68.9 | 32.7 | 52.5 | 8.49 | 55.95 | 31.9 | 39.4 | 28.7 | 1.45 | 0.69 | 5.9460 | 1.24 | 4.6560 | 0.022 |
| NR3 | 3 | 3 | 3.1121 | 69.7 | 36.9 | 47.1 | 8.82 | 61.76 | 20.5 | 38.6 | 40.9 | 1.47 | 0.78 | 5.9981 | | 4.7081 | 0.043 |
| NR3 | 4 | 4 | 4.1495 | 68.2 | 37.5 | 45.0 | 8.20 | 63.19 | 11.9 | 34.2 | 54.0 | 1.44 | 0.79 | 5.2525 | | 3.9625 | 0.022 |
| NR3 | 5 | 5 | 5.1869 | 82.6 | 46.9 | 43.2 | 8.32 | 65.10 | 9.8 | 51.2 | 39.0 | 1.74 | 0.99 | 5.0692 | 1.20 | 3.7792 | 0.034 |
| NR3 | 6 | 6 | 6.2243 | 92.6 | 64.3 | 30.6 | 6.40 | 75.84 | 6.3 | 37.3 | 56.3 | 1.95 | 1.35 | 3.7288 | | 2.4388 | 0.030 |
| NR3 | 7 | 7 | 7.2617 | 79.7 | 36 | 54.8 | 6.00 | 51.17 | 3.2 | 24.6 | 72.1 | 1.68 | 0.76 | 3.9459 | | 2.6559 | 0.022 |
| NR3 | 8 | 8 | 8.2991 | 85.7 | 51.3 | 40.1 | 6.51 | 66.37 | 4.9 | 27.6 | 67.5 | 1.80 | 1.08 | 3.8706 | 1.08 | 2.5806 | 0.016 |
| NR3 | 9 | 9 | 9.3364 | 70.1 | 43.5 | 37.9 | 6.48 | 68.54 | 7.0 | 32.1 | 61.0 | 1.48 | 0.92 | 2.7594 | | 1.4694 | 0.006 |
| NR3 | 10 | 10 | 10.3738 | 87.0 | 55.2 | 36.6 | 6.37 | 69.81 | 7.4 | 57.5 | 35.1 | 1.83 | 1.16 | 2.3198 | | 1.0298 | 0.008 |
| NR3 | 11 | 11 | 11.4000 | 106.0 | 68 | 35.8 | 8.00 | 72.15 | 9.1 | 34.1 | 56.8 | 2.23 | 1.43 | 1.7950 | 1.41 | 0.5050 | 0.004 |
| NR3 | 12 | 12 | 12.4000 | 83.3 | 53.5 | 35.8 | 7.49 | 71.72 | 8.3 | 40.7 | 51.0 | 1.75 | 1.13 | 1.8217 | | 0.5317 | 0.004 |
| NR3 | 13 | 13 | 13.4000 | 91.4 | 58.9 | 35.6 | 5.44 | 69.88 | 8.4 | 35.0 | 56.6 | 1.92 | 1.24 | 1.7774 | | 0.4874 | 0.004 |
| NR3 | 14 | 14 | 14.4000 | 87.0 | 55.4 | 36.3 | 5.32 | 69.00 | 8.4 | 34.4 | 57.3 | 1.83 | 1.17 | 1.5936 | 1.49 | 0.3036 | 0.002 |
| NR3 | 15 | 15 | 15.4000 | 84.8 | 54.3 | 36.0 | 5.30 | 69.33 | 8.1 | 27.9 | 64.1 | 1.78 | 1.14 | 1.9913 | | 0.7013 | 0.006 |
| NR3 | 16 | 16 | 16.4000 | 82.2 | 53 | 35.5 | 6.09 | 70.57 | 8.3 | 31.7 | 60.0 | 1.73 | 1.12 | 1.9986 | | 0.7086 | 0.008 |
| NR3 | 17 | 17 | 17.4000 | 105.0 | 68.1 | 35.1 | 5.80 | 70.66 | 9.3 | 17.3 | 73.4 | 2.21 | 1.43 | 1.9901 | 1.42 | 0.7001 | 0.009 |
| NR3 | 18 | 18 | 18.4000 | 107.7 | 70.1 | 34.9 | 5.10 | 70.19 | 8.6 | 22.3 | 69.1 | 2.27 | 1.48 | na | | na | na |
| NR3 | 19 | 19 | 19.4000 | 104.4 | 68 | 34.9 | 5.60 | 70.73 | 9.0 | 8.3 | 82.7 | 2.20 | 1.43 | 1.6988 | | 0.4088 | 0.002 |
| NR3 | 20 | 20 | 20.4000 | 87.1 | 56.2 | 35.5 | 5.60 | 70.12 | 7.8 | 28.5 | 63.8 | 1.83 | 1.18 | 1.6410 | 1.38 | 0.3510 | 0.002 |
| NR3 | 21 | 22 | 22.4000 | 147.6 | 96 | 35.0 | 4.76 | 69.80 | 6.9 | 45.5 | 47.6 | 1.55 | 1.01 | 1.3954 | | 0.1054 | 0.001 |
| NR3 | 22 | 24 | 24.4000 | 141.3 | 92.6 | 34.5 | 5.57 | 71.10 | 8.8 | 15.0 | 76.2 | 1.49 | 0.97 | 1.5242 | | 0.2342 | 0.004 |
| NR3 | 23 | 26 | 26.4000 | 183.6 | 120.7 | 34.3 | 6.08 | 71.82 | 8.8 | 35.0 | 56.1 | 1.93 | 1.27 | 1.2710 | 1.21 | -0.0190 | -0.001 |
| NR3 | 24 | 28 | 28.4000 | 170.3 | 112 | 34.2 | 6.10 | 71.86 | 8.8 | 57.7 | 33.5 | 1.79 | 1.18 | 1.4232 | | 0.1332 | 0.003 |
| NR3 | 25 | 30 | 30.4000 | 175.1 | 112.7 | 35.6 | 4.47 | 68.83 | 8.8 | 48.4 | 42.9 | 1.84 | 1.19 | 1.2960 | | 0.0060 | 0.000 |
| NR3 | 26 | 32 | 32.4000 | 153.3 | 100.3 | 34.6 | 5.43 | 70.86 | 9.4 | 37.0 | 53.6 | 1.61 | 1.06 | 1.4223 | 1.23 | 0.1323 | 0.001 |
| NR3 | 27 | 34 | 34.4000 | 172.4 | 112.2 | 34.9 | 7.55 | 72.63 | 7.7 | 57.1 | 35.2 | 1.81 | 1.18 | 1.2858 | | -0.0042 | 0.000 |
| NR3 | 28 | 36 | 36.4000 | 163.9 | 107.2 | 34.6 | 7.40 | 72.81 | 6.7 | 58.8 | 34.5 | 1.72 | 1.13 | 1.3475 | | 0.0575 | 0.000 |
| NR3 | 29 | 38 | 38.4000 | 154.5 | 101.7 | 34.2 | 7.46 | 73.28 | 8.7 | 74.3 | 17.0 | 1.63 | 1.07 | 1.2649 | 1.31 | -0.0251 | 0.000 |
| NR3 | 30 | 40 | 40.4000 | 168.0 | 111.4 | 33.7 | 6.76 | 73.07 | 9.9 | 68.7 | 21.4 | 1.77 | 1.17 | 1.2555 | | -0.0345 | -0.001 |
| NR3 | 31 | 42 | 42.4000 | 171.7 | 112.5 | 34.5 | 6.60 | 72.12 | 8.4 | 34.2 | 57.5 | 1.81 | 1.18 | 1.3062 | | 0.0162 | 0.000 |
| NR3 | 32 | 44 | 44.4000 | 142.2 | 93.2 | 34.5 | 6.14 | 71.68 | 10.4 | 64.8 | 24.8 | 1.50 | 0.98 | 1.3170 | 1.26 | 0.0270 | 0.000 |
| NR3 | 33 | 46 | 46.4000 | 151.4 | 101.2 | 33.2 | 6.17 | 73.01 | 8.7 | 40.8 | 50.5 | 1.59 | 1.06 | 1.2788 | | -0.0112 | 0.000 |
| NR3 | 34 | 48 | 48.4000 | 140.1 | 95.3 | 32.0 | 7.50 | 75.52 | 9.5 | 64.5 | 26.0 | 1.47 | 1.00 | 1.2736 | | -0.0164 | 0.000 |
| NR3 | 35 | 50 | 50.4000 | 162.9 | 110.5 | 32.2 | 7.40 | 75.23 | 7.6 | 42.5 | 49.8 | 1.71 | 1.16 | 1.2452 | | -0.0448 | -0.002 |
| NR3 | 36 | 52 | 52.5737 | 191.4 | 131.3 | 31.4 | 5.90 | 74.50 | 12.9 | 67.2 | 19.8 | 2.01 | 1.38 | 1.5215 | | 0.2315 | 0.007 |
| | | | | | | | | | | | | | | | Avg = 1.29 | | |

| Core No. | Sample No. | Uncorr. Depth (cm) | Corr. Depth (cm) | Wt. Wet Sample (g) | Wt. Dry Sample (g) | Water (%) | LOI (%) | Mineral (%) | Coarse Fraction (%) | Silt Fraction (%) | Clay Fraction (%) | Wet Bulk Dens (g/cc) | Dry Bulk Dens (g/cc) | Total Pb-210 (dpm/g) | Ra-226 (dpm/g) | USGS Excess Pb-210 (dpm/g) | +/- |
|---|---|---|---|---|---|---|---|---|---|---|---|---|---|---|---|---|---|
| NR 4 | 1 | 1 | 1.0000 | 45.2 | 20.1 | 55.5 | 16.74 | 27.73 | 37.3 | 37.3 | 25.4 | 0.95 | 0.42 | 6.4919 | | 5.4019 | 0.025 |
| NR 4 | 2 | 2 | 2.0000 | 69.0 | 33.6 | 51.3 | 14.44 | 34.25 | 25.9 | 45.4 | 28.7 | 1.45 | 0.71 | 5.5217 | | 4.4317 | 0.027 |
| NR 4 | 3 | 3 | 3.0000 | 69.0 | 37.3 | 45.9 | 15.69 | 38.37 | 16.3 | 46.1 | 37.6 | 1.45 | 0.78 | 3.8301 | 0.79 | 2.7401 | 0.017 |
| NR 4 | 4 | 4 | 4.0000 | 46.0 | 26.5 | 42.4 | 13.81 | 43.80 | 6.3 | 49.8 | 43.9 | 0.97 | 0.56 | 3.4065 | | 2.3165 | 0.014 |
| NR 4 | 5 | 5 | 5.0000 | 68.9 | 41.5 | 39.8 | 10.76 | 49.47 | 15.7 | 43.7 | 40.6 | 1.45 | 0.87 | 3.1395 | | 2.0495 | 0.014 |
| NR 4 | 6 | 6 | 6.0000 | 78.5 | 47.9 | 39.0 | 11.48 | 49.54 | 11.8 | 49.4 | 38.8 | 1.65 | 1.01 | 2.9447 | | 1.8547 | 0.020 |
| NR 4 | 7 | 7 | 7.0000 | 75.0 | 46.6 | 37.9 | 11.67 | 50.47 | 13.1 | 44.9 | 41.9 | 1.58 | 0.98 | 3.1239 | | 2.0339 | 0.010 |
| NR 4 | 8 | 8 | 8.0000 | 63.8 | 40.5 | 36.5 | 10.70 | 52.78 | 12.3 | 46.2 | 41.5 | 1.34 | 0.85 | 3.3906 | | 2.3006 | 0.012 |
| NR 4 | 9 | 9 | 9.0000 | 79.1 | 50.7 | 35.9 | 10.30 | 53.79 | 13.6 | 46.5 | 39.9 | 1.66 | 1.07 | 2.4281 | | 1.3381 | 0.009 |
| NR 4 | 10 | 10 | 10.0000 | 69.1 | 46.2 | 33.1 | 8.96 | 57.90 | 9.8 | 44.7 | 45.5 | 1.45 | 0.97 | 1.4049 | | 0.3149 | 0.001 |
| NR 4 | 11 | 11 | 11.0000 | 54.5 | 36.8 | 32.5 | 9.90 | 57.62 | 11.4 | 46.5 | 42.1 | 1.15 | 0.77 | 1.7758 | | 0.6858 | 0.002 |
| NR 4 | 12 | 12 | 12.0000 | 74.9 | 50.4 | 32.7 | 8.31 | 58.98 | 8.8 | 39.8 | 51.3 | 1.58 | 1.06 | 1.7313 | | 0.6413 | 0.003 |
| NR 4 | 13 | 13 | 13.0000 | 74.5 | 51.1 | 31.4 | 9.43 | 59.16 | 6.9 | 38.6 | 54.4 | 1.57 | 1.08 | 2.0374 | 1.2 | 0.9474 | 0.007 |
| NR 4 | 14 | 14 | 14.0000 | 61.9 | 42.4 | 31.5 | 8.85 | 59.65 | 5.1 | 41.4 | 53.5 | 1.30 | 0.89 | 1.6511 | | 0.5611 | 0.003 |
| NR 4 | 15 | 15 | 15.0000 | 67.1 | 46.1 | 31.3 | 9.58 | 59.12 | 7.6 | 36.8 | 55.6 | 1.41 | 0.97 | 1.6075 | | 0.5175 | 0.003 |
| NR 4 | 16 | 16 | 16.0000 | 67.2 | 46.2 | 31.3 | 9.38 | 59.37 | 9.2 | 32.2 | 58.6 | 1.41 | 0.97 | 1.7494 | | 0.6594 | 0.002 |
| NR 4 | 17 | 17 | 17.0000 | 73.9 | 51.4 | 30.4 | 10.75 | 58.80 | 11.7 | 43.4 | 44.9 | 1.56 | 1.08 | 1.8428 | | 0.7528 | 0.008 |
| NR 4 | 18 | 18 | 18.0000 | 63.0 | 43.7 | 30.6 | 7.68 | 61.68 | 15.1 | 43.2 | 41.7 | 1.33 | 0.92 | 1.2438 | | 0.1538 | 0.000 |
| NR 4 | 19 | 19 | 19.0000 | 74.9 | 52.2 | 30.3 | 9.35 | 60.34 | 12.5 | 45.7 | 41.8 | 1.58 | 1.10 | 1.7112 | | 0.6212 | 0.002 |
| NR 4 | 20 | 20 | 20.0000 | 74.6 | 52.1 | 30.2 | 7.67 | 62.17 | 13.7 | 46.3 | 40.0 | 1.57 | 1.10 | 1.3661 | | 0.2761 | 0.000 |
| NR 4 | 21 | 22 | 22.0400 | 132.6 | 91.8 | 30.8 | 10.25 | 58.98 | 13.2 | 47.2 | 39.6 | 1.40 | 0.97 | 1.8281 | | 0.7381 | 0.003 |
| NR 4 | 22 | 24 | 24.1200 | 111.2 | 76.8 | 30.9 | 9.02 | 60.05 | 11.9 | 46.2 | 41.9 | 1.17 | 0.81 | 1.5722 | | 0.4822 | 0.001 |
| NR 4 | 23 | 26 | 26.2000 | 124.9 | 87.1 | 30.3 | 10.02 | 59.72 | 7.8 | 43.8 | 48.4 | 1.31 | 0.92 | 2.2069 | 1.3 | 1.1169 | 0.005 |
| NR 4 | 24 | 28 | 28.2000 | 88.7 | 59.9 | 32.5 | 9.40 | 58.13 | 8.9 | 45.6 | 45.6 | 0.93 | 0.63 | 1.7375 | | 0.6475 | 0.008 |
| NR 4 | 25 | 30 | 30.2000 | 131.8 | 87.5 | 33.6 | 10.65 | 55.74 | 9.0 | 42.3 | 48.7 | 1.39 | 0.92 | 1.9707 | | 0.8807 | 0.005 |
| NR 4 | 26 | 32 | 32.2000 | 85.3 | 57.0 | 33.2 | na | | 10.4 | 32.3 | 57.3 | 0.90 | 0.60 | na | | na | na |
| NR 4 | 27 | 34 | 34.2000 | 157.2 | 104.0 | 33.8 | na | | 9.3 | 39.6 | 51.1 | 1.65 | 1.09 | na | | na | na |
| NR 4 | 28 | 36 | 36.2000 | 138.1 | 92.9 | 32.7 | na | | 11.1 | 36.4 | 52.5 | 1.45 | 0.98 | na | | na | na |
| NR 4 | 29 | 38 | 38.2000 | 144.8 | 97.4 | 32.7 | na | | 8.2 | 36.7 | 55.1 | 1.52 | 1.02 | na | | na | na |
| NR 4 | 30 | 40 | 40.2000 | 162.5 | 108.2 | 33.4 | na | | 5.4 | 34.7 | 59.8 | 1.71 | 1.14 | na | | na | na |
| NR 4 | 31 | 42 | 42.2000 | 138.7 | 94.4 | 31.9 | na | | 7.1 | 26.6 | 66.3 | 1.46 | 0.99 | na | | na | na |
| NR 4 | 32 | 44 | 44.2000 | 155.7 | 107.5 | 31.0 | na | | 9.6 | 28.7 | 61.7 | 1.64 | 1.13 | na | | na | na |
| NR 4 | 33 | 46 | 46.2000 | 123.9 | 83.4 | 32.7 | na | | 7.4 | 30.5 | 62.1 | 1.30 | 0.88 | na | | na | na |
| NR 4 | 34 | 48 | 48.2000 | 159.2 | 105.6 | 33.7 | na | | 10.8 | 31.0 | 58.2 | 1.68 | 1.11 | na | | na | na |
| | | | | | | | | | | | | | | | Avg = 1.09 | | |

| Core No. | Sample No. | Uncorr. Depth (cm) | Corr. Depth (cm) | Wt. Wet Sample (g) | Wt. Dry Sample (g) | Water (%) | LOI (%) | Mineral (%) | Coarse Fraction (%) | Silt Fraction (%) | Clay Fraction (%) | Wet Bulk Dens (g/cc) | Dry Bulk Dens (g/cc) | Total Pb-210 (dpm/g) | Ra-226 (dpm/g) | USGS Excess Pb-210 (dpm/g) 1.11 SPb | +/- |
|---|---|---|---|---|---|---|---|---|---|---|---|---|---|---|---|---|---|
| NR5 | 1 | 1 | 1.0308 | 63.3 | 50.2 | 20.7 | 11.13 | 68.17 | 13.7 | 57.0 | 29.3 | 1.33 | 1.06 | 3.4112 | | 2.2612 | 0.015 |
| NR5 | 2 | 2 | 2.0615 | 65.8 | 50.4 | 23.4 | 11.93 | 64.67 | 12.1 | 57.2 | 30.7 | 1.38 | 1.06 | 2.5192 | | 1.3692 | 0.008 |
| NR5 | 3 | 3 | 3.0923 | 71.6 | 54.5 | 23.9 | 11.61 | 64.50 | 11.9 | 51.2 | 36.9 | 1.51 | 1.15 | 2.2214 | | 1.0714 | 0.004 |
| NR5 | 4 | 4 | 4.1231 | 67.4 | 50.5 | 25.1 | 11.49 | 63.44 | 12.3 | 49.3 | 38.4 | 1.42 | 1.06 | 2.3041 | | 1.1541 | 0.006 |
| NR5 | 5 | 5 | 5.1538 | 61.7 | 46.5 | 24.6 | 10.58 | 64.79 | 11.9 | 45.8 | 42.3 | 1.30 | 0.98 | 1.9889 | | 0.8389 | 0.010 |
| NR5 | 6 | 6 | 6.1846 | 68.8 | 51.3 | 25.4 | 10.74 | 63.83 | 12.4 | 54.7 | 32.9 | 1.45 | 1.08 | 1.7430 | | 0.5930 | 0.006 |
| NR5 | 7 | 7 | 7.2154 | 75.6 | 55.7 | 26.3 | 11.66 | 62.02 | 8.8 | 37.3 | 53.8 | 1.59 | 1.17 | 1.8824 | | 0.7324 | 0.011 |
| NR5 | 8 | 8 | 8.2462 | 62.9 | 45.9 | 27.0 | 11.05 | 61.93 | 9.4 | 33.9 | 56.7 | 1.32 | 0.97 | 1.9927 | 1.18 | 0.8427 | 0.004 |
| NR5 | 9 | 9 | 9.2769 | 71.1 | 51.1 | 28.1 | 11.20 | 60.67 | 7.3 | 33.6 | 59.1 | 1.50 | 1.08 | 2.1655 | | 1.0155 | 0.005 |
| NR5 | 10 | 10 | 10.3077 | 71.8 | 51.4 | 28.4 | 11.78 | 59.81 | 7.0 | 39.8 | 53.1 | 1.51 | 1.08 | 2.1681 | | 1.0181 | 0.007 |
| NR5 | 11 | 11 | 11.3385 | 68.5 | 49.6 | 27.6 | 12.03 | 60.38 | 7.1 | 36.1 | 56.8 | 1.44 | 1.04 | 1.8840 | | 0.7340 | 0.004 |
| NR5 | 12 | 12 | 12.3692 | 77.2 | 55.5 | 28.1 | 12.01 | 59.88 | 8.6 | 37.9 | 53.5 | 1.62 | 1.17 | 2.0321 | | 0.8821 | 0.005 |
| NR5 | 13 | 13 | 13.4000 | 75.6 | 54.2 | 28.3 | 12.03 | 59.66 | 7.5 | 42.9 | 49.6 | 1.59 | 1.14 | 2.0170 | 1.08 | 0.8670 | 0.006 |
| NR5 | 14 | 14 | 14.4000 | 63.5 | 45.4 | 28.5 | 11.73 | 59.77 | 9.3 | 48.9 | 41.9 | 1.34 | 0.96 | 1.9575 | | 0.8075 | 0.007 |
| NR5 | 15 | 15 | 15.4000 | 72.3 | 51.8 | 28.4 | 11.68 | 59.96 | 9.9 | 50.5 | 39.6 | 1.52 | 1.09 | 2.4645 | | 1.3145 | 0.008 |
| NR5 | 16 | 16 | 16.4000 | 70.5 | 50 | 29.1 | 11.51 | 59.41 | 9.7 | 40.5 | 49.8 | 1.48 | 1.05 | 2.3881 | | 1.2381 | 0.004 |
| NR5 | 17 | 17 | 17.4000 | 63.6 | 45 | 29.2 | 11.68 | 59.07 | 10.3 | 49.4 | 40.2 | 1.34 | 0.95 | 2.3004 | | 1.1504 | 0.006 |
| NR5 | 18 | 18 | 18.4000 | 74.9 | 52.6 | 29.8 | 11.75 | 58.47 | 7.4 | 44.9 | 47.7 | 1.58 | 1.11 | 2.3042 | | 1.1542 | 0.004 |
| NR5 | 19 | 19 | 19.4000 | 77 | 54.3 | 29.5 | 11.46 | 59.06 | 7.6 | 49.6 | 42.8 | 1.62 | 1.14 | 2.1795 | | 1.0295 | 0.004 |
| NR5 | 20 | 20 | 20.4000 | 81.4 | 57.7 | 29.1 | 10.52 | 60.37 | 7.0 | 57.4 | 35.6 | 1.71 | 1.21 | 2.0863 | | 0.9363 | 0.004 |
| NR5 | 21 | 22 | 22.4000 | 140.9 | 98.9 | 29.8 | 10.93 | 59.26 | 7.2 | 47.1 | 45.7 | 1.48 | 1.04 | 2.1251 | | 0.9751 | 0.005 |
| NR5 | 22 | 24 | 24.4000 | 163.2 | 113.2 | 30.6 | 9.98 | 59.38 | 7.8 | 53.0 | 39.1 | 1.72 | 1.19 | 2.1740 | | 1.0240 | 0.007 |
| NR5 | 23 | 26 | 26.4000 | 160 | 113.3 | 29.2 | 10.22 | 60.60 | 10.5 | 56.2 | 33.3 | 1.68 | 1.19 | 1.6066 | | 0.4566 | 0.002 |
| NR5 | 24 | 28 | 28.4000 | 165.1 | 118.8 | 28.0 | 9.29 | 62.67 | 15.2 | 42.2 | 42.6 | 1.74 | 1.25 | 1.4833 | 1.2 | 0.3333 | 0.002 |
| NR5 | 25 | 30 | 30.4000 | 180.3 | 131.4 | 27.1 | 9.16 | 63.72 | 15.9 | 44.5 | 39.6 | 1.90 | 1.38 | 1.5641 | | 0.4141 | 0.002 |
| NR5 | 26 | 32 | 32.4000 | 184.4 | 136.9 | 25.8 | 8.70 | 65.55 | 22.9 | 30.9 | 46.2 | 1.94 | 1.44 | 1.0297 | | -0.1203 | 0.000 |
| NR5 | 27 | 34 | 34.4000 | 176.9 | 132.6 | 25.0 | 8.51 | 66.44 | 29.3 | 38.4 | 32.3 | 1.86 | 1.40 | 1.3888 | | 0.2388 | 0.002 |
| NR5 | 28 | 36 | 36.5125 | 198.6 | 151.9 | 23.5 | 8.00 | 68.49 | 34.0 | 25.6 | 40.4 | 2.09 | 1.60 | 1.0276 | | -0.1224 | 0.000 |
| NR5 | 29 | 38 | 39.1000 | 219.3 | 169.3 | 22.8 | 8.00 | 69.20 | 36.8 | 38.5 | 24.7 | 2.31 | 1.78 | 0.9619 | | -0.1881 | 0.000 |
| NR5 | 30 | 40 | 41.6000 | 198.6 | 152.6 | 23.2 | 7.66 | 69.18 | 34.1 | 28.7 | 37.3 | 2.09 | 1.61 | 2.0101 | | 0.8601 | 0.005 |
| | | | | | | | | | | | | | | | Avg. = 1.15 | | |

| Core No. | Sample No. | Uncorr. Depth (cm) | Corr. Depth (cm) | Wt. Wet Sample (g) | Wt. Dry Sample (g) | Water (%) | LOI (%) | Mineral (%) | Coarse Fraction (%) | Silt Fraction (%) | Clay Fraction (%) | Wet Bulk Dens (g/cc) | Dry Bulk Dens (g/cc) | Total Pb-210 (dpm/g) | Radium (dpm/g) | USGS Excess Pb-210 (dpm/g) | +/- |
|---|---|---|---|---|---|---|---|---|---|---|---|---|---|---|---|---|---|
| NR6 | 1 | 1 | 1.0000 | 47.9 | 15.8 | 67.0 | 21.70 | 11.28 | 52.6 | 23.0 | 24.4 | 1.05 | 0.34 | 9.2320 | | 8.3620 | 0.024 |
| NR6 | 2 | 2 | 2.0000 | 52.1 | 20.7 | 60.3 | 19.01 | 20.72 | 47.5 | 23.2 | 29.4 | 1.14 | 0.45 | 9.6026 | | 8.7326 | 0.021 |
| NR6 | 3 | 3 | 3.0000 | 90.6 | 43.2 | 52.3 | 16.90 | 30.78 | 6.0 | 30.9 | 63.1 | 1.98 | 0.94 | 6.2242 | | 5.3542 | 0.013 |
| NR6 | 4 | 4 | 4.0000 | 66.7 | 37.2 | 44.2 | 14.46 | 41.32 | 13.3 | 41.7 | 45.0 | 1.46 | 0.81 | 4.8421 | 0.69 | 3.9721 | 0.016 |
| NR6 | 5 | 5 | 5.0000 | 88.8 | 50.4 | 43.2 | 14.06 | 42.70 | 10.5 | 35.7 | 53.7 | 1.94 | 1.10 | 3.0042 | | 2.1342 | 0.005 |
| NR6 | 6 | 6 | 6.0000 | 74.2 | 43.9 | 40.8 | 12.08 | 47.09 | 3.4 | 43.6 | 53.0 | 1.62 | 0.96 | 3.2046 | | 2.3346 | 0.006 |
| NR6 | 7 | 7 | 7.0000 | 104.4 | 59.8 | 42.7 | 12.28 | 45.00 | 7.3 | 43.1 | 49.7 | 2.28 | 1.31 | 3.2338 | | 2.3638 | 0.014 |
| NR6 | 8 | 8 | 8.0000 | 70.9 | 41.4 | 41.6 | 12.50 | 45.89 | 3.4 | 40.7 | 56.0 | 1.55 | 0.90 | 2.9632 | 0.99 | 2.0932 | 0.008 |
| NR6 | 9 | 9 | 9.0000 | 88.7 | 52.6 | 40.7 | 12.28 | 47.02 | 2.1 | 39.5 | 58.4 | 1.94 | 1.15 | 2.9966 | | 2.1266 | 0.007 |
| NR6 | 10 | 10 | 10.0000 | 80.1 | 48.5 | 39.5 | 11.88 | 48.67 | 1.1 | 40.1 | 58.8 | 1.75 | 1.06 | 2.9173 | | 2.0473 | 0.008 |
| NR6 | 11 | 11 | 11.0000 | 60.5 | 37.2 | 38.5 | 12.33 | 49.16 | 2.4 | 34.4 | 63.2 | 1.32 | 0.81 | 2.7048 | | 1.8348 | 0.006 |
| NR6 | 12 | 12 | 12.0000 | 79.3 | 48 | 39.5 | 12.03 | 48.50 | 0.8 | 32.4 | 66.8 | 1.73 | 1.05 | 2.6353 | | 1.7653 | 0.006 |
| NR6 | 13 | 13 | 13.0000 | 68.2 | 42 | 38.4 | 12.33 | 49.26 | 1.1 | 29.8 | 69.1 | 1.49 | 0.92 | 2.8762 | | 2.0062 | 0.013 |
| NR6 | 14 | 14 | 14.0000 | 73.9 | 45.2 | 38.8 | 11.66 | 49.50 | 0.7 | 32.8 | 66.4 | 1.61 | 0.99 | 2.7940 | | 1.9240 | 0.008 |
| NR6 | 15 | 15 | 15.0000 | 69.9 | 43.5 | 37.8 | 12.20 | 50.03 | 1.5 | 36.5 | 62.0 | 1.53 | 0.95 | 3.1220 | | 2.2520 | 0.015 |
| NR6 | 16 | 16 | 16.0000 | 71.2 | 44.9 | 36.9 | 10.96 | 52.11 | 0.7 | 38.3 | 61.0 | 1.55 | 0.98 | 2.9589 | | 2.0889 | 0.006 |
| NR6 | 17 | 17 | 17.0000 | 69.1 | 43.4 | 37.2 | 11.66 | 51.15 | 1.8 | 27.6 | 70.6 | 1.51 | 0.95 | 2.6822 | | 1.8122 | 0.006 |
| NR6 | 18 | 18 | 18.0000 | 72.2 | 45.8 | 36.6 | 11.39 | 52.04 | 1.1 | 44.2 | 54.7 | 1.58 | 1.00 | 2.5748 | | 1.7048 | 0.006 |
| NR6 | 19 | 19 | 19.0000 | 65.2 | 41.1 | 37.0 | 11.22 | 51.82 | 1.5 | 49.8 | 48.7 | 1.42 | 0.90 | 2.4254 | | 1.5554 | 0.007 |
| NR6 | 20 | 20 | 20.0000 | 72.3 | 45.7 | 36.8 | 10.50 | 52.71 | 2.6 | 32.3 | 65.0 | 1.58 | 1.00 | 2.7427 | | 1.8727 | 0.008 |
| NR6 | 21 | 22 | 22.0000 | 106.8 | 67 | 37.3 | 11.22 | 51.51 | 0.7 | 44.8 | 54.5 | 1.17 | 0.73 | 2.1978 | | 1.3278 | 0.006 |
| NR6 | 22 | 24 | 24.0000 | 124.8 | 79.8 | 36.1 | 11.05 | 52.90 | 2.4 | 55.1 | 42.5 | 1.36 | 0.87 | 2.3372 | | 1.4672 | 0.006 |
| NR6 | 23 | 26 | 26.1067 | 146.6 | 93.6 | 36.2 | 10.69 | 53.15 | 2.1 | 55.7 | 42.2 | 1.60 | 1.02 | 2.1289 | | 1.2589 | 0.004 |
| NR6 | 24 | 28 | 28.2000 | 147.4 | 93.7 | 36.4 | 10.89 | 52.68 | 2.6 | 45.0 | 52.4 | 1.61 | 1.02 | na | | | na |
| NR6 | 25 | 30 | 30.6000 | 144.5 | 93.9 | 35.0 | 9.88 | 55.10 | 1.1 | 41.8 | 57.1 | 1.58 | 1.03 | 2.0500 | | 1.1800 | 0.007 |
| NR6 | 26 | 32 | 34.6000 | 175.4 | 113.9 | 35.1 | 10.08 | 54.86 | 2.1 | 41.8 | 56.1 | 1.91 | 1.24 | 2.0648 | 0.94 | 1.1948 | 0.008 |
| NR6 | 27 | 34 | 37.9600 | 187.5 | 122.6 | 34.6 | 9.66 | 55.72 | 1.3 | 48.2 | 50.5 | 2.05 | 1.34 | 1.9170 | | 1.0470 | 0.008 |
| NR6 | 28 | 36 | 41.1600 | 171.2 | 114.7 | 33.0 | 9.84 | 57.16 | 1.9 | 52.1 | 46.0 | 1.87 | 1.25 | 2.0358 | | 1.1658 | 0.007 |
| NR6 | 29 | 38 | 45.5429 | 178.5 | 118.9 | 33.4 | 8.86 | 57.75 | 1.6 | 51.9 | 46.5 | 1.95 | 1.30 | 1.7547 | | 0.8847 | 0.005 |
| | | | | | | | | | | | | | | | Avg=0.87 | | |

| Core No. | Sample No. | Uncorr. Depth (cm) | Corr. Depth (cm) | Wt. Wet Sample (g) | Wt. Dry Sample (g) | Water (%) | LOI (%) | Mineral (%) | Coarse Fraction (%) | Silt Fraction (%) | Clay Fraction (%) | Wet Bulk Dens (g/cc) | Dry Bulk Dens (g/cc) | Total Pb-210 (dpm/g) | Radium (dpm/g) | USGS Excess Pb-210 (dpm/g) | +/- |
|---|---|---|---|---|---|---|---|---|---|---|---|---|---|---|---|---|---|
| NR 7 | 1 | 1 | 1.0000 | 67.2 | 40.8 | 39.3 | 10.93 | 49.78 | 27.2 | 43.7 | 29.1 | 1.71 | 1.04 | 4.7458 | | 3.7658 | 0.018 |
| NR 7 | 2 | 2 | 2.0000 | 60.5 | 39.6 | 34.5 | 11.00 | 54.45 | 18.5 | 47.7 | 33.8 | 1.54 | 1.01 | 5.3559 | | 4.3759 | 0.023 |
| NR 7 | 3 | 3 | 3.0000 | 62.3 | 41.6 | 33.2 | 10.69 | 56.08 | 16.6 | 44.0 | 39.4 | 1.59 | 1.06 | 3.4786 | 1.01 | 2.4986 | 0.012 |
| NR 7 | 4 | 4 | 4.0000 | 72.8 | 50.3 | 30.9 | 10.47 | 58.62 | 10.3 | 49.6 | 40.1 | 1.85 | 1.28 | 2.6182 | | 1.6382 | 0.012 |
| NR 7 | 5 | 5 | 5.0000 | 80.5 | 54.4 | 32.4 | 10.34 | 57.24 | 14.4 | 44.8 | 40.7 | 2.05 | 1.39 | 3.0155 | | 2.0355 | 0.009 |
| NR 7 | 6 | 6 | 6.0000 | 87.0 | 59.6 | 31.5 | 10.50 | 58.01 | 17.1 | 50.6 | 32.3 | 2.22 | 1.52 | 2.8674 | | 1.8874 | 0.018 |
| NR 7 | 7 | 7 | 7.0000 | 60.1 | 40.8 | 32.1 | 10.50 | 57.39 | 16.5 | 40.4 | 43.1 | 1.53 | 1.04 | 1.9938 | | 1.0138 | 0.011 |
| NR 7 | 8 | 8 | 8.0000 | 70.9 | 48.0 | 32.3 | 10.87 | 56.83 | 7.9 | 39.9 | 52.2 | 1.81 | 1.22 | 2.0058 | | 1.0258 | 0.007 |
| NR 7 | 9 | 9 | 9.0000 | 80.2 | 54.1 | 32.5 | 10.36 | 57.10 | 8.9 | 44.0 | 47.1 | 2.04 | 1.38 | 1.6316 | | 0.6516 | 0.005 |
| NR 7 | 10 | 10 | 10.0000 | 82.2 | 55.8 | 32.1 | 10.34 | 57.55 | 10.1 | 42.9 | 47.0 | 2.09 | 1.42 | 1.5354 | | 0.5554 | 0.005 |
| NR 7 | 11 | 11 | 11.0000 | 69.6 | 47.1 | 32.3 | 10.45 | 57.22 | 7.4 | 36.0 | 56.6 | 1.77 | 1.20 | 1.6548 | | 0.6748 | 0.004 |
| NR 7 | 12 | 12 | 12.0000 | 76.7 | 51.8 | 32.5 | 10.81 | 56.73 | 6.8 | 46.4 | 46.8 | 1.95 | 1.32 | 1.5085 | 1.01 | 0.5285 | 0.004 |
| NR 7 | 13 | 13 | 13.0000 | 75.8 | 50.8 | 33.0 | 10.34 | 56.68 | 8.4 | 37.8 | 53.8 | 1.93 | 1.29 | 1.5507 | | 0.5707 | 0.006 |
| NR 7 | 14 | 14 | 14.0000 | 82.0 | 55.4 | 32.4 | 10.22 | 57.34 | 10.1 | 44.4 | 45.5 | 2.09 | 1.41 | 1.5640 | | 0.5840 | 0.004 |
| NR 7 | 15 | 15 | 15.0000 | 96.6 | 64.9 | 32.8 | 10.71 | 56.47 | 10.3 | 36.8 | 52.9 | 2.46 | 1.65 | 1.5262 | | 0.5462 | 0.003 |
| NR 7 | 16 | 16 | 16.0000 | 82.2 | 55.8 | 32.1 | 10.34 | 57.55 | 10.3 | 43.2 | 46.5 | 2.09 | 1.42 | 1.5375 | | 0.5575 | 0.002 |
| NR 7 | 17 | 17 | 17.0000 | 90.2 | 60.8 | 32.6 | 10.26 | 57.15 | 9.6 | 33.8 | 56.6 | 2.30 | 1.55 | 1.5556 | | 0.5756 | 0.004 |
| NR 7 | 18 | 18 | 18.0000 | 79.6 | 54.2 | 31.9 | 9.36 | 58.73 | 10.9 | 39.3 | 49.8 | 2.03 | 1.38 | 1.4502 | | 0.4702 | 0.003 |
| NR 7 | 19 | 19 | 19.0000 | 94.9 | 64.6 | 31.9 | 10.06 | 58.01 | 8.8 | 35.2 | 56.0 | 2.42 | 1.65 | 1.1981 | | 0.2181 | 0.002 |
| NR 7 | 20 | 20 | 20.0000 | 84.8 | 58.9 | 30.5 | 9.66 | 59.79 | 10.8 | 35.3 | 53.8 | 2.16 | 1.50 | 1.6375 | | 0.6575 | 0.004 |
| NR 7 | 21 | 22 | 22.0000 | 167.7 | 115.9 | 30.9 | 9.41 | 59.70 | 9.7 | 28.5 | 61.8 | 2.14 | 1.48 | 1.4748 | | 0.4948 | 0.003 |
| NR 7 | 22 | 24 | 24.0000 | 108.6 | 76.2 | 29.8 | 8.25 | 61.91 | 11.5 | 28.2 | 60.3 | 1.38 | 0.97 | 1.6243 | 0.91 | 0.6443 | 0.002 |
| NR 7 | 23 | 26 | 26.0000 | 152.7 | 105.6 | 30.8 | 9.29 | 59.87 | 11.3 | 32.3 | 56.4 | 1.94 | 1.34 | 1.4549 | | 0.4749 | 0.003 |
| NR 7 | 24 | 28 | 28.0000 | 176.3 | 121.5 | 31.1 | 8.51 | 60.40 | 12.9 | 33.3 | 53.7 | 2.24 | 1.55 | 1.4341 | | 0.4541 | 0.002 |
| NR 7 | 25 | 30 | 30.0000 | 162.1 | 111.6 | 31.2 | 8.33 | 60.51 | 10.5 | 44.4 | 45.1 | 2.06 | 1.42 | 1.4126 | | 0.4326 | 0.002 |
| NR 7 | 26 | 32 | 32.0000 | 159.4 | 111.9 | 29.8 | 8.38 | 61.82 | 16.2 | 50.7 | 33.1 | 2.03 | 1.42 | 1.3923 | | 0.4123 | 0.003 |
| NR 7 | 27 | 34 | 34.0000 | 151.5 | 115.2 | 24.0 | 8.53 | 67.51 | 12.2 | 43.2 | 44.6 | 1.93 | 1.47 | 1.4244 | | 0.4444 | 0.003 |
| NR 7 | 28 | 36 | 36.0000 | 140.3 | 97.7 | 30.4 | 8.32 | 61.32 | 13.5 | 35.7 | 50.8 | 1.79 | 1.24 | 1.0771 | | 0.0971 | 0.000 |
| NR 7 | 29 | 38 | 38.0000 | 182.8 | 127.4 | 30.3 | 7.91 | 61.79 | 13.9 | 47.6 | 38.5 | 2.33 | 1.62 | 1.4745 | | 0.4945 | 0.016 |
| NR 7 | 30 | 40 | 40.0000 | 130.7 | 92.6 | 29.2 | 8.07 | 62.78 | 11.9 | 46.0 | 42.1 | 1.66 | 1.18 | 1.3228 | | 0.3428 | 0.002 |
| NR 7 | 31 | 42 | 42.0000 | 162.5 | 114.3 | 29.7 | 8.12 | 62.22 | 13.2 | 41.4 | 45.4 | 2.07 | 1.46 | 1.1440 | | 0.1640 | 0.001 |
| NR 7 | 32 | 44 | 44.0000 | 166.4 | 116.0 | 30.3 | 7.48 | 62.23 | 12.5 | 45.9 | 41.6 | 2.12 | 1.48 | 1.0625 | | 0.0825 | 0.002 |
| NR 7 | 33 | 46 | 46.0762 | 180.5 | 126.6 | 29.9 | 7.11 | 63.02 | 14.4 | 43.1 | 42.5 | 2.30 | 1.61 | 1.0506 | | 0.0706 | 0.000 |
| NR 7 | 34 | 48 | 48.1714 | 179.7 | 127.4 | 29.1 | 7.75 | 63.14 | 16.6 | 41.7 | 41.7 | 2.29 | 1.62 | 1.3057 | | 0.3257 | 0.009 |
| | | | | | | | | | | | | | | Avg = 0.98 | | | |

| Core No. | Sample No. | Uncorr. Depth (cm) | Corr. Depth (cm) | Wt. Wet Sample (g) | Wt. Dry Sample (g) | Water (%) | LOI (%) | Mineral (%) | Coarse Fraction (%) | Silt Fraction (%) | Clay Fraction (%) | Wet Bulk Dens (g/cc) | Dry Bulk Dens (g/cc) | Total Pb-210 (dpm/g) | Radium (dpm/g) | USGS Excess Pb-210 (dpm/g) | +/- |
|---|---|---|---|---|---|---|---|---|---|---|---|---|---|---|---|---|---|
| NR 8 | 1 | 1 | 1.0000 | 53.8 | 30.4 | 43.5 | 21.61 | 34.89 | 10.3 | 29.0 | 60.7 | 1.13 | 0.64 | 11.0118 | | 10.1018 | 0.067 |
| NR 8 | 2 | 2 | 2.0000 | 62.9 | 39.5 | 37.2 | 17.04 | 45.75 | 11.0 | 34.5 | 54.5 | 1.32 | 0.83 | 6.6259 | | 5.7159 | 0.034 |
| NR 8 | 3 | 3 | 3.0000 | 67.2 | 43.0 | 36.0 | 9.98 | 54.00 | 9.1 | 26.4 | 64.6 | 1.41 | 0.90 | 5.0639 | 0.98 | 4.1539 | 0.017 |
| NR 8 | 4 | 4 | 4.0000 | 78.6 | 51.6 | 34.4 | 11.20 | 54.45 | 12.4 | 29.1 | 58.5 | 1.65 | 1.09 | 5.1215 | | 4.2115 | 0.029 |
| NR 8 | 5 | 5 | 5.0000 | 71.7 | 46.4 | 35.3 | 21.71 | 43.00 | 10.2 | 20.4 | 69.4 | 1.51 | 0.98 | 2.7153 | | 1.8053 | 0.012 |
| NR 8 | 6 | 6 | 6.0000 | 83.3 | 54.5 | 34.6 | 9.18 | 56.25 | 15.5 | 24.7 | 59.8 | 1.75 | 1.15 | 4.6890 | | 3.7790 | 0.032 |
| NR 8 | 7 | 7 | 7.0000 | 66.7 | 44.4 | 33.4 | 7.83 | 58.73 | 22.7 | 35.4 | 41.9 | 1.40 | 0.93 | 2.5838 | | 1.6738 | 0.028 |
| NR 8 | 8 | 8 | 8.0000 | 72.7 | 48.3 | 33.6 | 7.74 | 58.70 | 20.3 | 33.0 | 46.7 | 1.53 | 1.02 | 2.9125 | | 2.0025 | 0.011 |
| NR 8 | 9 | 9 | 9.0000 | 106.0 | 70.8 | 33.2 | 6.88 | 59.92 | 18.9 | 39.8 | 41.3 | 2.23 | 1.49 | 2.6762 | | 1.7662 | 0.010 |
| NR 8 | 10 | 10 | 10.0000 | 81.8 | 55.9 | 31.7 | 8.87 | 59.46 | 22.4 | 37.6 | 39.9 | 1.72 | 1.18 | 2.6136 | | 1.7036 | 0.025 |
| NR 8 | 11 | 11 | 11.0000 | 99.7 | 67.5 | 32.3 | 7.88 | 59.82 | 23.5 | 30.2 | 46.3 | 2.10 | 1.42 | 2.5290 | 0.94 | 1.6190 | 0.010 |
| NR 8 | 12 | 12 | 12.0000 | 74.2 | 50.0 | 32.6 | 8.53 | 58.85 | 19.4 | 29.0 | 51.6 | 1.56 | 1.05 | 1.8801 | | 0.9701 | 0.012 |
| NR 8 | 13 | 13 | 13.0000 | 75.9 | 50.5 | 33.5 | 11.40 | 55.14 | 16.0 | 28.9 | 55.1 | 1.60 | 1.06 | 2.1565 | | 1.2465 | 0.022 |
| NR 8 | 14 | 14 | 14.0000 | 104.2 | 70.5 | 32.3 | 8.00 | 59.66 | 15.5 | 25.2 | 59.4 | 2.19 | 1.48 | 1.5858 | | 0.6758 | 0.004 |
| NR 8 | 15 | 15 | 15.0000 | 82.5 | 56.8 | 31.2 | 9.08 | 59.77 | 20.1 | 21.6 | 58.4 | 1.74 | 1.20 | 1.8149 | 0.82 | 0.9049 | 0.005 |
| NR 8 | 16 | 16 | 16.0000 | 87.0 | 60.0 | 31.0 | 7.27 | 61.70 | 14.9 | 23.5 | 61.6 | 1.83 | 1.26 | 1.8138 | | 0.9038 | 0.010 |
| NR 8 | 17 | 17 | 17.0000 | 76.3 | 52.6 | 31.1 | na | | 16.7 | 32.7 | 50.6 | 1.61 | 1.11 | na | | na | na |
| NR 8 | 18 | 18 | 18.0083 | 109.0 | 75.1 | 31.1 | na | | 15.4 | 38.3 | 46.2 | 2.29 | 1.58 | na | | na | na |
| NR 8 | 19 | 19 | 19.0500 | 69.5 | 48.4 | 30.4 | na | | 19.2 | 23.8 | 56.9 | 1.46 | 1.02 | na | | na | na |
| NR 8 | 20 | 20 | 20.0917 | 77.8 | 54.9 | 29.4 | na | | 18.4 | 23.8 | 57.9 | 1.64 | 1.16 | na | | na | na |
| NR 8 | 21 | 22 | 22.1750 | 141.6 | 99.1 | 30.0 | na | | 24.8 | 28.8 | 46.4 | 1.49 | 1.04 | na | | na | na |
| NR 8 | 22 | 24 | 24.2147 | 132.9 | 91.8 | 30.9 | na | | 21.2 | 21.2 | 57.6 | 1.40 | 0.97 | na | | na | na |
| NR 8 | 23 | 26 | 26.2358 | 160.0 | 111.2 | 30.5 | na | | 24.6 | 25.3 | 50.2 | 1.68 | 1.17 | na | | na | na |
| NR 8 | 24 | 28 | 28.2568 | 169.5 | 119.2 | 29.7 | na | | 24.1 | 28.9 | 47.0 | 1.78 | 1.25 | na | | na | na |
| NR 8 | 25 | 30 | 30.2779 | 166.1 | 118.7 | 28.5 | na | | 21.8 | 34.5 | 43.7 | 1.75 | 1.25 | na | | na | na |
| NR 8 | 26 | 32 | 32.2989 | 183.0 | 128.9 | 29.6 | na | | 23.6 | 31.6 | 44.9 | 1.93 | 1.36 | na | | na | na |
| NR 8 | 27 | 34 | 34.3200 | 138.0 | 95.0 | 31.2 | na | | 16.1 | 36.3 | 47.6 | 1.45 | 1.00 | na | | na | na |
| NR 8 | 28 | 36 | 36.3411 | 169.0 | 113.8 | 32.7 | na | | 17.0 | 37.7 | 45.3 | 1.78 | 1.20 | na | | na | na |
| NR 8 | 29 | 38 | 38.3621 | 166.7 | 112.3 | 32.6 | na | | 18.2 | 25.2 | 56.6 | 1.75 | 1.18 | na | | na | na |
| NR 8 | 30 | 40 | 40.3832 | 185.2 | 121.2 | 34.6 | na | | 18.9 | 30.7 | 50.4 | 1.95 | 1.28 | na | | na | na |
| NR 8 | 31 | 42 | 42.4119 | 128.2 | 83.4 | 34.9 | na | | 13.8 | 29.2 | 56.9 | 1.35 | 0.88 | na | | na | na |
| NR 8 | 32 | 44 | 44.4716 | 137.7 | 91.4 | 33.6 | na | | 20.3 | 28.6 | 51.0 | 1.45 | 0.96 | na | | na | na |
| NR 8 | 33 | 46 | 46.5313 | 179.7 | 117.9 | 34.4 | na | | 16.7 | 21.4 | 61.9 | 1.89 | 1.24 | na | | na | na |
| NR 8 | 34 | 48 | 48.5910 | 178.8 | 118.4 | 33.8 | na | | 21.8 | 22.9 | 55.3 | 1.88 | 1.25 | na | | na | na |
| NR 8 | 35 | 50 | 50.6507 | 151.8 | 101.6 | 33.1 | na | | 20.0 | 26.2 | 53.8 | 1.60 | 1.07 | na | | na | na |
| NR 8 | 36 | 52 | 52.7104 | 177.0 | 120.0 | 32.2 | na | | 22.7 | 23.9 | 53.4 | 1.86 | 1.26 | na | | na | na |
| NR 8 | 37 | 54 | 54.7701 | 199.7 | 129.4 | 35.2 | na | | 34.7 | 17.9 | 47.4 | 2.10 | 1.36 | na | | na | na |
| NR 8 | 38 | 56 | 56.8469 | 186.1 | 122.4 | 34.2 | na | | 35.1 | 22.9 | 42.1 | 1.96 | 1.29 | na | | na | na |
| NR 8 | 39 | 58 | 58.9406 | 162.5 | 104.4 | 35.8 | na | | 21.7 | 16.5 | 61.8 | 1.71 | 1.10 | na | | na | na |
| NR 8 | 40 | 60 | 61.0344 | 212.4 | 132.5 | 37.6 | na | | 19.0 | 21.3 | 59.7 | 2.24 | 1.39 | na | | na | na |
| NR 8 | 41 | 62 | 63.1281 | 146.2 | 93.4 | 36.1 | na | | 29.9 | 29.1 | 41.0 | 1.54 | 0.98 | na | | na | na |
| NR 8 | 42 | 64 | 65.2219 | 164.9 | 105.5 | 36.0 | na | | 42.0 | 16.3 | 41.6 | 1.74 | 1.11 | na | | na | na |
| NR 8 | 43 | 66 | 67.3156 | 156.0 | 97.2 | 37.7 | na | | 17.0 | 26.6 | 56.4 | 1.64 | 1.02 | na | | na | na |
| NR 8 | 44 | 68 | 69.2000 | 170.5 | 102.8 | 39.7 | na | | 12.5 | 26.7 | 60.8 | 1.79 | 1.08 | na | | na | na |
| NR 8 | 45 | 70 | 71.5222 | 164.3 | 97.7 | 40.5 | na | | 10.6 | 21.5 | 67.9 | 1.73 | 1.03 | na | | na | na |
| NR 8 | 46 | 72 | 73.6333 | 133.5 | 79.9 | 40.1 | na | | 12.3 | 25.7 | 62.1 | 1.40 | 0.84 | na | | na | na |
| NR 8 | 47 | 73 | 74.6889 | 119.6 | 72.8 | 39.1 | na | | 15.5 | 23.9 | 60.6 | 1.26 | 0.77 | na | | na | na |
| | | | | | | | | | | | | | | | Avg = 0.91 | | |

| Core No. | Sample No. | Uncorr. Depth (cm) | Corr. Depth (cm) | Wt. Wet Sample (g) | Wt. Dry Sample (g) | Water (%) | LOI (%) | Mineral (%) | Coarse Fraction (%) | Silt Fraction (%) | Clay Fraction (%) | Wet Bulk Dens (g/cc) | Dry Bulk Dens (g/cc) | Total Pb-210 (dpm/g) | Radium (dpm/g) | USGS Excess Pb-210 (dpm/g) | +/- |
|---|---|---|---|---|---|---|---|---|---|---|---|---|---|---|---|---|---|
| NR 9 | 1 | 1 | 1.0000 | 65.0 | 49.6 | 23.7 | 11.64 | 64.67 | 24.2 | 48.4 | 27.4 | 1.32 | 1.01 | 4.6208 | | 3.6308 | 0.093 |
| NR 9 | 2 | 2 | 2.0000 | 59.7 | 47.0 | 21.3 | 22.43 | 56.30 | 28.6 | 39.4 | 32.0 | 1.21 | 0.95 | 3.2768 | | 2.2868 | 0.017 |
| NR 9 | 3 | 3 | 3.0000 | 53.2 | 42.7 | 19.7 | 8.45 | 71.81 | 24.6 | 44.4 | 31.0 | 1.08 | 0.87 | 2.2588 | 1.1 | 1.2688 | 0.012 |
| NR 9 | 4 | 4 | 4.0000 | 78.5 | 61.4 | 21.8 | 8.24 | 69.98 | 15.2 | 41.2 | 43.7 | 1.59 | 1.25 | 1.8010 | | 0.8110 | 0.020 |
| NR 9 | 5 | 5 | 5.0000 | 79.9 | 60.9 | 23.8 | 8.89 | 67.33 | 15.5 | 35.9 | 48.6 | 1.62 | 1.24 | 1.5851 | | 0.5951 | 0.004 |
| NR 9 | 6 | 6 | 6.0000 | 83.7 | 63.6 | 24.0 | 21.14 | 54.84 | 18.1 | 41.3 | 40.6 | 1.70 | 1.29 | na | | | na |
| NR 9 | 7 | 7 | 7.0000 | 92.1 | 73.3 | 20.4 | 20.86 | 58.73 | 30.6 | 43.0 | 26.5 | 1.87 | 1.49 | 1.3142 | | 0.3242 | 0.004 |
| NR 9 | 8 | 8 | 8.0000 | 81.1 | 65.2 | 19.6 | 20.93 | 59.47 | 33.7 | 30.6 | 35.8 | 1.65 | 1.32 | na | | | na |
| NR 9 | 9 | 9 | 9.0000 | 59.8 | 48.2 | 19.4 | 6.24 | 74.36 | 33.7 | 37.2 | 29.1 | 1.21 | 0.98 | 1.3045 | | 0.3145 | 0.003 |
| NR 9 | 10 | 10 | 10.0000 | 56.0 | 44.6 | 20.4 | 7.86 | 71.79 | 25.7 | 34.6 | 39.8 | 1.14 | 0.91 | na | | | na |
| NR 9 | 11 | 11 | 11.0000 | 90.0 | 71.7 | 20.3 | 7.38 | 72.29 | 37.1 | 35.3 | 27.6 | 1.83 | 1.46 | na | | | na |
| NR 9 | 12 | 12 | 12.0000 | 57.6 | 46.3 | 19.6 | 8.41 | 71.97 | 31.4 | 36.8 | 31.8 | 1.17 | 0.94 | 0.9576 | | -0.0324 | -0.001 |
| NR 9 | 13 | 13 | 13.0000 | 109.4 | 88.0 | 19.6 | 2.33 | 78.11 | 39.9 | 24.7 | 35.4 | 2.22 | 1.79 | 0.7424 | 0.82 | -0.2476 | -0.003 |
| NR 9 | 14 | 14 | 14.0000 | 70.1 | 56.7 | 19.1 | 6.33 | 74.55 | 39.0 | 25.5 | 35.6 | 1.42 | 1.15 | 0.9296 | | -0.0604 | -0.001 |
| NR 9 | 15 | 15 | 15.0000 | 81.5 | 65.2 | 20.0 | 7.60 | 72.40 | 40.1 | 28.2 | 31.8 | 1.65 | 1.32 | na | | | na |
| NR 9 | 16 | 16 | 16.0000 | 75.8 | 58.8 | 22.4 | 7.36 | 70.22 | 40.5 | 32.7 | 26.8 | 1.54 | 1.19 | 0.9593 | | -0.0307 | -0.001 |
| NR 9 | 17 | 17 | 17.0000 | 80.3 | 64.0 | 20.3 | 16.44 | 63.26 | 43.7 | 28.4 | 28.0 | 1.63 | 1.30 | 0.6657 | | -0.3243 | -0.003 |
| NR 9 | 18 | 18 | 18.0000 | 91.9 | 72.8 | 20.8 | 11.88 | 67.34 | 43.1 | 34.5 | 22.4 | 1.87 | 1.48 | na | 1.06 | na | na |
| NR 9 | 19 | 19 | 19.0000 | 100.2 | 78.5 | 21.7 | na | | 35.4 | 39.3 | 25.4 | 2.03 | 1.59 | na | | na | na |
| NR 9 | 20 | 20 | 20.0000 | 61.3 | 48.4 | 21.0 | na | | 36.3 | 32.4 | 31.3 | 1.24 | 0.98 | na | | na | na |
| NR 9 | 21 | 22 | 22.0000 | 220.5 | 174.1 | 21.0 | na | | 41.4 | 27.5 | 31.1 | 2.24 | 1.77 | na | | na | na |
| NR 9 | 22 | 24 | 24.0000 | 163.9 | 130.1 | 20.6 | na | | 48.2 | 31.2 | 20.6 | 1.66 | 1.32 | na | | na | na |
| NR 9 | 23 | 26 | 26.0000 | 204.2 | 160.7 | 21.3 | na | | 43.9 | 26.8 | 29.4 | 2.07 | 1.63 | na | | na | na |
| NR 9 | 24 | 28 | 28.0000 | 184.7 | 143.4 | 22.4 | na | | 46.4 | 24.0 | 29.6 | 1.87 | 1.46 | na | | na | na |
| NR 9 | 25 | 30 | 30.0000 | 182.8 | 141.8 | 22.4 | na | | 42.1 | 36.7 | 21.2 | 1.86 | 1.44 | na | | na | na |
| NR 9 | 26 | 32 | 32.0000 | 192.0 | 149.0 | 22.4 | na | | 35.4 | 38.8 | 25.8 | 1.95 | 1.51 | na | | na | na |
| NR 9 | 27 | 34 | 34.0000 | 173.9 | 135.2 | 22.3 | na | | 46.0 | 29.6 | 24.4 | 1.77 | 1.37 | na | | na | na |
| NR 9 | 28 | 36 | 36.0000 | 178.9 | 138.7 | 22.5 | na | | 40.9 | 29.2 | 29.9 | 1.82 | 1.41 | na | | na | na |
| NR 9 | 29 | 38 | 38.0000 | 190.3 | 146.5 | 23.0 | na | | 29.2 | 37.9 | 32.8 | 1.93 | 1.49 | na | | na | na |
| NR 9 | 30 | 40 | 40.0000 | 178.6 | 138.0 | 22.7 | na | | 37.7 | 32.6 | 29.7 | 1.81 | 1.40 | na | | na | na |
| NR 9 | 31 | 42 | 42.0000 | 183.0 | 141.7 | 22.6 | na | | 42.7 | 33.7 | 23.5 | 1.86 | 1.44 | na | | na | na |
| NR 9 | 32 | 44 | 44.0000 | 180.0 | 140.3 | 22.1 | na | | 41.4 | 26.5 | 32.1 | 1.83 | 1.42 | na | | na | na |
| NR 9 | 33 | 46 | 46.0000 | 210.7 | 161.6 | 23.3 | na | | 41.4 | 29.7 | 28.9 | 2.14 | 1.64 | na | | na | na |
| NR 9 | 34 | 48 | 48.0000 | 174.8 | 134.8 | 22.9 | na | | 43.0 | 28.5 | 28.5 | 1.77 | 1.37 | na | | na | na |
| NR 9 | 35 | 50 | 50.0000 | 188.5 | 137.9 | 26.8 | na | | 41.2 | 34.2 | 24.6 | 1.91 | 1.40 | na | | na | na |
| NR 9 | 36 | 52 | 52.0000 | 168.2 | 128.2 | 23.8 | na | | 40.1 | 28.8 | 31.2 | 1.71 | 1.30 | na | | na | na |
| NR 9 | 37 | 54 | 54.0000 | 219.1 | 166.5 | 24.0 | na | | 43.1 | 24.2 | 32.7 | 2.22 | 1.69 | na | | na | na |
| NR 9 | 38 | 56 | 56.0308 | 172.0 | 130.7 | 24.0 | na | | 40.7 | 28.1 | 31.2 | 1.75 | 1.33 | na | | na | na |
| NR 9 | 39 | 58 | 58.3385 | 201.2 | 154.3 | 23.3 | na | | 53.1 | 24.0 | 22.9 | 2.04 | 1.57 | na | | na | na |
| NR 9 | 40 | 60 | 60.6462 | 175.5 | 134.4 | 23.4 | na | | 47.0 | 21.7 | 31.2 | 1.78 | 1.36 | na | | na | na |
| NR 9 | 41 | 61 | 61.8000 | 159.7 | 119.0 | 25.5 | na | | 36.8 | 25.7 | 37.5 | 1.62 | 1.21 | na | | na | na |
| | | | | | | | | | | | | | | | Avg = 0.99 | | |

| Core No. | Sample No. | Uncorr. Depth (cm) | Corr. Depth (cm) | Wt. Wet Sample (g) | Wt. Dry Sample (g) | Water (%) | LOI (%) | Mineral (%) | Coarse Fraction (%) | Silt Fraction (%) | Clay Fraction (%) | Wet Bulk Dens (g/cc) | Dry Bulk Dens (g/cc) | Total Pb-210 (dpm/g) | Radium (dpm/g) | USGS Excess Pb-210 (dpm/g) | +/- |
|---|---|---|---|---|---|---|---|---|---|---|---|---|---|---|---|---|---|
| NR 10 | 1 | 1 | 1.0000 | 41.1 | 34.9 | 15.1 | 11.78 | 73.14 | 3.6 | 57.3 | 39.1 | 0.97 | 0.82 | 3.8828 | | 2.3128 | 0.006 |
| NR 10 | 2 | 2 | 2.0000 | 47.8 | 39.3 | 17.8 | 11.68 | 70.53 | 4.2 | 61.5 | 34.3 | 1.13 | 0.93 | 3.0244 | 1.30 | 1.4544 | 0.004 |
| NR 10 | 3 | 3 | 3.0000 | 42.7 | 34.8 | 18.5 | 11.71 | 69.79 | 5.0 | 60.2 | 34.8 | 1.01 | 0.82 | 3.2737 | | 1.7037 | 0.004 |
| NR 10 | 4 | 4 | 4.0000 | 46.9 | 37.4 | 20.3 | 11.22 | 68.52 | 3.9 | 58.9 | 37.2 | 1.10 | 0.88 | 2.6864 | | 1.1164 | 0.002 |
| NR 10 | 5 | 5 | 5.0000 | 53.8 | 42.0 | 21.9 | 11.53 | 66.54 | 2.3 | 49.0 | 48.7 | 1.27 | 0.99 | 1.4646 | 1.60 | -0.1054 | 0.000 |
| NR 10 | 6 | 6 | 6.0000 | 52.4 | 40.7 | 22.3 | 11.33 | 66.34 | 1.9 | 53.5 | 44.6 | 1.23 | 0.96 | 2.8113 | | 1.2413 | 0.004 |
| NR 10 | 7 | 7 | 7.0000 | 59.0 | 45.9 | 22.2 | 11.26 | 66.53 | 3.3 | 52.7 | 44.0 | 1.39 | 1.08 | 3.3776 | | 1.8076 | 0.007 |
| NR 10 | 8 | 8 | 8.0000 | 74.4 | 56.5 | 24.1 | 11.09 | 64.85 | 2.2 | 52.0 | 45.7 | 1.75 | 1.33 | 2.4304 | 1.60 | 0.8604 | 0.002 |
| NR 10 | 9 | 9 | 9.0000 | 49.6 | 37.4 | 24.6 | 11.73 | 63.67 | 2.5 | 57.4 | 40.1 | 1.17 | 0.88 | 1.1461 | | -0.4239 | -0.001 |
| NR 10 | 10 | 10 | 10.0000 | 72.1 | 53.8 | 25.4 | 10.76 | 63.86 | 2.7 | 49.0 | 48.2 | 1.70 | 1.27 | 1.8585 | | 0.2885 | 0.001 |
| NR 10 | 11 | 11 | 11.0000 | 81.0 | 60.0 | 25.9 | 10.76 | 63.32 | 2.1 | 47.8 | 50.2 | 1.91 | 1.41 | 2.8517 | 1.42 | 1.2817 | 0.005 |
| NR 10 | 12 | 12 | 12.0000 | 73.3 | 53.8 | 26.6 | 11.95 | 61.44 | 1.4 | 45.4 | 53.2 | 1.73 | 1.27 | 2.2882 | | 0.7182 | 0.001 |
| NR 10 | 13 | 13 | 13.0000 | 73.4 | 53.4 | 27.2 | 10.85 | 61.90 | 1.5 | 73.7 | 24.8 | 1.73 | 1.26 | 2.1500 | | 0.5800 | 0.002 |
| NR 10 | 14 | 14 | 14.0000 | 89.5 | 64.3 | 28.2 | 11.11 | 60.73 | 1.0 | 85.0 | 14.0 | 2.11 | 1.51 | 0.8423 | 1.72 | -0.7277 | -0.005 |
| NR 10 | 15 | 15 | 15.0000 | 85.2 | 61.3 | 28.1 | 11.44 | 60.51 | 1.8 | 74.7 | 23.5 | 2.01 | 1.44 | 1.7054 | | 0.1354 | 0.001 |
| NR 10 | 16 | 16 | 16.0000 | 67.5 | 48.8 | 27.7 | 10.78 | 61.52 | 0.8 | 73.4 | 25.8 | 1.59 | 1.15 | 2.1604 | | 0.5904 | 0.007 |
| NR 10 | 17 | 17 | 17.0000 | 79.6 | 56.8 | 28.6 | 11.55 | 59.80 | 1.6 | 63.2 | 35.3 | 1.87 | 1.34 | 1.8702 | 1.51 | 0.3002 | 0.002 |
| NR 10 | 18 | 18 | 18.0000 | 74.3 | 53.3 | 28.3 | 10.76 | 60.98 | 1.1 | 73.2 | 25.7 | 1.75 | 1.25 | 1.6269 | | 0.0569 | 0.000 |
| NR 10 | 19 | 19 | 19.0000 | 71.8 | 51.8 | 27.9 | 11.02 | 61.12 | 1.5 | 57.7 | 40.8 | 1.69 | 1.22 | 1.8910 | | 0.3210 | 0.002 |
| NR 10 | 20 | 20 | 20.0000 | 73.6 | 53.0 | 28.0 | 10.47 | 61.54 | 1.2 | 52.0 | 46.8 | 1.73 | 1.25 | 1.9072 | 1.67 | 0.3372 | 0.002 |
| NR 10 | 21 | 22 | 22.0000 | 141.6 | 100.3 | 29.2 | 11.42 | 59.42 | 1.2 | 52.7 | 46.1 | 1.67 | 1.18 | 1.8701 | | 0.3001 | 0.001 |
| NR 10 | 22 | 24 | 24.0000 | 155.2 | 110.0 | 29.1 | 10.65 | 60.23 | 1.9 | 74.5 | 23.6 | 1.83 | 1.29 | 1.7327 | 1.71 | 0.1627 | 0.001 |
| NR 10 | 23 | 26 | 26.0000 | 108.2 | 77.3 | 28.6 | 11.46 | 59.98 | 1.8 | 46.6 | 51.6 | 1.27 | 0.91 | 1.9965 | | 0.4265 | 0.003 |
| NR 10 | 24 | 28 | 28.0000 | 129.4 | 91.5 | 29.3 | 10.45 | 60.26 | 2.0 | 53.8 | 44.2 | 1.52 | 1.08 | 1.8174 | | 0.2474 | 0.001 |
| NR 10 | 25 | 30 | 30.0000 | 141.5 | 99.9 | 29.4 | 10.52 | 60.08 | 1.8 | 48.5 | 49.6 | 1.67 | 1.18 | 1.3888 | | -0.1812 | -0.003 |
| NR 10 | 26 | 32 | 32.0000 | 122.8 | 86.6 | 29.5 | 10.54 | 59.98 | 1.9 | 58.6 | 39.5 | 1.45 | 1.02 | 1.6823 | | 0.1123 | 0.001 |
| NR 10 | 27 | 34 | 34.0000 | 148.2 | 103.8 | 30.0 | 11.24 | 58.80 | 2.7 | 56.5 | 40.8 | 1.74 | 1.22 | 1.9930 | | 0.4230 | 0.004 |
| NR 10 | 28 | 36 | 36.0000 | 141.4 | 98.8 | 30.1 | 10.74 | 59.14 | 1.6 | 50.6 | 47.8 | 1.66 | 1.16 | 1.9681 | | 0.3981 | 0.003 |
| NR 10 | 29 | 38 | 38.0000 | 142.9 | 99.6 | 30.3 | 10.93 | 58.76 | 2.7 | 79.5 | 17.9 | 1.68 | 1.17 | 2.0166 | | 0.4466 | 0.003 |
| NR 10 | 30 | 40 | 40.0000 | 153.7 | 106.9 | 30.4 | 10.30 | 59.25 | 5.1 | 60.2 | 34.8 | 1.81 | 1.26 | 1.8050 | | 0.2350 | 0.002 |
| NR 10 | 31 | 42 | 42.0000 | 163.9 | 112.6 | 31.3 | 11.42 | 57.28 | 2.9 | 57.8 | 39.4 | 1.93 | 1.33 | 1.5224 | | -0.0476 | 0.000 |
| NR 10 | 32 | 44 | 44.1111 | 183.8 | 126.1 | 31.4 | 10.76 | 57.85 | 2.9 | 68.0 | 29.0 | 2.16 | 1.48 | 1.8262 | | 0.2562 | 0.005 |
| NR 10 | 33 | 46 | 46.5556 | 158.8 | 109.6 | 31.0 | 11.16 | 57.86 | 1.5 | 59.3 | 39.2 | 1.87 | 1.29 | 1.9179 | | 0.3479 | 0.002 |
| NR 10 | 34 | 48 | 49.0000 | 153.8 | 106.2 | 30.9 | 10.91 | 58.14 | 3.9 | 73.2 | 22.8 | 1.81 | 1.25 | na | | na | na |
| NR 10 | 35 | 50 | 51.5714 | 158.9 | 110.2 | 30.6 | 12.03 | 57.32 | 3.5 | 63.8 | 32.7 | 1.87 | 1.30 | 2.5290 | | 0.9590 | 0.007 |
| NR 10 | 36 | 52 | 54.2500 | 147.9 | 102.1 | 31.0 | 10.50 | 58.54 | 4.8 | 57.8 | 37.5 | 1.74 | 1.20 | 2.1618 | | 0.5918 | 0.003 |
| | | | | | | | | | | | | | | | Avg = 1.57 | | |

| Core No. | Sample No. | Uncorr. Depth (cm) | Corr. Depth (cm) | Wt. Wet Sample (g) | Wt. Dry Sample (g) | Water (%) | LOI (%) | Mineral (%) | Coarse Fraction (%) | Silt Fraction (%) | Clay Fraction (%) | Wet Bulk Dens (g/cc) | Dry Bulk Dens (g/cc) | Total Pb-210 (dpm/g) | Radium (dpm/g) | USGS Excess Pb-210 (dpm/g) | +/- |
|---|---|---|---|---|---|---|---|---|---|---|---|---|---|---|---|---|---|
| NR 11 | 1 | 1 | 1.0000 | 81.8 | 30.8 | 62.3 | 10.80 | 26.85 | 13.8 | 37.1 | 49.1 | 2.08 | 0.78 | 4.3043 | | 3.3643 | 0.044 |
| NR 11 | 2 | 2 | 2.0000 | 67.5 | 25.5 | 62.2 | 8.49 | 29.29 | 9.6 | 31.4 | 59.0 | 1.72 | 0.65 | 4.3657 | | 3.4257 | 0.055 |
| NR 11 | 3 | 3 | 3.0000 | 65.7 | 25.3 | 61.5 | 8.82 | 29.69 | 10.3 | 40.6 | 49.1 | 1.67 | 0.64 | 4.2482 | | 3.3082 | 0.054 |
| NR 11 | 4 | 4 | 4.0000 | 61.9 | 23.8 | 61.6 | 8.20 | 30.25 | 9.4 | 34.9 | 55.7 | 1.58 | 0.61 | 4.0670 | | 3.1270 | 0.023 |
| NR 11 | 5 | 5 | 5.0000 | 50.2 | 20.1 | 60.0 | 8.32 | 31.72 | 2.8 | 28.7 | 68.5 | 1.28 | 0.51 | 3.5721 | 0.87 | 2.6321 | 0.022 |
| NR 11 | 6 | 6 | 6.0000 | 71.1 | 28.1 | 60.5 | 6.40 | 33.12 | 6.7 | 34.8 | 58.5 | 1.81 | 0.72 | 3.8408 | | 2.9008 | 0.028 |
| NR 11 | 7 | 7 | 7.0000 | 62.6 | 25.9 | 58.6 | 6.00 | 35.37 | 3.9 | 43.3 | 52.8 | 1.59 | 0.66 | 3.2790 | | 2.3390 | 0.051 |
| NR 11 | 8 | 8 | 8.0000 | 65.8 | 28.5 | 56.7 | 6.51 | 36.80 | 5.7 | 39.8 | 54.4 | 1.68 | 0.73 | 3.4285 | | 2.4885 | 0.013 |
| NR 11 | 9 | 9 | 9.0000 | 58.7 | 25.4 | 56.7 | 6.48 | 36.79 | 4.8 | 46.3 | 48.9 | 1.49 | 0.65 | 2.6304 | | 1.6904 | 0.035 |
| NR 11 | 10 | 10 | 10.0000 | 70.5 | 30.1 | 57.3 | 6.37 | 36.33 | 6.7 | 37.8 | 55.6 | 1.80 | 0.77 | 2.7722 | | 1.8322 | 0.021 |
| NR 11 | 11 | 11 | 11.0000 | 62.8 | 27.5 | 56.2 | 8.00 | 35.79 | 4.1 | 50.4 | 45.5 | 1.60 | 0.70 | 2.7647 | | 1.8247 | 0.022 |
| NR 11 | 12 | 12 | 12.0000 | 60.4 | 26.7 | 55.8 | 7.49 | 36.71 | 4.2 | 40.6 | 55.2 | 1.54 | 0.68 | 3.5565 | | 2.6165 | 0.017 |
| NR 11 | 13 | 13 | 13.0000 | 65.1 | 28.8 | 55.8 | 25.44 | 18.80 | 7.0 | 47.3 | 45.7 | 1.66 | 0.73 | 2.9294 | 1.01 | 1.9894 | 0.045 |
| NR 11 | 14 | 14 | 14.0000 | 67.9 | 29.7 | 56.3 | 5.32 | 38.42 | 6.3 | 40.4 | 53.3 | 1.73 | 0.76 | 2.5652 | | 1.6252 | 0.018 |
| NR 11 | 15 | 15 | 15.0000 | 72.4 | 34.7 | 52.1 | 5.30 | 42.63 | 17.1 | 50.8 | 32.2 | 1.84 | 0.88 | 2.4228 | | 1.4828 | 0.017 |
| NR 11 | 16 | 16 | 16.0000 | 64.4 | 31.8 | 50.6 | 6.09 | 43.28 | 19.8 | 45.5 | 34.7 | 1.64 | 0.81 | 2.3575 | | 1.4175 | 0.013 |
| NR 11 | 17 | 17 | 17.0000 | 69.1 | 32.4 | 53.1 | 5.80 | 41.09 | 15.3 | 42.6 | 42.2 | 1.76 | 0.83 | 2.3970 | | 1.4570 | 0.043 |
| NR 11 | 18 | 18 | 18.0000 | 65.5 | 32.3 | 50.7 | 5.10 | 44.21 | 19.5 | 44.2 | 36.3 | 1.67 | 0.82 | 2.5361 | | 1.5961 | 0.025 |
| NR 11 | 19 | 19 | 19.0000 | 59.2 | 29.8 | 49.7 | 5.60 | 44.74 | 26.7 | 37.1 | 36.3 | 1.51 | 0.76 | 1.7740 | | 0.8340 | 0.006 |
| NR 11 | 20 | 21 | 21.0000 | 95.5 | 46.1 | 51.7 | 5.60 | 42.67 | 30.7 | 32.3 | 37.1 | 1.22 | 0.59 | 1.5906 | | 0.6506 | 0.005 |
| NR 11 | 21 | 23 | 23.0542 | 98.3 | 56.2 | 42.8 | 4.76 | 52.41 | 21.4 | 34.6 | 44.0 | 1.25 | 0.72 | 1.6890 | | 0.7490 | 0.004 |
| NR 11 | 22 | 25 | 25.1375 | 114.8 | 56.6 | 50.7 | 5.57 | 43.74 | 14.9 | 29.3 | 55.8 | 1.46 | 0.72 | 1.8331 | | 0.8931 | 0.007 |
| NR 11 | 23 | 27 | 27.2208 | 100 | 57 | 43.0 | 6.08 | 50.92 | 8.4 | 30.7 | 60.9 | 1.27 | 0.73 | 1.6566 | | 0.7166 | 0.004 |
| NR 11 | 24 | 29 | 29.3042 | 95 | 55.5 | 41.6 | 6.10 | 52.33 | 5.9 | 20.1 | 74.0 | 1.21 | 0.71 | 1.8290 | | 0.8890 | 0.003 |
| NR 11 | 25 | 31 | 31.3875 | 111.3 | 65.8 | 40.9 | 4.47 | 54.65 | 6.0 | 29.7 | 64.3 | 1.42 | 0.84 | 1.9667 | | 1.0267 | 0.004 |
| NR 11 | 26 | 33 | 33.4708 | 92.6 | 55.7 | 39.8 | 5.43 | 54.72 | 7.9 | 27.0 | 65.1 | 1.18 | 0.71 | 1.8770 | | 0.9370 | 0.004 |
| NR 11 | 27 | 35 | 35.7600 | 106.7 | 63.3 | 40.7 | 7.55 | 51.77 | 7.9 | 17.6 | 74.5 | 1.36 | 0.81 | 2.2434 | | 1.3034 | 0.006 |
| NR 11 | 28 | 37 | 38.1600 | 131.9 | 80.8 | 38.7 | 7.40 | 53.86 | 2.6 | 33.5 | 63.9 | 1.68 | 1.03 | 2.1123 | | 1.1723 | 0.004 |
| NR 11 | 29 | 39 | 40.5600 | 123.9 | 76.2 | 38.5 | 7.46 | 54.04 | 3.2 | 36.6 | 60.2 | 1.58 | 0.97 | 2.3385 | | 1.3985 | 0.004 |
| NR 11 | 30 | 41 | 42.9600 | 120.1 | 72.4 | 39.7 | 6.76 | 53.52 | 2.3 | 31.3 | 66.4 | 1.53 | 0.92 | na | | na | na |
| NR 11 | 31 | 43 | 45.0000 | 102.4 | 60.8 | 40.6 | 6.60 | 52.78 | 1.4 | 22.8 | 75.8 | 1.30 | 0.77 | 2.5941 | | 1.6541 | 0.025 |
| NR 11 | 32 | 45 | 47.0000 | 115 | 67.8 | 41.0 | 6.14 | 52.82 | 1.8 | 22.5 | 75.6 | 1.46 | 0.86 | 1.7795 | | 0.8395 | 0.005 |
| NR 11 | 33 | 47 | 49.0000 | 117.7 | 70.6 | 40.0 | 6.17 | 53.82 | 2.6 | 19.1 | 78.3 | 1.50 | 0.90 | 2.8901 | | 1.9501 | 0.010 |
| NR 11 | 34 | 49 | 51.0000 | 121.9 | 74.2 | 39.1 | 7.50 | 53.37 | 0.4 | 15.3 | 84.3 | 1.55 | 0.94 | 2.8026 | | 1.8626 | 0.013 |
| NR 11 | 35 | 51 | 53.0000 | 119.5 | 74.6 | 37.6 | 7.40 | 55.03 | 0.4 | 34.3 | 65.4 | 1.52 | 0.95 | 1.8782 | | 0.9382 | 0.004 |
| NR 11 | 36 | 53 | 55.0000 | 115.9 | 70.4 | 39.3 | 5.90 | 54.84 | 1.1 | 30.5 | 68.4 | 1.48 | 0.90 | na | na | na | na |
| NR 11 | 37 | 55 | 57.0000 | 123.8 | 77.2 | 37.6 | na | | 1.9 | 30.9 | 67.2 | 1.58 | 0.98 | na | na | na | na |
| NR 11 | 38 | 57 | 59.0000 | 124.9 | 78.9 | 36.8 | na | | 1.5 | 35.9 | 62.5 | 1.59 | 1.00 | na | na | na | na |
| NR 11 | 39 | 59 | 61.0000 | 116.3 | 67 | 42.4 | na | | 2.4 | 30.6 | 67.1 | 1.48 | 0.85 | na | na | na | na |
| NR 11 | 40 | 61 | 63.0000 | 125.8 | 80.7 | 35.9 | na | | 0.4 | 28.1 | 71.5 | 1.60 | 1.03 | na | na | na | na |
| NR 11 | 41 | 63 | 65.0000 | 135.3 | 83 | 38.7 | na | | 0.8 | 37.7 | 61.5 | 1.72 | 1.06 | na | na | na | na |
| NR 11 | 42 | 65 | 67.0000 | 133.7 | 83.2 | 37.8 | na | | 0.4 | 41.1 | 58.5 | 1.70 | 1.06 | na | na | na | na |
| NR 11 | 43 | 67 | 69.0000 | 147.4 | 89.8 | 39.1 | na | | 1.5 | 16.6 | 81.9 | 1.88 | 1.14 | na | na | na | na |
| NR 11 | 44 | 69 | 71.0000 | 144.4 | 90.6 | 37.3 | na | | 0.4 | 37.1 | 62.5 | 1.84 | 1.15 | na | na | na | na |
| NR 11 | 45 | 71 | 73.0000 | 85.6 | 52.7 | 38.4 | na | | 1.6 | 23.0 | 75.5 | 1.09 | 0.67 | na | na | na | na |
| | | | | | | | | | | | | | | | Avg = 0.94 | | |

# APPENDIX C

## Laboratory Procedures for Determining $^{210}Pb$ Activities

## USGS Laboratory Procedures for Determining $^{210}Pb$ Activities

The U.S. Geological Survey's Analytical Laboratory at Denver analyzed $^{210}Pb$ activity in the cores. Analyses were completed under the direction of Dr. Charles W. Holmes. Other USGS personnel involved in the analyses were James D. Cathcart and Margaret Marot. The cores were sampled at either 1 cm or 2 cm intervals from the center of each core from top to bottom. Analyzed samples were prepared using the following 14 steps modified from Flynn (1968) and Martin and Rice (1981).

1. Wet samples are placed into clean, preweighed procelain evaporating dishes, weighed, dried at 40°C, and reweighed to determine water loss.

2. Dried samples are ground to a fine powder (75-100 U.S. Standard mesh) in a grinding mill to obtain an homogeneous sample for analysis.

3. Sample splits of approximately 5 g are made and weighed, placed into precleaned, preweighed crucibles and heated in a muffle furnace at 450°C for 6 hrs until a stable weight is obtained. The samples are allowed to cool to room temperature and reweighed.

4. Each sample is transferred to a 100-ml Teflon beaker using 5-10 m. of reagent grade 16N nitric acid ($HNO_3$). A known amount of calibrated $^{209}Po$ spike is added and the sample swirled to mix the spike. The beaker is covered with a watchglass and allowed to stand overnight.

5. The solution is evaporated under heat lamps at 109°C. The dried sample is washed from the sides of the beaker using 8N hydrochloric acid (HCL) and swirled again to insure proper mixing. The solution is evaporated to dryness and allowed to cool.

6. One-milliliter aliquots of 30 percent hydrogen peroxide ($H_2O_2$) are added to the sample until it is completely wet, and the resulting solution is again evaporated to dryness. The sample is placed under heat lamps only after the peroxide reaction has subsided. The cooling and peroxide steps are repeated twice more.

7. The sample is then washed twice with 8N HCL and evaporated to dryness between each washing. This step is to remove all traces of the nitric acid which interferes with the autoplating onto the silver planchet.

8. Five milliliters of 8N HCL are added to the dried sample, which is then transferred to a 100-ml glass beaker using additional amounts of HCL and deionized water.

9. To minimize the interference of $Fe^{+3}$, $Cr^{+6}$, and other oxidants, 5 ml of hydroxylamine hydrochloride and 2 ml of 25% sodium citrate are added to each sample. Additionally, 1 ml of holdback carrier, bismuth nitrate ($BiN0_3$), is added to prevent deposition of $^{212}Bi$. A plastic coated magnetic stir bar is added to each beaker for stirring during the autoplating.

10. The pH of the solution is adjusted to between 1.85 and 1.95 using ammonium hydoxide ($NH_4OH$) and HCL to inhibit any tellurium and selenium whose presence decreases the plating efficiency.

11. The beaker is placed on a stirring hot plate and heated between 85°C and 90°C for 5 minutes to reduce any $Fe^{+3}$, $Cr^{+6}$, or other oxidants that might be present.

12. A Teflon plating device holding the silver foil disc is placed in the solution. This allows plating on one side of the disc only. The plating device covers the beaker and therefore minimal evaporation occurs during the plating procedure.

13. The heating and stirring proceeds for a minimum of 90 minutes.

14. The plating device is disassembled, the silver disc washed with deionized water, dried and then counted on a alpha counting system.

**Counting Procedure**

1. The sample is positioned beneath an alpha detector in a counting chamber and put under vacuum.

2. The sample is counted for 24-48 hrs or until enough counts are obtained for each spectra.

3. Counts for each spectrum are routed to the proper channel in the Pulse Height Analyzer (PHA) and stored by a computer.

4. The PHA supports form 1-16 counting chambers at any given time.

5. The raw spectrum is transferred from the computer via a 5 1/4 inch floppy disk for later data reduction.

# APPENDIX D

## BEG Data on Moisture and Bulk Density

# APPENDIX D

| Location I.D. | Most Complete Sample Extraction | Sample Length (cm) | Volume (cc) | Moisture (wt%) | Dry Bulk Density (g/cc) |
|---|---|---|---|---|---|
| NRD1 /top - 5 cm | | 5.5 | 5.91 | 32.6 | 0.61 |
| NRD1 /top - 23 | | 5.6 | 6.02 | 31.7 | 0.80 |
| NRD1 /top - 50 | | 5.9 | 6.34 | 31.3 | 0.90 |
| NRD2 /top - 5 | | 5.0 | 5.38 | 51.7 | 0.71 |
| NRD2 /top - 35 | | 5.3 | 5.70 | 37.5 | 0.89 |
| NRD2 /top - 62 | | 5.7 | 6.13 | 29.2 | 1.23 |
| NRD3 /top - 5 | | 5.0 | 5.38 | 43.5 | 0.52 |
| NRD3 /top - 33 | | 4.8 | 5.16 | 34.7 | 0.85 |
| NRD3 /top - 54 | | 4.9 | 5.27 | 32.5 | 0.92 |
| NRD4 /top - 5 | | 5.1 | 5.48 | 43.9 | 0.68 |
| NRD4 /top - 25 | | 5.0 | 5.38 | 33.2 | 0.81 |
| NRD4 /top - 45 | | 4.8 | 5.16 | 35.1 | 0.72 |
| NRD5 /top - 5 | X | 5.0 | 5.38 | 26.1 | 0.71 |
| NRD5 /top - 24 | X | 5.0 | 5.38 | 31.2 | 0.75 |
| NRD5 /top - 39 | X | 5.1 | 5.48 | 23.8 | 1.00 |
| NRD6 /top - 11 | | 5.0 | 5.38 | 43.4 | 0.51 |
| NRD6 /top - 22 | | 5.3 | 5.70 | 38.4 | 0.79 |
| NRD6 /top - 36 | | 5.4 | 5.81 | 35.9 | 0.80 |
| NRD7 /top - 11 | | 5.1 | 5.48 | 34.3 | 0.64 |
| NRD7 /top - 25 | | 5.5 | 5.91 | 32.0 | 0.84 |
| NRD7 /top - 44 | | 5.4 | 5.81 | 32.8 | 0.75 |
| NRD8 /top - 12 | X | 4.9 | 5.27 | 32.0 | 0.85 |
| NRD8 /top - 42 | X | 5.0 | 5.38 | 37.6 | 0.72 |
| NRD8 /top - 72 | X | 5.0 | 5.38 | 41.0 | 0.84 |
| NRD9 /top - 5 | X | 5.0 | 5.38 | 26.3 | 0.58 |
| NRD9 /top - 32 | X | 4.5 | 4.84 | 25.5 | 1.40 |
| NRD9 /top - 59 | X | 4.9 | 5.27 | 25.4 | 1.39 |
| NRD10 /top - 10 | X | 5.1 | 5.48 | 29.8 | 0.61 |
| NRD10 /top - 27 | | 4.7 | 5.05 | 31.0 | 0.68 |
| NRD10 /top - 48 | | 4.9 | 5.27 | 33.4 | 0.92 |
| NRD11 /top - 28 | X | 5.3 | 5.70 | 43.9 | 0.55 |
| NRD11 /top - 62 | X | 5.0 | 5.38 | 36.6 | 0.64 |
| NRD11 /top - 67 | X | 5.1 | 5.48 | 41.9 | 0.73 |